MODS

A Multi-Object Double Spectrograph for the Large Binocular Telescope

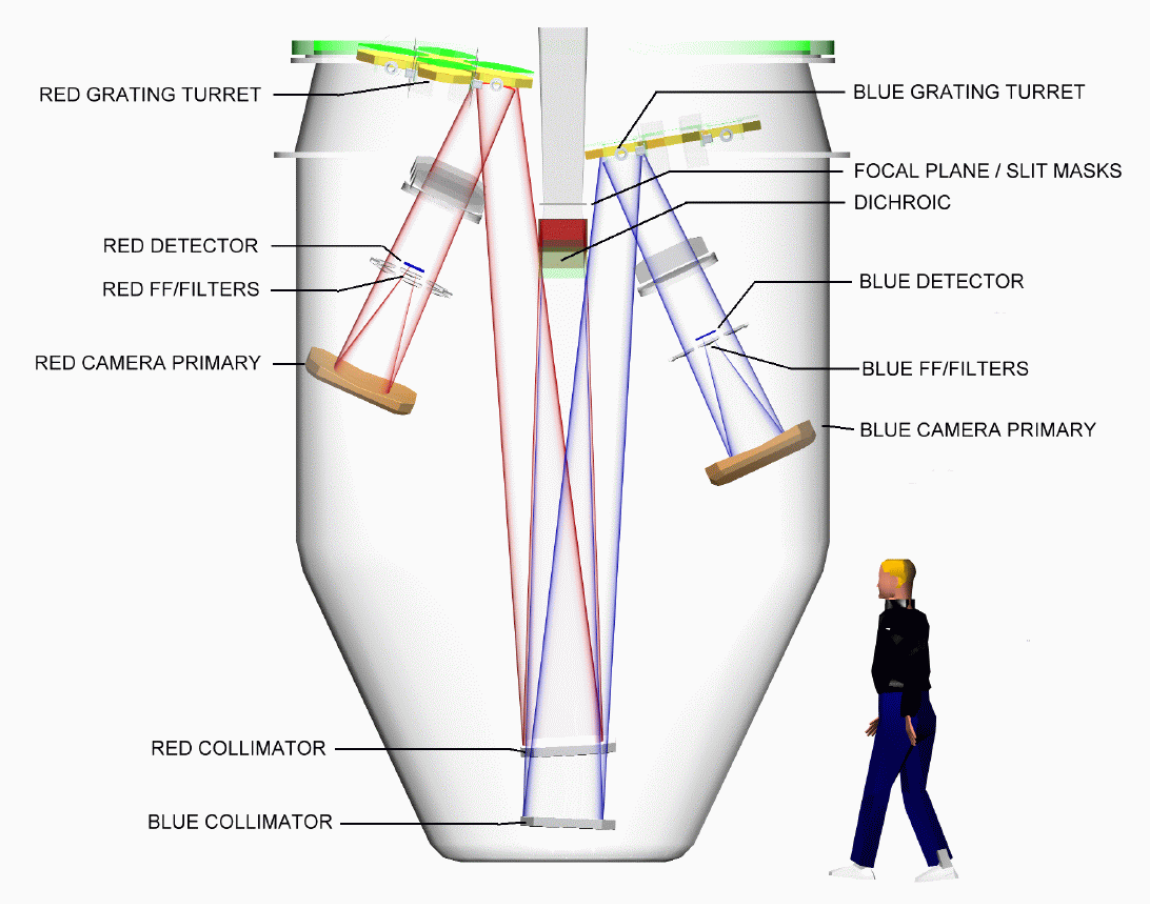

Preliminary Design Review

11 June 2001

The Ohio State University, Department of Astronomy

Columbus, Ohio

MODS PDR

Compiled & Edited by Darren DePoy & Richard Pogge

Authors & Project Team:

Patrick Osmer	Project PI (Overview §1)
Darren DePoy	(Project Management §7, Overview §1)
Richard Pogge	(Software §6, Overview §1)
Bruce Atwood	(Detectors §5)
Thomas O'Brien	(Mechanical §3 & Appendix B)
Paul Byard	(Optics, §2 & Appendices A & B)
Dan Pappalardo	(Mechanism Control §4)
Jerry Mason	(Software §6)
David Weinberg	(Overview §1)

MODS PDR Committee:

Tom Herbst (Chair; MPIA, Heidelberg)

Dan Fabricant (Referee, Harvard-Smithsonian CfA)

Gary Hill (Referee, University of Texas, Austin)

Gary Bernstein (Referee, University of Michigan)

Walter Seifert (Referee, Landessternwarte Heidelberg-Königstuhl)

Klaus Meisenheimer (Referee, MPIA Heidelberg)

Giampaolo Vettolani (Referee, CNR)

Mark Wagner (LBTPO)

John Hill (LBTPO)

Table of Contents

1 Overview

1.1 Introduction

The Large Binocular Telescope (LBT) project is a partnership of the University of Arizona, the German LBTB consortium (MPIA, lead institute), the Italian astronomical community (through Arcetri Observatory), the Ohio State University, and the Research Corporation to build the world's largest telescope on a single mount. The telescope construction is progressing well and first light is expected in late 2003/early 2004. The initial instrument complement of the telescope will include a near-infrared camera/spectrograph (LUCIFER), a wide field prime-focus CCD camera (WFPFC), infrared interferometric beam combiners, and an optical spectrograph (MODS). As part of the Ohio State University Astronomy Department contribution to the project, we are building the optical spectrograph, which will be a facility instrument for the entire LBT community. The primary science driver for the instrument for our group is a set of observational programs designed to address several key research topics on the evolution of galaxies and structure in the Universe. We plan to devote a significant fraction of our LBT observing time to these programs, the ultimate outcome of which should be major advances in our understanding of galaxy evolution. Our LBT partners will use the instrument for a wide variety of other research programs as well.

MODS (Multi-Object Double Spectrograph) is designed to deliver the highest possible throughput from 320 to 1000 nm, with spectral resolutions of 10^3 to 10^4, and multi-object capability over an ~6' field. Our design is highly modular, so future upgrades (e.g., additional cameras, new gratings, and integral field units) should be straightforward.

To provide the context of the MODS design described in detail in the rest of this PDR document, this overview of MODS describes the history of our astronomical instrumentation activities at Ohio State (§1.2), and outlines a scientific program for MODS from which we developed the general description and scientific requirements for MODS (§1.3 and §1.4). We then present the basic MODS instrument specifications (§1.5), and describe the scope of this design review document (§1.6).

1.2 Astronomical Instrumentation at Ohio State

The Ohio State University Department of Astronomy has a long history of astronomical instrumentation development stretching back into the late 1970s. Since 1988, we have built a number of advanced facility instruments for our own telescopes and for partners in observatories throughout the world.

We have constructed 5 major facility instruments:

1. Imaging Fabry-Perot Spectrometer (IFPS) deployed at the 1.8-m Perkins telescope between 1988 and 1998.
2. The Ohio State Infrared Imager and Spectrometer (OSIRIS), first deployed at the 1.8-m Perkins telescope, then serving first as a guest investigator instrument at CTIO, and it is now a facility instrument at the CTIO 1.5-m and 4-m telescopes. Next year it will serve as a commissioning instrument on the new SOAR 4m telescope.

3. The MDM-Ohio State-Array Infrared Camera (TIFKAM, The Instrument Formerly Known As MOSAIC), which has been a facility instrument at KPNO and MDM.
4. ANDICAM (A Novel Double-Imaging CAMera), which is a facility instrument on the YALO 1-meter telescope at CTIO, in operation since 1998. A copy of ANDICAM built for a Dutch/South African collaboration (named DANDICAM, for Dutch ANDICAM) has been deployed at the 1-m Elizabeth telescope at SAAO in Sutherland South Africa since 1999.
5. CCDS, a retrofit of a Boller & Chivens optical long-slit spectrometer to use a CCD camera and provide motor controls for mechanisms. It was first deployed in 1986 at the 1.8-m Perkins telescope, and has been in use at MDM since 1999.

All of these instruments have seen substantial use by both Ohio State personnel and the general astronomical community (typically via shared use of the instruments at national observatories) and have produced a large number of papers in refereed journals.

The IFPS is a two-dimensional imaging spectrophotometer for the 320–1000nm-wavelength region. It uses four etalons providing spectral resolutions ($\lambda/\Delta\lambda$) of 1200 at 450-750nm and 4500 at 320-700nm, making it applicable to a wide range of galactic and extragalactic imaging spectrophotometric problems. The IFPS has also been used extensively for direct imaging. A comprehensive description of the instrument is given in Pogge et al. (1995). The IFPS was deployed at the 1.8-m Perkins Telescope of the Lowell Observatory where it saw substantial use as a Fabry-Perot and a direct imaging camera from 1988 until it was retired in 1998.

OSIRIS is a multipurpose infrared instrument providing imaging and spectroscopy in the 0.9–2.5μm wavelength region. In imaging mode the instrument has two plate scales provided by selectable camera lenses. In spectroscopic mode a grating replaces a folding flat and slit is introduced in the focal plane (replacing an imaging mask). Different slits and cameras provide resolutions of 1200 and 3200. There is also a cross-dispersed mode that allows simultaneous observation of all of the J, H, and K bands at R=1200 with an 85 pixel long slit. DePoy et al. (1993) gives a detailed description of the instrument. We recently upgraded OSIRIS to a 1024×1024 HgCdTe detector array (provided by NOAO) and currently support its use as a facility instrument at CTIO on the 1.5-meter and 4-meter telescopes. Next year OSIRIS will be deployed to the new SOAR 4m telescope. While there it will serve as a facility infrared camera and as the primary infrared commissioning instrument for the telescope. In all, OSIRIS is one of the most successful instruments we have produced.

TIFKAM is an infrared imager/spectrometer built on the heritage of OSIRIS, and incorporating many improvements learned from the OSIRIS project. It uses one of the first science-quality large-format ALADDIN InSb arrays, provided by an agreement with the US Naval Observatory and NOAO. The larger format detector allows for higher dispersion than OSIRIS, and improved image sampling with a wide field of view. It is primarily used on the 2.4-m Hiltner telescope by the MDM Consortium and was available for community use as a facility instrument at KPNO telescopes as part of the agreement that provided the ALADDIN array until 2001, when KPNO deployed its updated SQIID

IR camera. TIFKAM has been used on either the 2.4m or 1.3m telescope during every bright run at MDM since 2000.

ANDICAM is capable of simultaneous imaging at an optical and a near-infrared wavelength. The light from a telescope is split by a dichroic so that optical wavelengths (300–900nm) are imaged onto a 2048×2048 CCD and infrared wavelengths (1.1–2.4μm) are imaged onto a 1024×1024 HgCdTe array (there are filter wheels in both channels to select appropriate bands). ANDICAM is primarily intended for multi-color synoptic observing programs and is permanently mounted on the CTIO/Yale 1m telescope. We also received funding from the Dutch and South African governments to build a copy of ANDICAM for the SAAO 1m telescope as part of a program to detect extra-solar-system planets using observations of gravitational microlensing events (DANDICAM for Dutch-funded ANDICAM). ANDICAM has been in continuous operations every clear night at CTIO for the last 2 years, and regularly produces between 1 and 2 GB of CCD and IR imaging per night. As part of the ANDICAM project OSU also developed the web-based queue/service observer preparation and scheduling system in use. See http://www.astronomy.ohio-state.edu/YALO/ for details. DANDICAM is used approximately 180 nights per year at SAAO.

CCDS was first deployed at the 1.8-m Perkins telescope of the Lowell Observatory in 1986, after retrofitting it with a CCD (to replace an image tube), and adding new mechanism controls. In 1998, it was moved to OSU where it was modified for deployment on the MDM telescopes, and equipped with a new Loral CCD and updated (and vastly improved) mechanisms and control computers. It has been available as a facility spectrometer at MDM on the 2.4-m and 1.3-m telescopes since 2000 and has been heavily used for a variety of spectroscopic projects.

There has been substantial community use of these instruments. OSIRIS was used as a facility instrument at CTIO for 15 months in 1993-1994, where it was scheduled for ~150 nights on either the 4-m or 1.5-m telescopes. Under the agreement that provided the 1024×1024 detector, OSIRIS is available for use by the general community at CTIO during 1999-2001. OSU, Lowell, and visitors heavily used the IFPS on the Perkins 1.8-m telescope at Lowell Observatory. Nine Ph.D. dissertations have been completed using the IFPS and OSIRIS, six from OSU and three from other institutions. TIFKAM is used at KPNO as a facility infrared imager/spectrometer on the 2.1m and 4m telescopes approximately 30 nights per semester. ANDICAM is available for community use for observing programs via the NOAO TAC process. In the past few years, more than 100 papers have been published in refereed journals using data from these instruments. DANDICAM has been heavily subscribed by astronomers at SAAO, and together with the ANDICAM produced much of the southern-hemisphere data for the PLANET microlensing consortium during the 1998, 1999, and 2000 Galactic Bulge seasons.

In addition to these major instruments, we have produced and deployed the following minor instruments:

1. 2K×2K CCD Cameras for Michigan State
2. 2K×4K CCD for the Wise Observatory (Israel)
3. 512×512 CCD Camera for Perth Observatory (Australia).

4. 2K×2K CCD Camera for Lowell Observatory.
5. 512×512 CCD Camera for the Crimean Astrophysical Observatory.

Our instrumentation group consists of a core of professional personnel all in full-time salaried positions. This has allowed us to maintain a stable instrumentation group over the last decade, and so our instruments reflect a general evolution rather than new projects that start from scratch each time. This will be critical to enabling us to build an instrument as large and complex as MODS because we can fall back upon a 10-year heritage of working solutions and experience.

The instrumentation team is closely integrated with the Department of Astronomy, rather than existing as an autonomous "group" separate from the scientific faculty and students. The MODS effort grew out of an effort to pool all of our resources, from engineers to cosmology theorists, to define the scientific and technical cases for MODS. The success of this integrated approach is shown in the scientific output of the facility instruments we have deployed over the last decade: every one of our instruments was built combining sound engineering principles with well-defined scientific goals. While this PDR document is primarily concerned with the technical aspects of MODS (optics, mechanism, etc.), the next section gives the scientific drivers behind the project from which we have derived the basic specifications for MODS.

1.3 A Scientific Research Program that defines MODS

Recent increases in the aperture and image quality of ground-based optical telescopes and the sensitivity of their instruments have greatly enhanced their power as cosmic time machines, capable of studying the populations of objects present when the universe was a small fraction of its current age. Unraveling cosmic history by studying the properties of faint, highly redshifted sources and the absorption by intervening material is one of the most compelling challenges for observational astronomy in the next decade. The OSU astronomy department will have a 1/6 share of observing time on the Large Binocular Telescope (LBT). During the first five years of LBT operation, the department plans to devote a substantial fraction (more than 50%) of its observing time to spectroscopic surveys aimed at understanding the formation and evolution of galaxies and active galactic nuclei and the evolution of large scale structure. Furthermore, since the spectrograph will serve as the LBT facility optical spectrograph, the instrument should see extensive service with the other LBT partners for a wide variety of research programs.

There are numerous open questions that our observations will address. What is the cosmic history of star formation and chemical enrichment? What physical processes determine this history? When did galaxies of different luminosities and morphologies assemble most of their mass into coherent units? What is the relation between galaxies observed at high redshift and galaxies in the universe today? What are the relations between the populations of high-z quasars, low-z AGN, and supermassive black holes in local galaxies? What is the typical lifetime of luminous quasars? What mechanisms trigger quasar activity, and what physics drives the turn-on and turn-off of the quasar population? What are the relations between the diverse populations of objects by which we trace the evolution of structure in the universe: galaxies, quasars, damped Lyα

systems, Lyman limit systems, and low column density Lyα forest absorbers? How does the structure traced by these populations relate to the structure in the underlying distribution of dark matter?

The last few years have seen major observational advances in these areas, including redshift surveys of flux-limited samples that probe the galaxy distribution out to z≈1 (e.g., Lilly et al. 1995, Lin et al. 1999), HST studies of the morphological evolution of galaxies over this redshift range (e.g., Abraham et al. 1996), and "demographic" studies of the population of supermassive black holes in nearby galaxies (e.g., Magorrian et al. 1998, van der Marel 1999). Most dramatic has been the discovery of a large population of "normal" star-forming galaxies at z>3, through a combination of multi-color selection of "Lyman-break" candidates and spectroscopic confirmation with the LRIS spectrograph on Keck (e.g., Steidel et al. 1996, Lowenthal et al. 1997). More recently, this population has also been probed with Lyα emission-line surveys (e.g., Hu et al. 1998), and discoveries of distant galaxies and quasars are now reaching to z=5 and beyond (Weymann et al. 1998, Spinrad et al. 1998, Chen et al. 1999, and Fan et al. 1999). These developments have made possible the first serious attempts at one of the major objectives of observational cosmology: a determination of the global history of star formation in the universe (e.g., Madau et al. 1996, Madau 1997, and Steidel et al. 1999). However, this determination suffers from many uncertainties, such as the poorly constrained contribution from low-luminosity systems and the possibility, supported by some studies of faint sub-millimeter sources (e.g., Blain et al 1999), that a large fraction of the star formation occurs in regions enshrouded by dust. Even the basic properties of the Lyman-break objects at z≈3 are a matter of debate. Some argue that these UV-luminous objects are massive systems forming stars at a fairly steady rate (e.g., Steidel et al. 1996), and others that they are small systems whose UV emission has been temporarily boosted by sudden bursts of star formation (e.g., Sawicki & Yee 1998, Kolatt et al. 1999). These disparate points of view have radically different implications for the place of Lyman-break systems in the overall story of galaxy formation and evolution.

Alongside the observational breakthroughs have come major advances in the theoretical framework for describing galaxy formation and evolution, with increasing sophistication of semi-analytic models (e.g., Kauffmann et al. 1993; Cole et al. 1994; Somerville & Primack 1999) and hydrodynamic numerical simulations (e.g., Navarro & Steinmetz 1997; Weinberg et al. 1997 and references therein). In contrast to the traditional picture in which galaxies maintain their identity and evolve largely in isolation, theoretical studies of hierarchical galaxy formation suggest that mergers and radical morphological transformations are a common feature of galaxy evolution, and that many of a galaxy's stars form in sub-units that only later assemble into the galaxy itself. Recent analytic models have begun to explore the connection between the formation of galaxies and the onset and eventual decline of quasar activity (e.g., Haehnelt et al. 1998). Perhaps the most revolutionary theoretical transformation has been the new understanding of the low column density Lyα forest that has emerged from hydrodynamic cosmological simulations (e.g., Cen et al. 1994; Zhang et al. 1995, Hernquist et al. 1996, Miralda-Escudé et al. 1996) and related analytic models (e.g., Bi & Davidsen 1997, Hui et al. 1997). These investigations imply that there is a tight and physically straightforward correlation between observable Lyα optical depth and underlying dark matter density.

They also imply that the statistical properties of absorption in Lyα forest spectra with resolution R≈2000-8000 can provide powerful constraints on cosmological models and on the structure of the dark matter distribution (see, e.g., Croft et al. 1999, Nusser & Haehnelt 1999, Weinberg et al. 1999a).

We plan to pursue three linked observing programs that would lead to major advances in the understanding of cosmic structure formation and the evolution of the galaxy and quasar populations:

1. A spectroscopic survey of galaxies with z<1
2. A spectroscopic survey of galaxies and quasars with 1<z<7
3. A multiple-tracer study of structure evolution focused on the redshift range z≈1.7–4

The last of these programs is the most observationally challenging and the most novel, and we believe that it will ultimately prove the most revealing. It is predicated on the idea that the clustering of a population of objects can reveal a great deal about the physics of their formation. This notion has already gained currency in the study of Lyman-break galaxy clustering (see, e.g., Adelberger et al. 1998, Katz et al. 1999), but we believe that it has much broader applicability, and that it becomes especially powerful when one considers cross-correlations between different tracer populations as well as clustering of the populations on their own. We further expect that the instrument will have a long lifetime as the facility optical spectrograph on the LBT and, hence, needs to satisfy the future needs of the department and meet the science goals of our LBT partners.

These observational programs then define the required capabilities for the LBT optical spectrometer:

- High throughput, to take full advantage of the LBT's aperture for studies of faint objects.
- A multi-slit mode is required for efficient operation of most aspects of these programs.
- Long-slit capability, for the fluorescent Lyα emission searches and detailed kinematic studies of selected objects from program (1).
- Wavelength coverage to the atmospheric cutoff at 320nm, to obtain maximum overlap of observable spectral features over the redshift range of program (1) and, more importantly, to allow detection of Lyα absorption and emission features down to z=1.65 for programs (2) and (3). Because the background targets for absorption studies become fainter at higher redshifts, we will probably get our most detailed measurements of structure at the lowest redshifts where we can observe Lyα, and the observing time required for fluorescent emission detection rises steeply with increasing redshift (Gould & Weinberg 1996).
- Wavelength coverage to the CCD sensitivity cutoff at 1000nm, to allow Lyα detection to z≈7 for program (2) and to maximize the accessibility of spectral diagnostics for programs (1) and (2), in particular allowing the detection of spectral features near 400nm rest wavelength out to z=1.5.

- Resolution R≈2000 for identifications and redshifts of faint objects, moderate resolution studies of the Lyα forest, and detection of high column density absorption systems against faint background targets.
- Resolution R≈8000 for chemical and kinematic studies of galaxies in program (1), higher resolution maps of the Lyα forest against the brighter background targets in program (3), measurements of neutral hydrogen column densities of DLA systems, and fluorescent Lyα emission searches matched to the expected width of typical features.
- Flexibility to upgrade in the future to make use of on-going technological innovations.

With these scientific requirements in mind, we have developed the basic specifications of the MODS spectrograph described in the next section. An LBT-appointed working group reviewed and endorsed these goals for the instrument in 1999 (see Appendix for the documentation from this review).

1.4 MODS General Description

MODS will work at the straight *f*/15 Gregorian focus of each of the 8.4-m LBT primary mirrors. Our scientific interests (as described above) dictate that MODS offer moderate spectral resolutions (10^3–10^4), wide wavelength coverage (320–1000nm), and the ability to observe extremely faint objects (≥25 mag). These objectives require that the instrument have excellent throughput from the atmospheric cut-off in the ultraviolet to the practical sensitivity limit of CCDs in the far red. No single reflective or antireflective coating will work optimally over this wavelength range without sacrificing one extreme or the other. This has led us to adopt a double spectrograph design (like the Palomar DBSP; Oke & Gunn 1982) with separate blue- and red-optimized channels to maximize the throughput. We plan to use detectors that are of sufficiently large format (~8000 pixels) to simultaneously obtain spectra at moderate resolution of the entire wavelength span of the channel. This again will ensure optimal observing efficiency and effectiveness by minimizing the required number of grating tilt settings to obtain spectra over a broad wavelength range.

To further improve the effective throughput, a multi-object capability over a field large enough to include many typical objects is also required. There is sufficient density of objects within an ~4′ field of view to give considerable multiplex advantage with a multislit system. At the urging of the LBT-appointed conceptual review committee, we expanded the field of MODS to 6′, although with reduced image quality.

The seeing expected at the LBT is ~0.6″ (similar to that currently obtained at the MMT, WIYN, and KPNO). We have designed MODS around the assumption that slit widths of ~0.6″ will be typical. Slit widths should also allow for the best-anticipated conditions (i.e. ~0.3″; active/adaptive optics are planned, and the LBT image error budget is 0.34″) and for worse-than-average conditions (i.e. ~1.2″).

Finally, given the unique configuration of the LBT, the most effective use of the full LBT collecting area is to employ two independent spectrographs, providing costs can kept

reasonable and CCDs capable of very low readout noise can be obtained. Our ultimate goal, therefore, is two build two copies of MODS for LBT.

MODS will have three baseline observing modes: *long-slit*, *multi-slit*, and *imaging*:

Long-slit mode, in which a slit mask provides continuous spatial coverage across one axis of the MODS field-of-view. Long slits are useful for point sources, especially faint objects where sky subtraction is critical, and for spatially extended objects with a definite axis of symmetry. A 0.6″slit is matched to four pixels of the detector (assuming an anamorphic factor of 1.2), but a wider slit can be used with no noise penalty by binning the detector.

Multi-slit mode, in which an aperture mask is used to define a series of precisely located "slitlets" centered on objects falling within the MODS field of view. At a penalty of slightly reduced spectral coverage near the ends of the field along the dispersion axis of the system, spectra can be obtained of objects distributed in 2 dimensions, effectively multiplying the throughput of the spectrograph by the number of slitlets used. For example, we could easily accommodate 48 slitlets 5″ long across a 4′ field. Consideration of adequate sky subtraction suggests that for the faintest objects, 10″-long slits (for ~24 slitlets) would be optimal. Multislit modes are features of all major spectrographs being designed for use by the current and coming generation of large telescopes (e.g., GMOS, DEIMOS, and FORS). For flexibility and simplicity of operation, the best option appears to be custom aperture plates machined on-site.

Direct-Imaging mode, in which the spectrograph is used without a slit mask and the grating is replaced by a flat mirror. In addition to applications requiring direct imaging *per se*, MODS ability to quickly switch between direct imaging and slit spectroscopic modes provides a foolproof method of precise target acquisition and placement on the slits or multislits. Furthermore, the faintest objects observed with the LBT will be much fainter than the night sky brightness, and direct imaging will be essential for target acquisition.

1.5 MODS Specification Goals and Requirements

Table 1 lists some of the important performance requirements for MODS. These arise primarily from consideration of the science projects we envision for the instrument. The throughput goal is set so that MODS can reach limiting magnitudes sufficiently faint to enable much of the science discussed above. The image quality specification ensures that if the telescope delivers good images (~0.6″ FWHM), then these images will not be substantially degraded by the instrument optics. The image quality over the larger extended field again should ensure that little light is lost to slit effects even in the outer part of the field in multi-slit operational modes. The image/spectral stability specification is set largely by our experience with other spectrographs. The detector format is large enough that the entire wavelength region spanned by a channel of the instrument will be observed with a single grating setting at resolution ($\lambda/\Delta\lambda$) ~2000. The detector read noise is specified so that the signal-to-noise ratio of digitally combined observations are <20% worse than single 11.8m telescope measurements, assuming typical observing conditions of resolutions $<10^4$, slits > 0.3″ wide, and dark sky conditions.

There are also goals for the instrument that we will attempt to meet. These are extensions of the requirements driven by the science objectives that will typically enhance the performance of the instrument significantly. For example, CCD read noises of <2 electrons will ensure that digital combination of spectra will be <5% worse than data taken with a single 11.8m telescope.

Table 1.1: Performance Goals for MODS

Specification	Requirement	Goal
High throughput from atmospheric cut-off to CCD red limit	>50% 350-900 nm (exclusive of grating efficiency, telescope, and atmosphere)	>80% 320-1000 nm (exclusive of grating efficiency, telescope, and atmosphere)
Excellent image quality over a 4′×4′ field of view	<0.5″ 80% encircled energy diameter center-to-edge	<0.3″ 80% encircled energy diameter center-to-edge
Adequate image quality over a 6′×6′ field of view	<1″ 80% encircled energy center-to-edge	<0.5″ 80% encircled energy center-to-edge
Excellent image/spectral stability	<0.5 pixel (7.5 μm) image motion during 1 hour integration	<0.1 pixel (1.5 μm) image motion during 1 hour integration
Detector format	2K×4K in each channel	>2K×8K in each channel
Detector read noise	<5 electrons	<2 electrons

1.6 MODS Deployment Plan

The ultimate aim of MODS is to take spectra of the faintest objects known. To accomplish this, our approach is to build two spectrographs, one for each of the two LBT primary mirrors, and combine measurements digitally after the observations using standard data reduction processes. Functionally, this is equivalent to taking two consecutive observations to build signal-to-noise ratio on a faint object, but the observations are obtained simultaneously. Such digital beam combination is practical since modern CCDs can deliver very low read noise, so co-addition of two data sets incurs little additional noise penalty. Furthermore, if the two spectrographs are identical, there are significant cost savings due to non-recurring design and engineering expenses. We believe that this approach is the most efficient and practical way of using the LBT as an 11.8m telescope at optical wavelengths for spectroscopy.

The two LBT primary mirrors will not be deployed simultaneously. The current schedule for the telescope suggests that first light with the initial primary mirror will be in late-2003. First light with both mirrors in place is scheduled for early-2005.

Our plan is to deploy MODS in a staged fashion. We will first take a version of MODS with a restricted feature set (one functional channel, a single grating, and a limited set of

slits) to the LBT in early-2004. This simplified version of the instrument will be fully capable of interesting and exciting science projects and will allow us to thoroughly field test the basic instrument package (interfaces, communications, etc.). While this is happening, we will be assembling a full two-channel version of MODS in Columbus. This full version will be built around the support structure, large optics, etc. that we will acquire as part of our longer term plan to complete two full two-channel instruments. We expect to deploy the first full two-channel MODS in mid-2005.

Once the deployment of the first full version of MODS is complete, we will upgrade the original (reduced capability set) version to its fully featured configuration. Plans and schedule for this upgrade are not fully developed, since we have not yet identified sources needed to fund the purchases required to fully outfit the second full MODS. Our goal, however, is to complete this second MODS by early-2006.

1.7 Scope of this Design Review Document

The main purpose of this review is to check the mapping of our design for MODS to our scientific objectives for the instrument. In part, this document serves as a status report on our progress to date on the design and construction of MODS. The sections that follow briefly describe the decisions we have made and designs we have developed for MODS. Inevitably, some details and information will be incomplete or missing. We look forward to the review committee's comments on the design and seek the committee's input on techniques and approaches that will improve the performance of the instrument or save time and costs.

References:

Abraham, R. G., Tanvir, N. R., Santiago, B. X., Ellis, R. G., Glazebrook, K., & Van Den Bergh, S. 1996, MNRAS, 279, L47

Adelberger, K. L., Steidel, C. C., Giavalisco, M., Dickinson, M., Pettini, M., & Kellogg, M. 1998, ApJ, 505, 18

Allington-Smith, J., Content, R., Haynes, R., & Lewis, I. 1996, SPIE preprint.

Bacon, R., et al. 1995, A&AS, 113, 347.

Bacon, R., 1995, in *3D Optical Spectroscopic Methods in Astronomy,* G. Comte, M. Marcelin, eds., ASP Conf. Ser. 71, 239

Barden, S., Arns, J., & Colburn, J. 1999, Proc SPIE 3749, 52 (see also http://www.noao.edu/ets/vpgratings)

Bi, H.G., & Davidsen, A. 1997, ApJ , 479, 523

Blain, A. W., Smail, I., Ivison, R. J., & Kneib, J.-P. 1999, MNRAS, 302, 632

Bunker, A. J., Marleau, F. R., & Graham, J. R. 1998, AJ, 116, 2086

Cen, R., Miralda-Escudé, J., Ostriker, J.P., & Rauch, M. 1994, ApJ, 437, L9

Chen, H.-W., Lanzetta, K. M., & Pascarelle, S. 1999, Nature, 398, 586

Cole, S., Aragon-Salamanca, A., Frenk, C. S., Navarro, J. F., & Zepf, S. E. 1994, MNRAS, 271, 781

Croft, R. A. C., Weinberg, D. H., Pettini, M., Katz, N., & Hernquist, L. 1999, ApJ, 520, 1

Dobrzycki, A., & Bechtold, J. 1991, ApJ, 377, L69

Fan, X., et al. 1999, AJ, 118, 1

Gallego, J., Zamorano, J., Aragon-Salamanca, A., & Rego, M. 1995, ApJ, 455, L1

Gould, A., & Weinberg, D. H. 1996, ApJ, 468, 462

Haehnelt, M. G., Natarajan, P., & Rees, M. J. 1998, MNRAS, 300, 817

Hernquist L., Katz, N., Weinberg, D. H., & Miralda-Escudé, J. 1996, ApJ, 457, L5

Hogan, C. J. & Weymann, R. J. 1987, MNRAS, 225, L1
Hu, E. M., Cowie, L. L., & McMahon, R. G. 1998, ApJ, 502, L99
Hui, L., Gnedin, N., & Zhang, Y. 1997, ApJ, 486, 599
Jannuzi, B T. & Dey, A. 1999 in *Photometric Redshifts and High Redshift Galaxies*, eds. R. Weymann, L. Storrie-Lombard, M. Sawicki, & R. Brunner, ASP Conference Series, San Francisco, in press
Kaiser, N. 1984, ApJ, 294, L9
Katz, N., Hernquist, L., & Weinberg, D. H. 1999, ApJ, in press, astro-ph/9806257
Kauffmann, G., White, S. D. M., & Guideroni, B. 1993, MNRAS, 264, 201
Kolatt, T. S., et al. 1999, ApJ, submitted, astro-ph/9906104
Lilly, S. J., LeFevre, O., Crampton, D. Hammer, F., & Tresse, L. 1995, ApJ, 455, 50
Lilly, S. J., LeFevre, O., Hammer, F., & Crampton, D. 1996, ApJ, 460, L1
Lin, H., Yee, H. K. C., Carlberg, R. G., Morris, S. L., Sawicki, M., Patton, D. R., Wirth, G., Shepherd, C. W. 1999, ApJ, 518, 533
Lowenthal, J. D., Koo, D. C., Guzman, R., Gallego, J., Phillips, A. C., Faber, S. M., Vogt, N. P., Illingworth, G. D., & Gronwall, C. 1997, ApJ, 481, 673
Madau, P. 1997, in *The Hubble Deep Field*, eds. M. Livio, S. M. Fall, & P. Madau (Cambridge: Cambridge University Press)
Madau, P., Ferguson, H. C., Dickinson, M. E., Giavalisco, M., Steidel, C. C., & Fruchter, A. 1996, MNRAS, 283, 1388
Miralda-Escudé J., Cen R., Ostriker, J.P., & Rauch, M. 1996, ApJ, 471, 582
Magorrian, J., et al. 1998, AJ, 115, 2285
Navarro, J. F., & Steinmetz, M. 1997, ApJ, 478, 13
Nusser, A., & Haehnelt, M. 1998, MNRAS, 303, 179
Osmer, P.S. 1998, in *The Young Universe*, ASP Conf. Ser. 146, 1, eds. S. D'Odorico, A, Fontana, & E. Giallongo.
Sawicki, M., & Yee, H. K. C. 1998, AJ, 115, 1329
Somerville, R. S., & Primack, J. R. 1999, MNRAS, in press, astro-ph/9802268
Spinrad, H., Stern, D., Bunker, A., Dey, A., Lanzetta, K., Yahil, A., Pascarelle, S., & Fernandez-Soto, A. 1998, AJ, 116, 2617
Steidel, C., Adelberger, K., Giavalisco, M., Dickinson, M., & Pettini, M. 1999, ApJ, 519, 1
Steidel, C. C., Giavalisco, M., Pettini, M., Dickinson, M., & Adelberger, K. L. 1996, ApJ, 462, L17
Turnshek, D. A., Wolfe, A. M., Lanzetta, K. M., Briggs, F. H., Cohen, R. D., Foltz, C. B., Smith, H. E., Wilkes, B. J. 1989, ApJ, 344, 567
van der Marel, R. P. 1999, AJ, 117, 744
Weinberg, D. H., et al. 1999a, in *Evolution of Large Scale Structure: From Recombination to Garching*, eds. A.J. Banday et al., (Twin Press: Vledder NL), astro-ph/9810142
Weinberg, D. H., Davé, R., Gardner, J. P., Hernquist, L., & Katz, N. 1999b, in *Photometric Redshifts and High Redshift Galaxies*, eds. R. Weymann, L. Storrie-Lombard, M. Sawicki, & R. Brunner, ASP Conference Series, San Francisco, in press
Weinberg, D. H., Katz, N., & Hernquist, L. 1998, in *Origins*, C. E. Woodward, J. M. Shull, & H. Thronson, eds., ASP Conf. Ser. 121, astro-ph/9708213
Weymann, R. J., Stern, D., Bunker, A., Spinrad, H., Chaffee, F. H., Thompson, R. I., & Storrie-Lombardi, L. J. 1998, ApJ, 505, L95
Vanderreist, C. 1995, in *3D Optical Spectroscopic Methods in Astronomy*, G. Comte, M. Marcelin, eds., ASP Conf. Ser. 71, 209.
Zhang, Y., Anninos, P., & Norman, M. L. 1995, ApJ, 453, L57

2 Optics

This section describes the optical design of the MODS spectrograph.

2.1 Design Constraints

The basic design constraints for the MODS optical design are high throughput over a wavelength range of 320 nm to1000 nm, moderate spectroscopic resolution ($\lambda/\Delta\lambda \sim 10^3$-$10^4$) with a 0.6″ wide slit, and imaging performance over a 4′×4′ field without serious compromise of telescope delivered image quality (expected to be ≤0.6″). An LBT-appointed working group conducted a conceptual design review of the instrument and made several recommendations that were adopted as part of the design (see Appendices). In particular, the available field of the instrument was increased to 6′×6′, although with reduced image quality outside of the inner 4′×4′. Note that a preliminary description of the MODS optical design appears in Byard & O'Brien (2000, SPIE Proceedings, Vol. 4008, pp 40-49).

The optical design is further constrained by the location of the spectrograph at the Gregorian focus of the LBT and a relatively slow *f*/15 final focal ratio. The Gregorian instrument volume is the only space large enough for the spectrograph and the focal ratio is dictated by the only secondary available on the telescope at first light.

2.2 Design Approach

After considering a number of options for MODS, we elected to pursue a double-spectrograph design with reflective collimators, de-centered Maksutov-Schmidt cameras, and gratings as primary dispersers. For example, we investigated the possibility of using a doublet spherical corrector instead of the aspheric singlet, but found the performance was worse and the cost higher. Furthermore, our adopted approach will maximize the throughput in the blue and red regions of the spectrum for several reasons:

- The number of surfaces is a minimum for reflective designs.
- The effectiveness of anti-reflection and reflective coatings can be individually optimized for separate red and blue channels.
- The double design allows the use of different optical materials and optimization in each wavelength range.
- Grating spectra cover a spectral range of only one octave without the confusion of overlapping orders, and grating blaze functions are too narrow to provide high throughput over a wavelength range from 320 nm – 1000 nm.
    - Separate red and blue channels permit greater wavelength coverage in a single exposure, when appropriate.

The design also includes other elements necessary for science operations: an atmospheric dispersion corrector, field lens for control of pupil placement, provision for additional dispersing elements (cross-dispersion, low resolution prisms, etc.), and filters. The entire design was developed using the *CodeV* optical design software package from Optical Research Associates. An independent consultant verified the entire design using a

different software package; B. Gregory (CTIO) used *OSLO* to check the design and confirm our analysis and performance results.

2.3 Design Description

This section describes the optical components in the current MODS design. Refer to Figure 2.1 for the locations of these components; the general sequence is as light enters MODS to the detector. Note that complete specifications and prescriptions for the optical elements are given in the Appendix A.

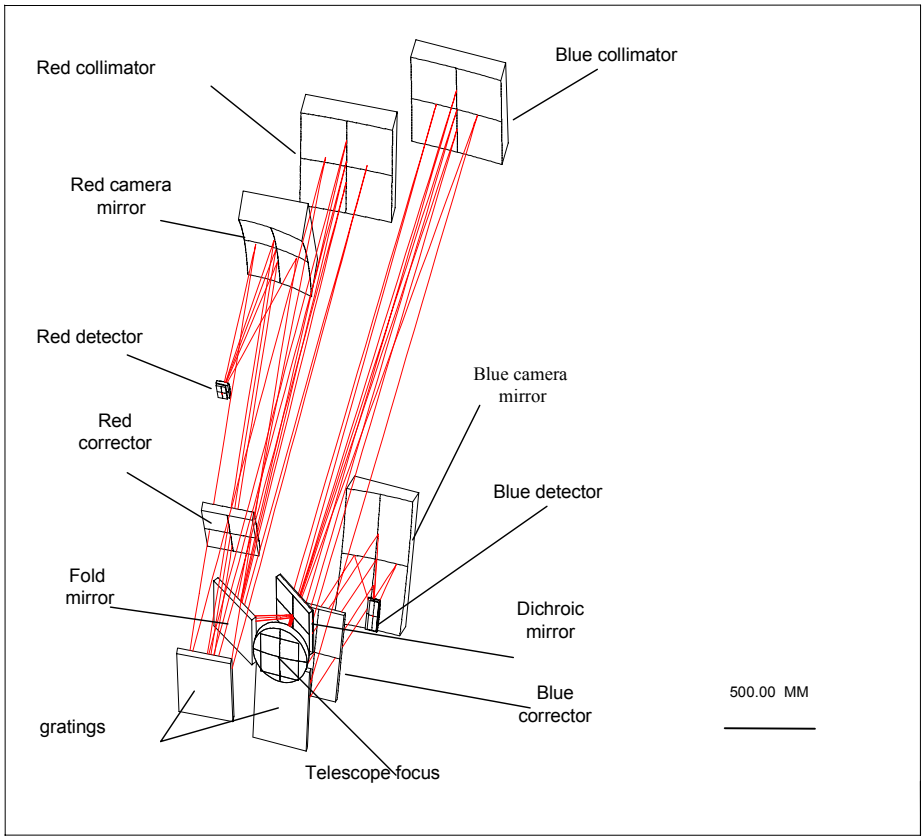

Figure 2.1: Optical layout for MODS.

2.3.1 Atmospheric dispersion compensator

Dispersion by the atmosphere affects the image quality and apparent location of the target when observing away from the zenith. An ADC capable of covering up to the central 4×4-arcminute FOV can be accommodated by the current design without difficulty. This FOV is for an ADC located ~900mm ahead of the MODS focal plane and ~200mm in diameter. Currently an ADC is *not* part of the baseline instrument plan and is considered a potential upgrade.

Given the image quality in the extended 6-arcmin FOV, it is clear that an ADC makes most sense in the inner 2-arcmin region where we get the best (0.3") image quality, and

arguably might be useful for the 4-arcmin main FOV. We have adopted the 4-arcminute FOV limitation as trying to provide an ADC for the full 6-arcmin FOV would be prohibitively expensive and difficult to package. Note that the decision to not deploy an ADC with the baseline instrument is similar to that made by nearly every other optical spectrometer for 8-10m class telescopes (e.g., DEIMOS, ESI, and VIMOS).

2.3.2 Telescope focal surface

The focal surface of the Gregorian LBT is convex toward the secondary mirror. The radius of curvature of this surface is approximately 1 meter. The slit, or multi-object slitlet array, will be placed on this surface. This ensures the best match of slit sizes to telescope image quality with the greatest exclusion of background sky emission. The 6′×6′ imaging field of the instrument is defined by a field stop at this surface.

2.3.3 Field Lens

A fused silica meniscus field lens is placed after the focal surface. This lens, in combination with the collimator mirror, positions the exit pupil of the telescope on the spectrograph grating at a convenient location in the instrument volume.

2.3.4 Dichroic

A dichroic beamsplitter reflects red light to the red channel of the spectrograph via an additional fold mirror. Light transmitted through the dichroic illuminates the blue channel. The dichroic can be removed to illuminate the blue channel only or replaced with a mirror to illuminate the red channel only. Light loss in either channel due to the dichroic will be less than 5%. The dichroic will have a transition from reflecting to transmitting over 50 nm band centered at approximately 550 nm allowing overlap between red and blue spectra to simultaneously calibrate both channels. The flat substrate of the dichroic introduces astigmatism into the blue channel. A weak cylindrical surface on the rear surface of the substrate can reduce the astigmatism to an insignificant value.

2.3.5 Collimators

Two decentered paraboloidal mirrors 3.45-m from the *f*/15 Gregorian focal plane collimate the two beams. The mirrors are identical except for their reflective coatings. Each mirror produces 230-mm diameter collimated beams that converge to pupil images at the red and blue gratings.

The angle between the collimator axis and the camera axis is 30 degrees. As this angle increases the anamorphic magnification of the grating increases. As the angle is reduced, the camera moves away from the grating. Both effects increase the dispersed beam size at the camera. The minimum camera aperture occurs close to a 30-degree value.

2.3.6 Gratings

Three gratings and a mirror are available in each channel. Rotating selectors allow quick changes from imaging to spectroscopy at a choice of three different resolutions. More detail about possible grating selections is available in section 2.6.

2.3.7 Cross-dispersion

Observations over the full spectral range at high spectral resolution can use gratings in a high order and filters or an order separating grism just in front of the red camera. The grism will be a replica of approximately 170 lines/mm attached to an index matched glass substrate with an 80 mm base and will disperse the 600 nm to 1000 nm wavelength range perpendicular to the primary dispersion direction. There are no plans to provide cross-dispersion in the blue channel of the instrument.

2.3.8 Cameras

Nearly identical 700 mm focal length cameras derived from a Maksutov-Schmidt design are used in both channels giving 0.15" per 15-micron pixel in imaging mode and mapping a 0.6" slit onto four pixels when accounting for an anamorphic magnification of 1.2. Figure 2.2 shows a schematic layout of the cameras. The design incorporates an off-axis, Schmidt-like, aspherical, transmissive corrector plate, a spherical primary mirror, and a plano-convex, spherical, transmissive field flattener. Note that we currently plan to use the field flattener as the detector dewar window and that filters will be placed just in front of the field flattener (not shown in Figure 2.2). The camera can accommodate a dispersed beam from the grating with an anamorphic factor of 1.2 with no vignetting for a slit height of up to 6′ and a ~125 mm long spectrum (roughly the length of a 8196 15 μm pixel detector).

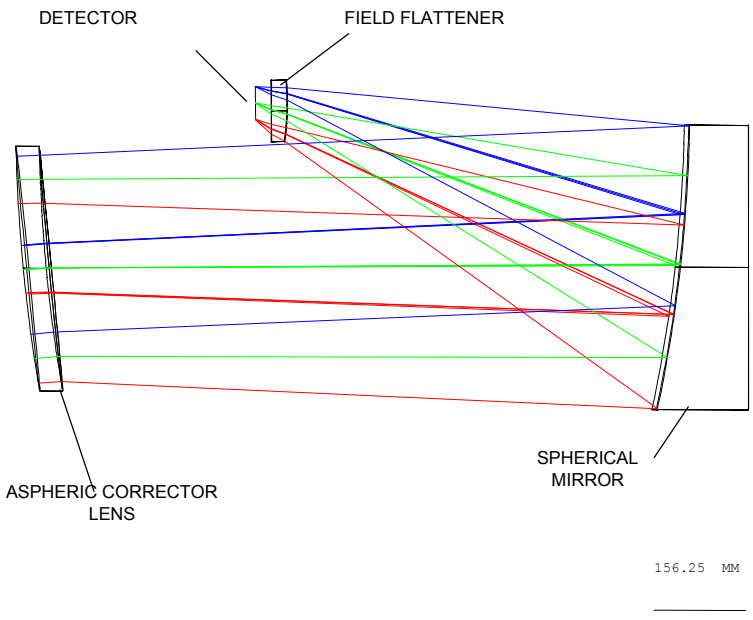

Figure 2.2: Cross-sectional view MODS camera through the center of the parent camera. The axis of the system passes through the center of the field flattener lens parallel to the chief ray

An important feature of these cameras is that the dispersed beams are de-centered with respect to the camera optical axes. The detectors and field flattening lenses are positioned entirely outside the incoming beams to the camera mirrors. This has two important

advantages. First, the obstruction associated with the trapped focus of single mirror reflective cameras is eliminated. Second, any radiation reflected from the detector is not reflected back towards the grating to be reflected or re-dispersed into the camera. This eliminates narcissus reflections, an important source of the undesirable ghost images found in many spectrographs.

2.4 Design Optimization

The components of the MODS optical design were optimized together with the optical design of the LBT telescope. The optimization procedure is briefly described below.

2.4.1 Field lens

A meniscus field lens is placed between the focal surface of the telescope and the dichroic. This lens forms an image of the telescope stop (the LBT secondary mirror) near the blue and red grating surfaces. Without a field lens the collimated beams from a 6-arcminute field would overfill the available gratings and the field would be severely vignetted. Since the lens is near the telescope focus its thickness is kept small in order to reduce the probability of defects such as small bubbles or inclusions in the lens and maximize transmission.

2.4.2 Dichroic

A tilted dichroic mirror separates the red and blue beams. Since the dichroic is a flat in non-collimated light, it introduces astigmatism into the transmitted (blue) beam. This astigmatism is minimal in comparison with the image quality of the instrument for field of 4–6 arcminutes in diameter. The dichroic can be removed and the blue channel used alone for those cases where the highest possible image quality in the blue over a small field is required by particular science projects. Alternatively we could obtain a dichroic with a small cylindrical figure on one side and have no diminution in image quality.

2.4.3 Collimators

The MODS collimators are very simple: a single reflection off a decentered paraboloidal surface. Both collimators are identical and have focal lengths of 3450 mm. The angles between the telescope axis and the collimated beam axes (5.7^{o}) were chosen to allow the collimated beam from each collimator to clear the additional fold mirrors of the red channel as well as the field stop.

The collimators are the primary source of optical aberrations in the MODS optical design. Table 2.1 shows a comparison of the collimator performance with a perfect camera (simulated in *CodeV*) with the expected performance of the collimator including the rest of the MODS optics (see the other parts of this section) for the red channel over the R-band. Note that in the complete design these aberrations are partially compensated for by other system optical elements and expected mechanical deformations. Clearly collimator aberrations dominate the optical performance over the entire field of the instrument. Performance of the blue channel collimator is similar.

Table 2.1: Performance of MODS decentered paraboloidal collimators: Red channel at R-band

Field Radius (')	D_{80} (80% Encircled Energy in arcsec)	
	Collimator + Perfect camera	Complete Design
0.0	0.00	0.17
0.5	0.09	0.18
1.0	0.21	0.23
1.5	0.36	0.37
2.0	0.53	0.54
2.5	0.75	0.76
3.0	0.93	1.01

2.4.4 Cameras

A camera focal length of 700 mm was selected to match a slit width of 0.6″ to four 15 μm CCD pixels at an anamorphic magnification factor of 1.2. The monochromatic *f*/ratio of the camera is roughly *f*/3.0 in the cross dispersion direction and about *f*/2.5 in the dispersion direction (as defined by the 230 mm collimated beam) at an anamorphic factor of 1.2. However, the camera design uses a sub-aperture from an 840 mm diameter parent optic for the corrector plate. Thus, for comparison with many other designs the camera can be thought of as *f*/0.83.

The camera aperture in the dispersion direction is 420 mm to provide unvignetted performance across the whole width of the detector. Detectors up to a length of ~125 mm in the dispersion direction can be accommodated. Thus, an 8196 pixel long detector with

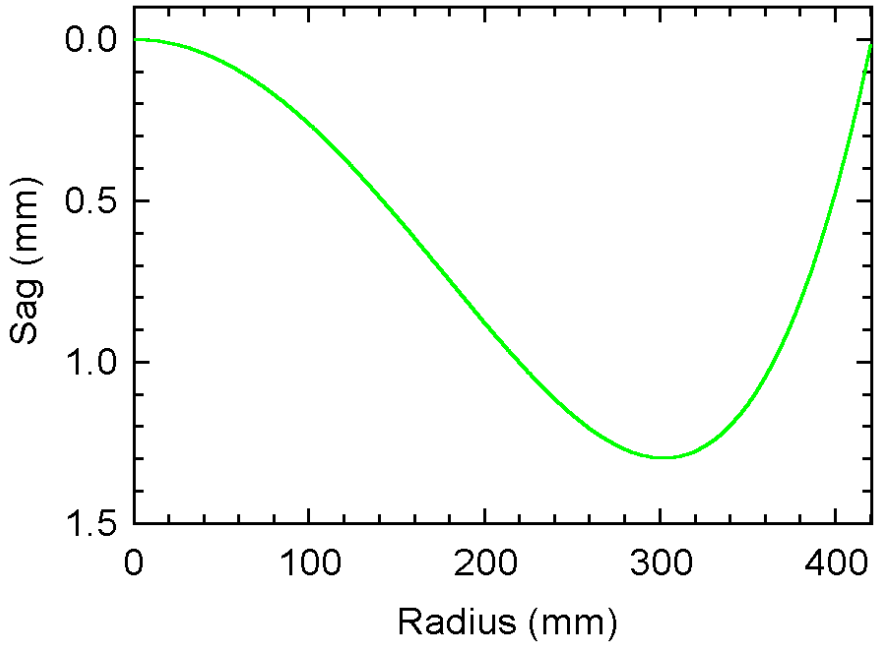

Figure 2.3: Departure from the nearest sphere of the red Camera Corrector lens.

15 μm pixels can be used, which will provide ~2000 4-pixel resolution elements. A spectrum covering a 2:1 ratio in wavelength will have a resolution ($\lambda/\Delta\lambda$) at the center of ~3000. Each camera was optimized with gratings to give wavelength ranges of 300 nm – 600 nm for the blue and 500 nm – 1000 nm for the red. The *CodeV* optimization procedure used five zoom positions for wavelengths distributed over the selected spectral ranges at several field positions and included the effects of the collimator and telescope.

The camera corrector lens material is different for each channel. BK7 is relatively inexpensive and gives superior performance in the red channel. Fused silica has excellent ultraviolet and blue transmission and performs well in the blue channel. We have identified vendors for the blanks required for the correctors and determined methods to reduce the material costs. There is some lateral color in the camera design that arises from dispersion in the corrector lens. This is not important for spectroscopic observations with the instrument (the effect will show up as a term in the spectral wavelength calibration), but does somewhat degrade performance in imaging modes.

All the optical surfaces of the cameras are spherical except one surface of the corrector. This surface is a section of an asphere with departures from the vertex radii of curvatures of several millimeters. Figure 2.3 shows the sag of the aspheric surface of the red corrector as a function of radius; the sag of the blue corrector is nearly identical. The departure from a best fit to the *nearest sphere* for the red corrector is ~720 μm (similar for the blue corrector). Four separate optical vendors have agreed that the surfaces can be accurately produced. The radii of curvatures for the camera mirrors are identical.

2.5 Performance of the Complete Design

In this section we give various image quality performance estimates of the entire MODS optical design. We include the telescope optics (primary and secondary) in the estimates, but do not include the atmosphere. In general, the image quality of the design is adequate to meet the science goals for the instrument. The performance is particularly good on-axis. For example, for the nominal image quality specification for the telescope delivered image quality of 0.3″, MODS will deliver on-axis a monochromatic image with FWHM=0.34″ and 80% encircled energy (D_{80})=0.51″. For a telescope delivered image quality of 0.15″ (as would be available using some AO correction, for example) the on-axis monochromatic images produced by the MODS design have FWHM=0.22″ and D_{80}=0.33″.

2.5.1 Imaging Mode

In Fig. 2.4 we show values of the 80% encircled energy diameters (D_{80}) measured in arc-seconds for the images in the V-band. The curves show D_{80} for five y-axis values of the field, as a function of the positions on the x-axis, for a 4′×4′ square field. Even at a field diameter of nearly 8.5′, in the corners of a 6′×6′ field, the D_{80} is still only 1.20″ after re-focus for the best images. If the focus is optimized for a smaller field, the image quality is substantially better. For example, refocus of the system for a 1′×1′ field results in D_{80} values of <0.3″ for all bands at all positions over that field. Performance is similar in other broadband filters for both the red and blue channels. For more imaging performance plots, see Appendix D.

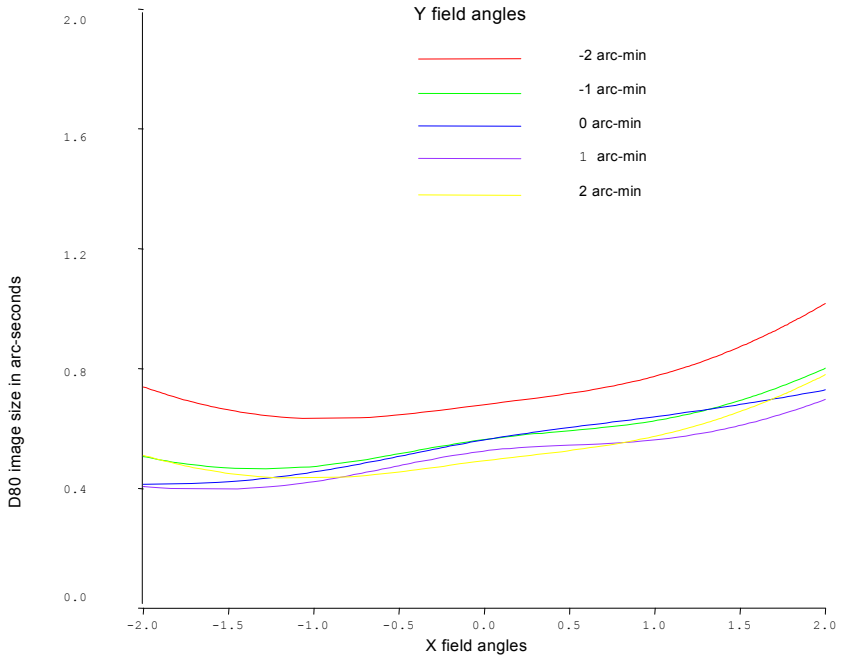

Figure 2.4: Imaging performance of the MODS red camera in a 4'×4' FOV with a V-band filter at the optical full-field focus.

2.5.2 Spectrographic Mode

Fig. 2.5 shows D_{80} measures in microns for a spectrum covering the entire range of the red camera (600nm–1000nm) for monochromatic images at several positions on a long (4′) slit centered on the axis of the telescope.

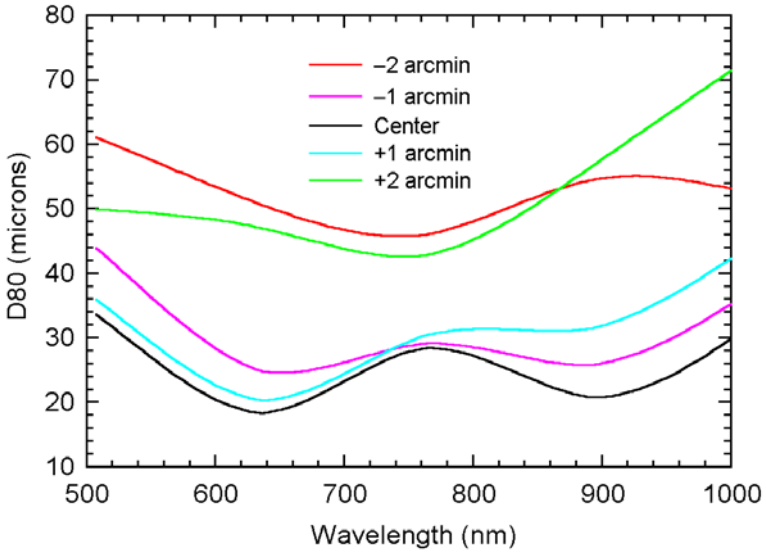

Figure 2.5: Imaging performance as a function of slit position and wavelength for optimal focus.

For a 6-arcminute slit, we need to refocus. The best focus performance for a full 6-arcminute slit is shown in Figure 2.6. For more performance plots, see Appendix D.

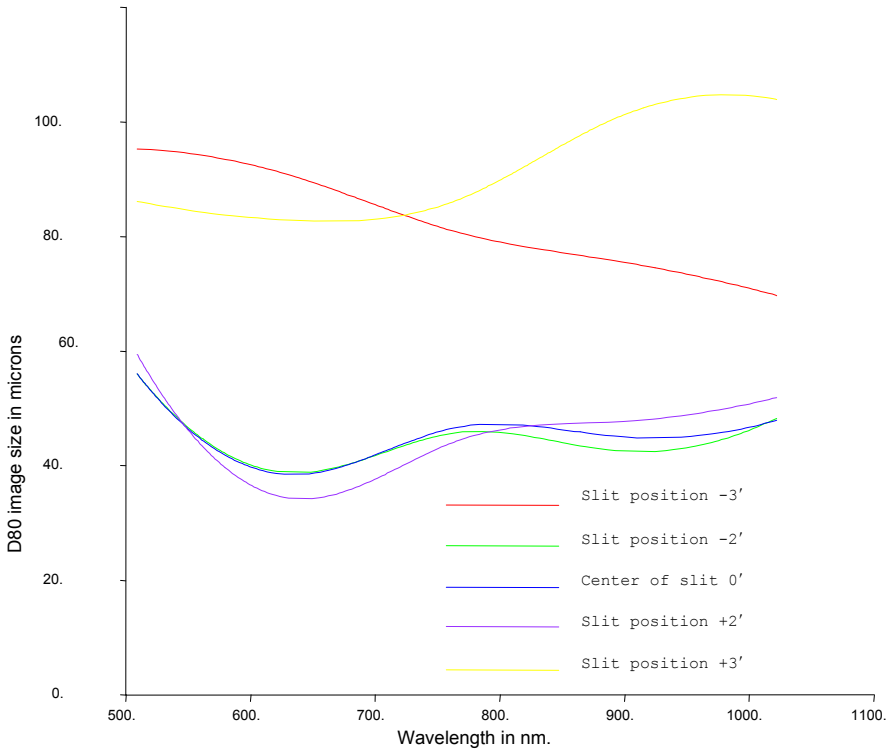

Figure 2.6: Imaging performance as a function of position along the slit and wavelength in spectroscopic mode at the optimal focus for a 6-arcminute slit.

2.6 Performance of Available Gratings

The MODS beam size (230 mm) limits the number of available diffraction gratings. The only gratings from Richardson Grating Laboratory that will accommodate this beam diameter are the Large Astronomical Reflectance Gratings. Although there are 11 gratings listed in this category only 7 of these are large enough to use in MODS without vignetting the collimated beam.

The published efficiency curves versus wavelength are typically for gratings used in near Littrow conditions. However, MODS uses gratings at an angle of 30° between incident and diffracted beams. Therefore, we have calculated the efficiency curves for suitable gratings used in this non-Littrow mode using *GSOLVER*. This program calculates the efficiency of gratings in arbitrary configurations and is available from Grating Solver Development Company (Allen, TX). The predicted efficiencies for the 5 most suitable gratings are shown in Figures 2.7-2.14. The wavelength ranges, center wavelength for the geometrical blaze, center resolution and other data in order of decreasing groove spacing are summarized in Table 2.2.

Some of these gratings will work fine for MODS, but others are clearly unacceptable. In particular, RGL #75-45-273 would make an acceptable red low-dispersion grating, and

RGL #73-45-584 an acceptable blue low-dispersion grating. The peak diffraction efficiencies for these gratings is >80% and they perform well over nearly the entire wavelength range of each respective channel. An interesting grating is RGL #73-45-571, which would give MODS a reasonably high resolution capability in the red, although at a cost of relatively low throughput.

We anticipate that MODS will eventually require additional rulings. We plan to design these using *GSOLVER* and then get someone else to pay for them.

Table 2.2: Properties of Available Thermo RGL Large Astronomical Gratings

RGL Number	Groove Per mm	Blaze Angle	Order	Center λ nm.	λ range nm.	A factor	Slit width ″/4 pixels	pixels per/0.6″	R@center 4 pixels	R@center 0.6″
75-45-271	250	5	1	673	341 –1010	1.048	0.52″	4.58	1990	1727
75-45-273	270	4.13	1	515	Atmos – 827	1.039	0.52″	4.6	1800	1417
73-49-505	316	11	1	1166	900 –CCD limit	1.11	0.55″	4.32	4304	3959
73-49-505	316	11	2	583	450 – 718	1.11	0.55″	4.32	4304	3959
73-45-584	400	4.76	1	401	Atmos – 611	1.045	0.52″	4.58	2100	1636
73-45-561	632	22.3	1	1160	1025 – CCD lim.	1.25	0.63″	3.8	8610	8917
73-45-561	632	22.3	2	580	513 – 646	1.25	0.63″	3.8	8610	8917
73-45-571*	632	57	5	513	491 – 513	2.40*	1.22″	1.96	25,555	51,370
73-45-109**	1000	13	1	435	350 – 520	1.13	0.56″	4.22	5053	4752

* Because of the high angles of incidence and diffraction on this grating the collimated beam overfills the grating. There is also considerable groove shadowing that flattens and broadens the blaze function. The net result is to reduce both the effective aperture of the telescope and the blaze efficiency. The estimated total throughput of the grating is ~16%.

** Because this grating is so close to the collimated beam size the field will be very slightly vignetted with the vignetting being a function of field angle in the multi-slit mode.

The diffraction efficiency for the above gratings has been calculated using the *GSOLVER* program. The program calculates the diffraction efficiency for polarizations parallel and perpendicular to the rulings. The results are plotted for the average of these values. The accuracy of the results depends on a number of factors and should only be regarded as approximate. However it does give an indication of the useful wavelength ranges of the gratings and the resolutions available.

Calculated blaze efficiency of gratings in non-Littrow mode

Richardson Grating Lab Catalog Number 73-45-271

Aluminum index values used from gsolver Table values

Angle between collimator and camera axes is 30 degrees

Angle of incidence 20 degrees

Marker shows blue limit for this wavelength.red limit is at 1.01 microns

The efficiency is plotted for unpolarised light and is the average value of the P-plane and S-plane responses.

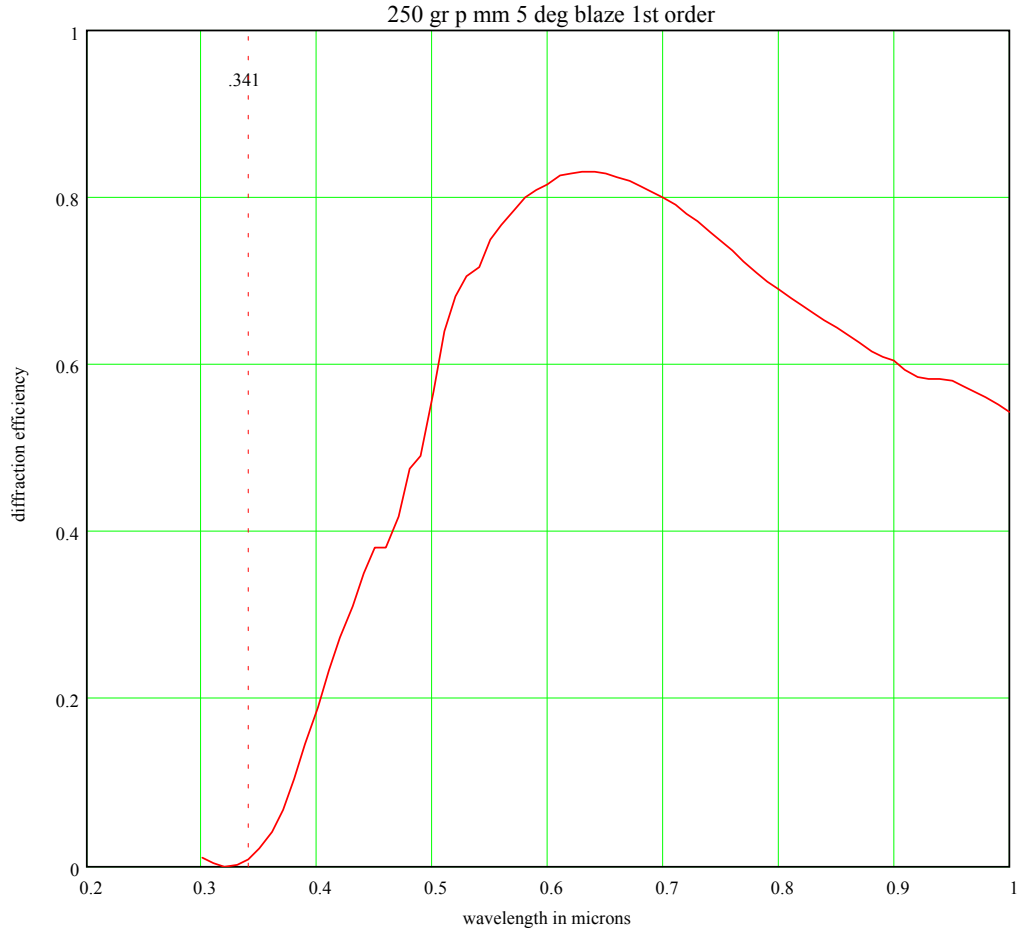

Figure 2.7: Resolving power R = λ/dλ at center of spectrum 1727

Calculated blaze efficiency of gratings in non-Littrow mode

Richardson Grating Lab Catalog Number 73-45-273

Aluminum index values used from gsolver Table values

Angle between collimator and camera axes is 30 degrees

Angle of incidence 19.13 degrees

Markers show red and blue limits for blazed wavelength at center

The efficiency is plotted for unpolarised light and is the average value or the P-plane and S-plane responses.

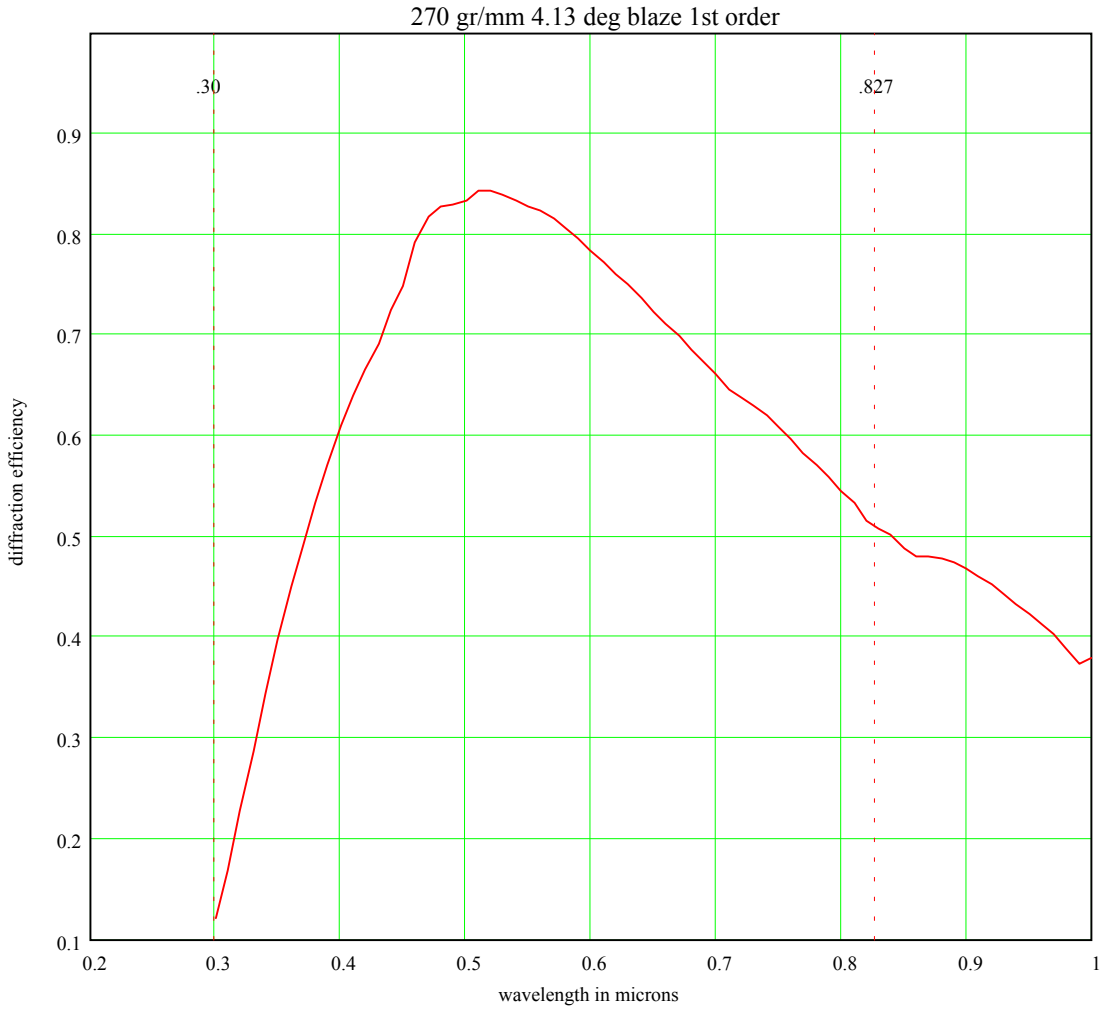

Figure 2.8: Resolving power R = λ/dλ at center of spectrum 1417

Calculated blaze efficiency of gratings in non-Littrow mode

Richardson Grating Lab Catalog Number 73-49-505

Aluminum index values used from gsolver Table values

Angle between collimator and camera axes is 30 degrees

Angle of incidence 26 degrees

Markers show blue and red limits for blazed wavelength at center

The efficiency is plotted for unpolarised light and is the average value or the P-plane and S-plane responses.

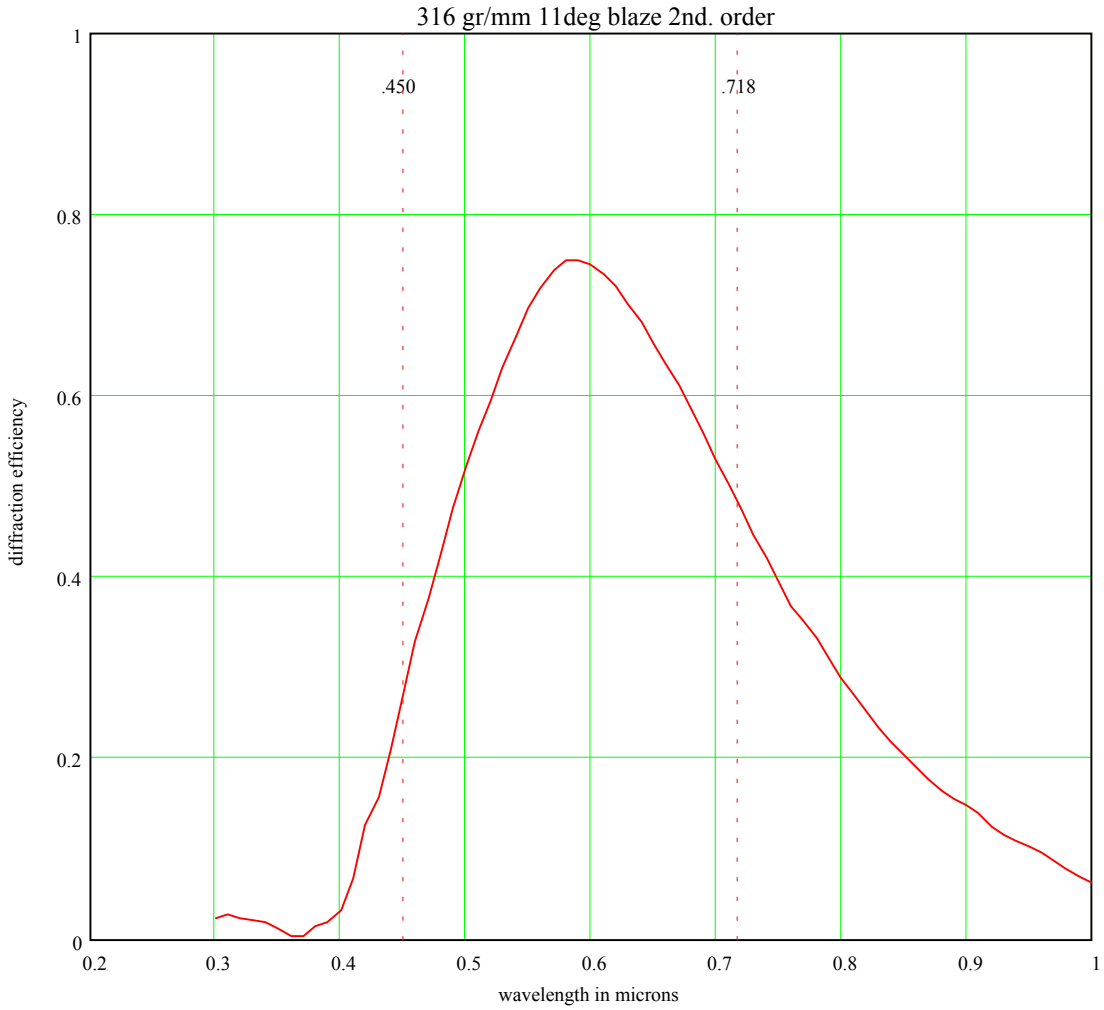

Figure 2.9: Resolving power R = λ/dλ at center of spectrum 3959

Calculated blaze efficiency of gratings in non-Littrow mode

Richardson Grating Lab Catalog Number 73-49-505

Aluminum index values used from gsolver Table values

Angle between collimator and camera axes is 30 degrees

Angle of incidence 26 degrees

Markers show blue limit for blazed wavelength at center

The efficiency is plotted for unpolarised light and is the average value or the P-plane and S-plane responses.

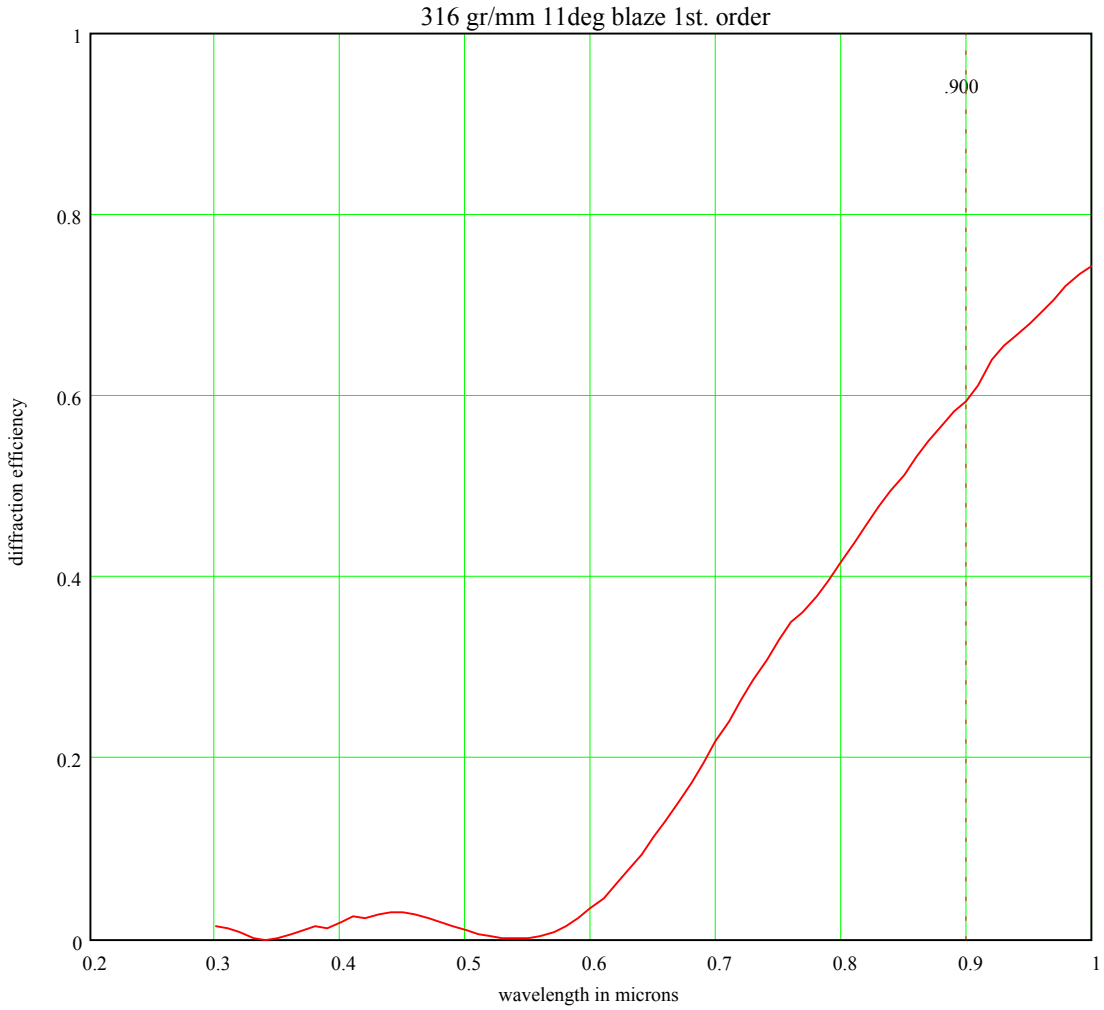

Figure 2.10: Resolving power R = λ/dλ at center of spectrum 3959

Calculated blaze efficiency of gratings in non-Littrow mode

Richardson Grating Lab Catalog Number 73-45-584

Aluminum index values used from gsolver Table values

Angle between collimator and camera axes is 30 degrees

Angle of incidence 19.76 degrees

Markers show blue and red limits for blazed wavelength at center

The efficiency is plotted for unpolarised light and is the average value or the P-plane and S-plane responses.

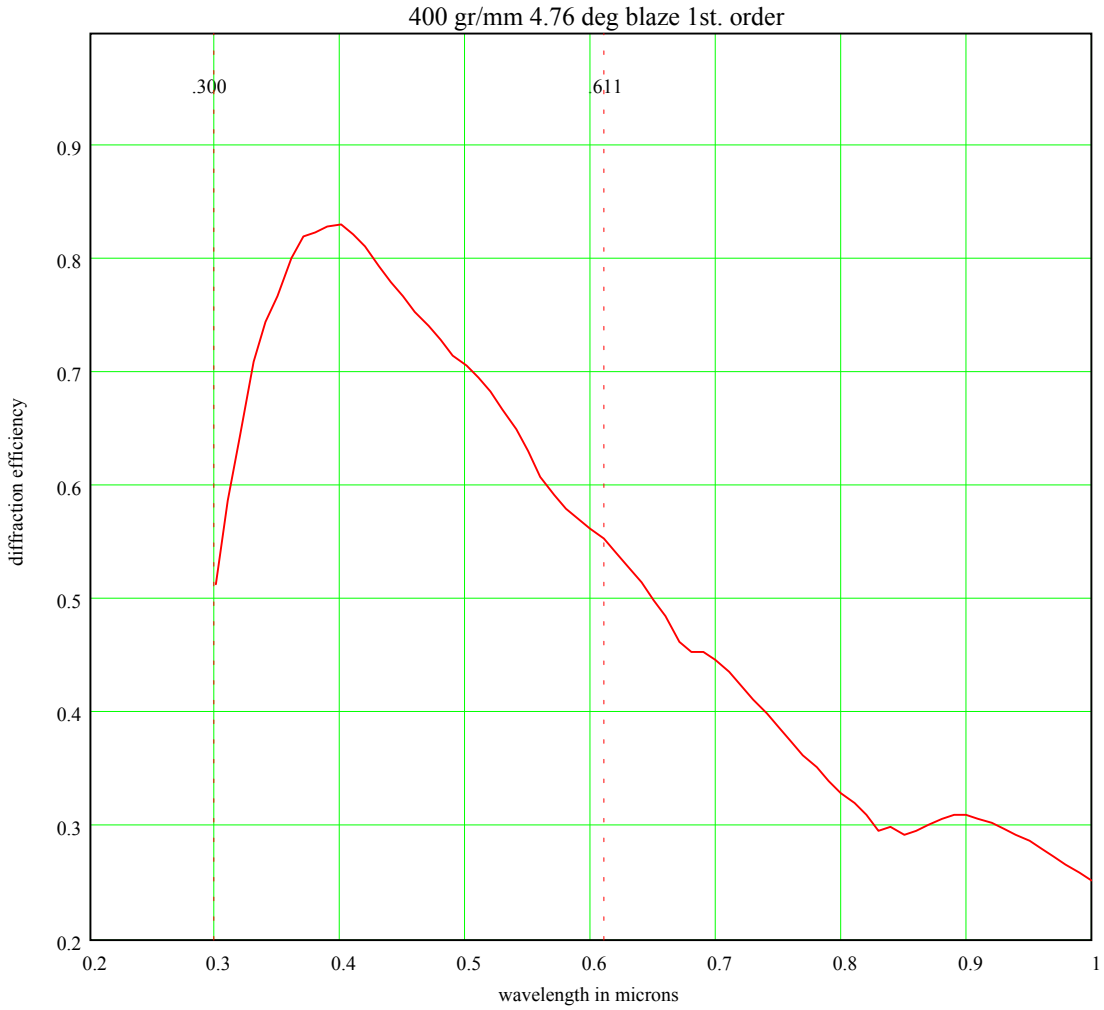

Figure 2.11: Resolving power R = λ/dλ at center of spectrum 1636

Calculated blaze efficiency of gratings in non-Littrow mode

Richardson Grating Lab Catalog Number 73-45-561

Aluminum index values used from gsolver Table values

Angle between collimator and camera axes is 30 degrees

Angle of incidence 37.3 degrees

Markers show blue and red limits for blazed wavelength at center

The efficiency is plotted for unpolarised light and is the average value or the P-plane and S-plane responses.

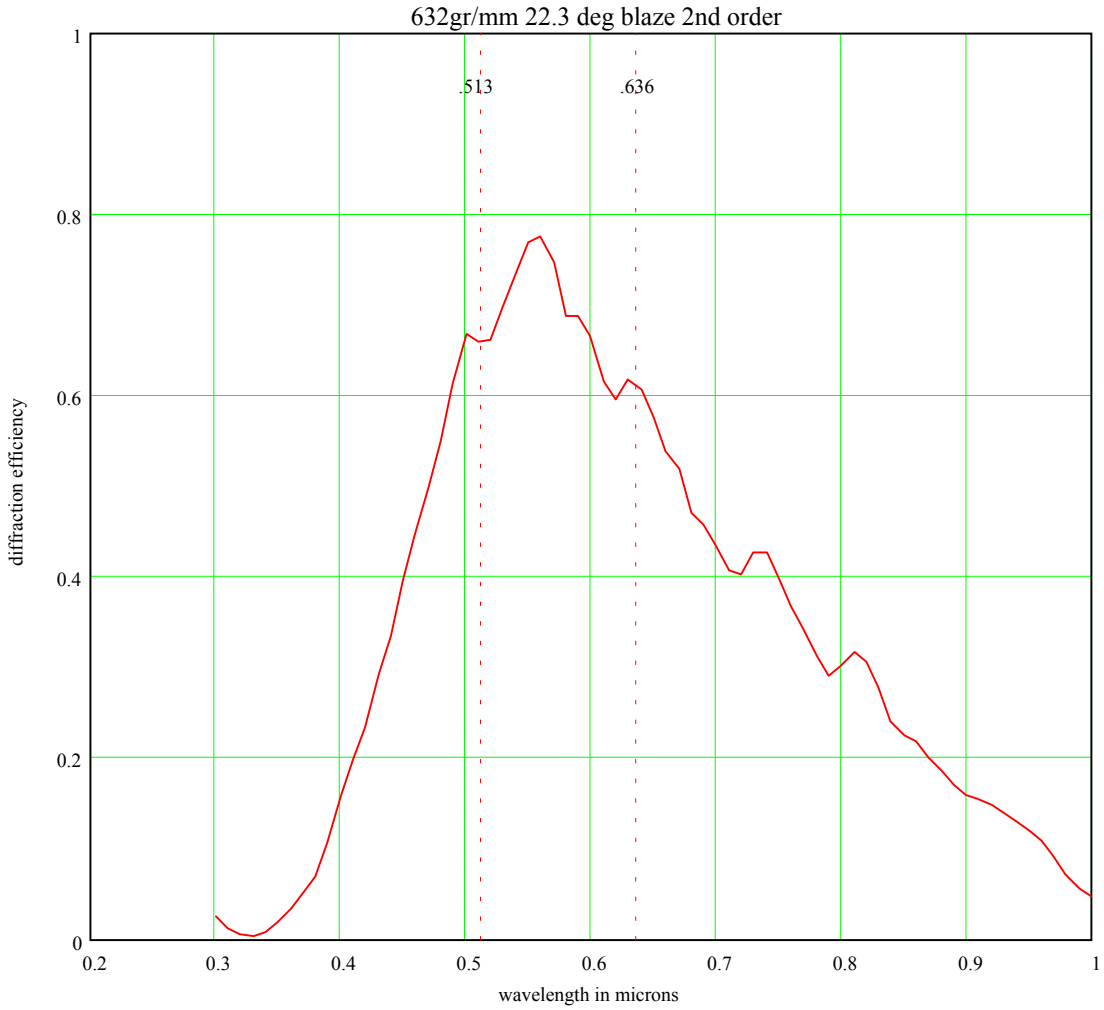

Figure 2.12: Resolving power R = λ/dλ at center of spectrum 8917

Calculated blaze efficiency of gratings in non-Littrow mode

Richardson Grating Lab Catalog Number 73-45-561

Aluminum index values used from gsolver Table values

Angle between collimator and camera axes is 30 degrees

Angle of incidence 37.3 degrees

Center of blaze is at 1.16 microns

The efficiency is plotted for unpolarised light and is the average value or the P-plane and S-plane responses.

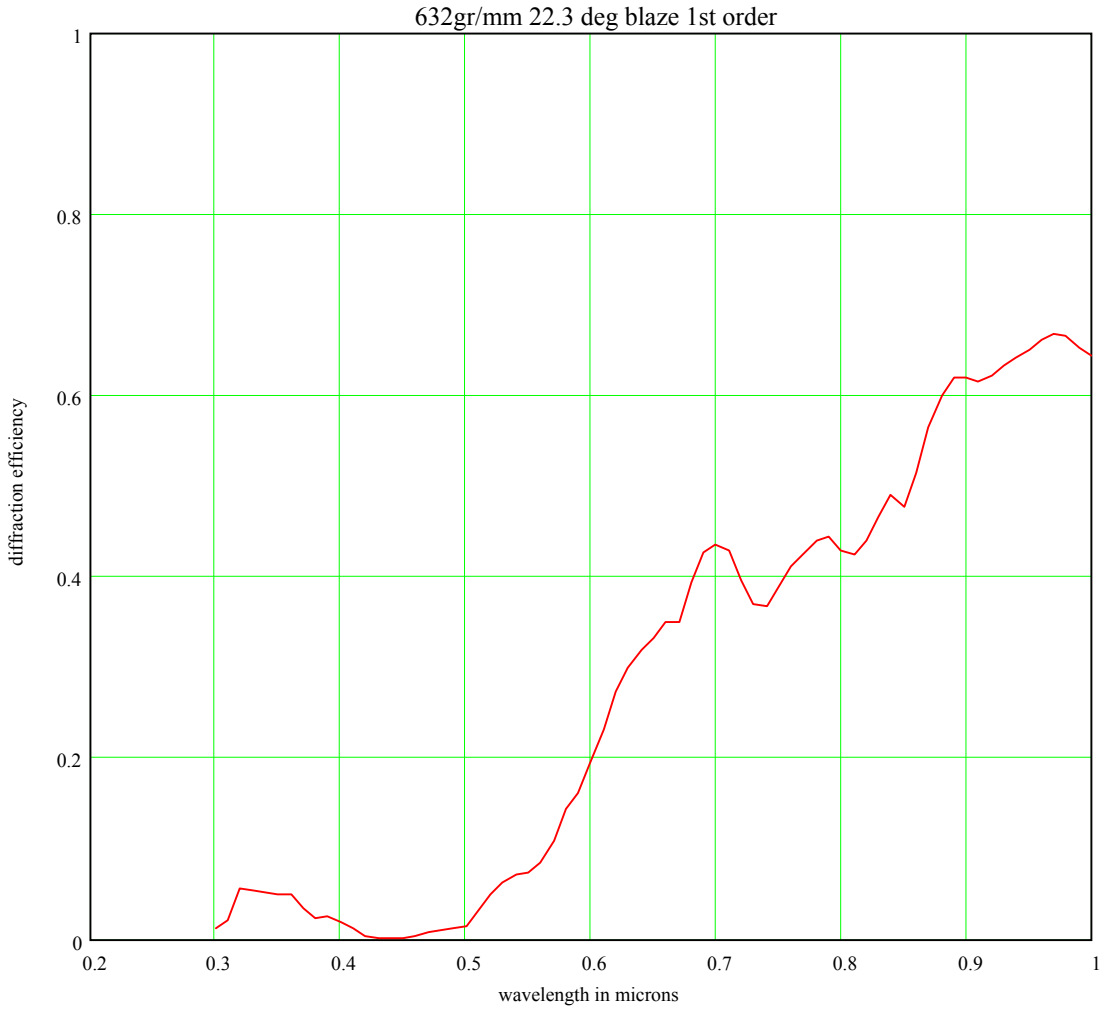

Figure 2.13: Resolving power R = λ/dλ at center of spectrum 8917

Calculated blaze efficiency of gratings in non-Littrow mode

Richardson Grating Lab Catalog Number 73-45-109

Aluminum index values used from gsolver Table values

Angle between collimator and camera axes is 30 degrees

Angle of incidence 21.5 degrees

Markers show red and blue limits for blazed wavelength at center

The efficiency is plotted for unpolarised light and is the average value or the P-plane and S-plane responses.

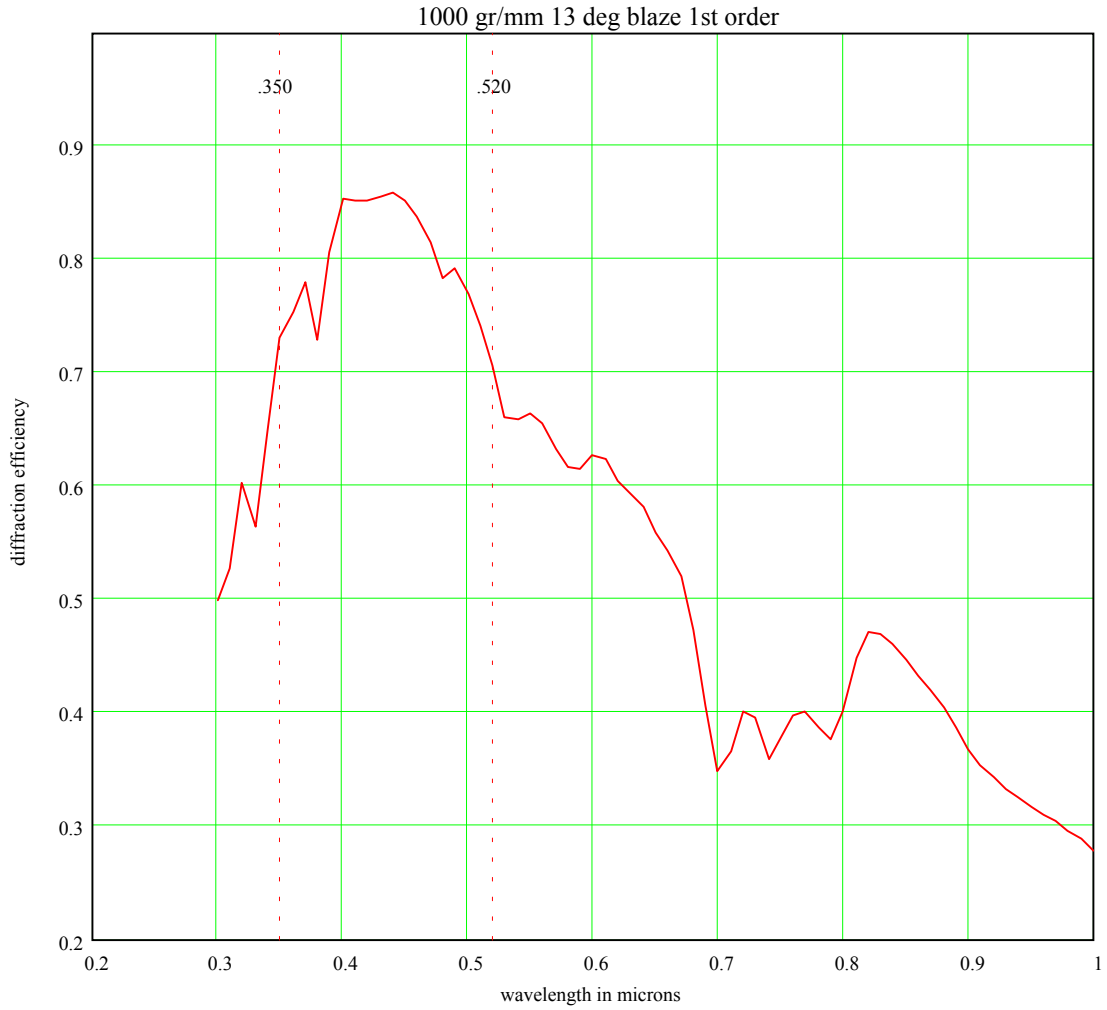

Figure 2.14: Resolving power R = λ/dλ at center of spectrum 4752

2.7 Estimated Throughput

The total throughput of the instrument is determined by the combination of the transmission and reflectance of the optical surfaces, the efficiency of the grating in use, and the CCD quantum efficiency. Figure 2.15 shows the estimated throughput with a particular selection of gratings. For this estimate we assumed:

- A field lens anti-reflection coating with 98% transmission over a 320-1000 nm wavelength range
- Blue reflecting surfaces with 90% reflectivity (enhanced Al)
- Blue refracting surfaces with transmission of 99.5%
- Red reflecting surfaces with 95% reflectivity (protected Ag)
- Red refracting surfaces with 99.5% transmission
- Predicted grating efficiencies for our nominal choice of existing rulings.
- Dichroic efficiency (transmission and reflection) of ~90% away from the cutoff, and a cutoff half-width of ~20nm.

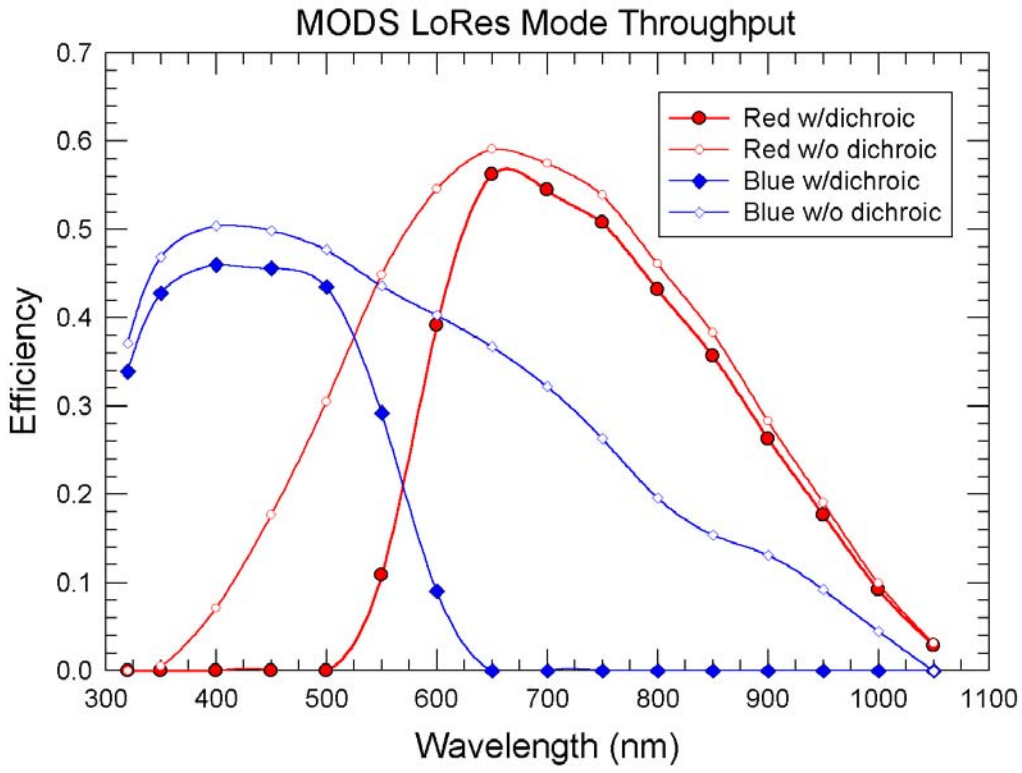

Figure 2.15: Estimated MODS low-resolution mode throughput.

These assumptions were based on published reflectivities of mirrors, actual traces of anti-reflection coatings we have used on similar transmissive optics, measured detector

quantum efficiency, and published grating characteristics. Note that the telescope, atmosphere, or slit losses were not included in the estimate.

2.8 Optical Surface Accuracy Tolerance and Fabrication Requirements

The previous sections have shown the expected optical performance of the instrument assuming that all the optics are fabricated without errors and that the wavefront delivered by the telescope optics is undisturbed by the atmosphere. Neither is likely to be the case. We have developed manufacturing tolerances for potential fabricators based on structure-function arguments; these arguments are similar to the sort of strategies used to define telescope image quality error budgets. In particular, we can associate each surface in the optical design with a length parameter r_0 that can be equated to errors at a variety of different scales. Similarly, the wavefront reaching the telescope through the atmosphere also has the same type of structure at different scales. The quadrature sum of the r_0 values can then predict the final delivered image quality. This analysis technique is convenient, since if the instrument and individual surfaces are made to deliver r_0 values better than any expected from the atmosphere, then the optical manufacturing tolerances will not meaningfully degrade the delivered image quality for that particular optical design.

We start by assuming that the telescope delivers an image with a FWHM of 0.15″. This corresponds to an adaptively corrected image with a typical r_0 value of 67 cm (assuming a standard atmospheric turbulence length scale spectrum). We next determine that the total optical design should at its best produce images with a value of r_0=91 cm, which corresponds to a FWHM of 0.11″. Each surface in the optical design was then assigned an r_0 value consistent with values expected using reasonable manufacturing processes. For example, the most difficult surface to manufacture in MODS is the aspheric surface of the corrector plate. In discussion with various optical fabricators, we determined that realistic tolerances for this surface should be 1.5 to 2 times looser than for the other surfaces in the instrument. Conversely, we also elected to include reasonably tight values on some of the simpler optics that should straightforward for the optical fabricators to meet.

The r_0 values assigned to the individual surfaces in MODS are given in Table 2.3. Note that the values have been assigned in accordance with whether the surface is refractive or reflective and that the largest errors be permitted on the difficult aspheric surface of the corrector lens. The first two values ("AO images" and "Optical design") are for the telescope using the adaptive Gregorian secondary and from the *CodeV* design for the spectrograph. The image FWHM values in the table are determined by from the assigned r_0 values. Note that we have not included the ADC, field lens, or the dichroic and other flat surfaces in the error budget. The reason is that these surfaces are straightforward to make with high precision (corresponding to r_0 values >> 300 cm) and will not significantly affect the wavefront as it passes through the instrument.

Table 2.3: Values of r_0 at 500 nm scaled by LBT aperture/MODS pupil

Design Parameter	r_0 value (cm)	Image FWHM (″)
AO image	67	0.15
Optical Design	91	0.11
Collimator	200	0.05
Corrector spherical surface	300	0.03
Corrector aspherical surface	150	0.07
Camera mirror	200	0.05
Optical support	220	0.05

Table 2.4 gives the permissible optics surface tolerances for the MODS components at several length scales. These were derived from the assigned r_0 values for each surface (again the ADC, field lens, and flats are not included). Discussions with various optical manufacturers indicate that these surface tolerances are achievable with standard techniques and at reasonable cost (particularly for the aspheric surface).

Table 2.4: Permissible rms surface errors (waves at 633 nm)

Scale length (mm)	Collimator Mirror	Corrector Spherical Surface	Corrector Aspheric Surface	Camera Mirror	Optical Support
10	1/20	1/10	1/5	1/20	1/10
25	1/20	1/5	1/3	1/20	1/8
50	1/8	1/4	1/2	1/8	1/4
100	1/3	1/2	1.3	1/3	1/2
230	1/2	1	2.4	1/2	1

2.9 Optical Alignment Strategy

The accurate alignment of the optical components of MODS is critical to the successful operation of the instrument. We plan to fully configure and align the instrument in the lab (using the high bay space available for instrument assembly). The camera optics can be aligned separately. The procedure will begin with careful mechanical alignment of the structure and optics. We estimate that standard techniques should allow the optics to be aligned to less than 1 mm. We will then illuminate system with an expanded collimated He/Ne laser source and measure the resulting on-axis images using a lab CCD camera. This CCD camera will over-sample the images and provide an accurate representation of the on-axis monochromatic point-spread-function. We will then compare this on-axis point-spread-function with CodeV predictions. The left panel of Figure 2.16 shows the PSF of a perfectly adjusted camera for the above conditions. This will actually be an out of adjustment condition for wide field spectrographic illumination. A smaller overall error function results when the camera is adjusted to produce an on-axis PSF corresponding to the right panel of Figure 2.16. This change corresponds to an added decenter of the corrector lens of 0.99 mm and a refocus of the camera mirror of 0.258

mm. We have used this technique to align a variety of optical systems in the past (e.g., offner relays, collimator-camera lens systems, etc.). We have used this technique in the past to align various optical systems (Offner relays, other camera-collimator systems, etc.). Typically, no more than a few iterations are required to achieve optimal optical alignment. Figure 2.16 shows examples of well-aligned and misaligned (by ~0.5mm) configurations of MODS. The difference is dramatic and the suggested direction of the correction to the alignment obvious.

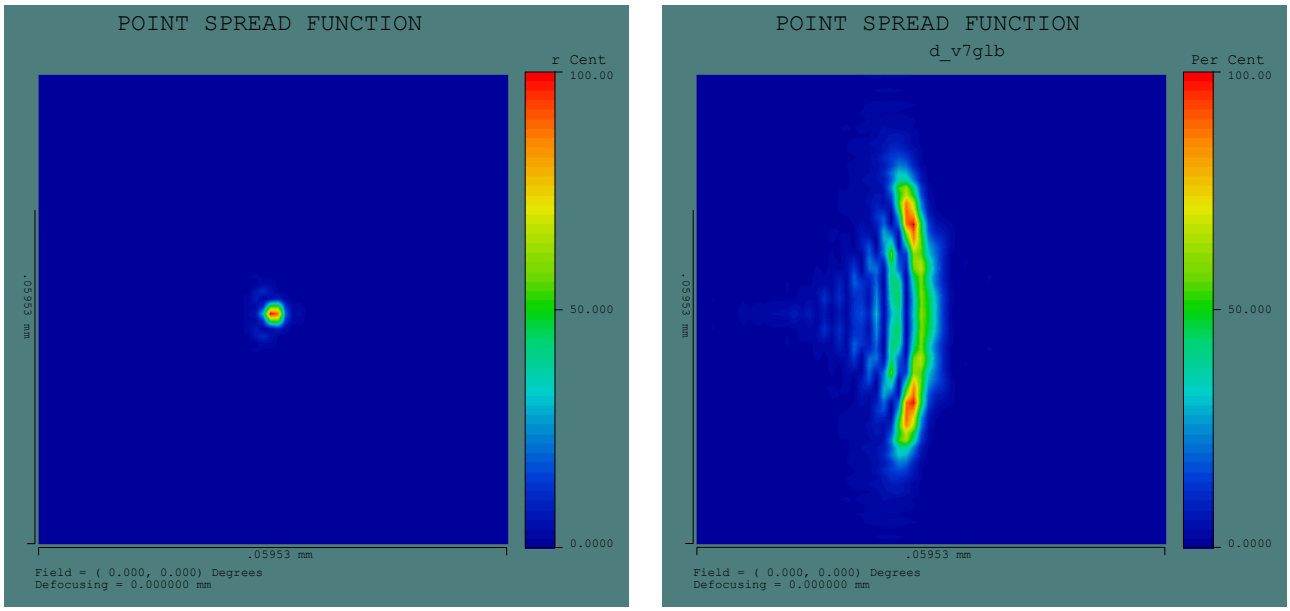

Figure 2.16: Best on-axis monochromatic PSF (left). Optics re-aligned (right) for best polychromatic wide field performance. The PSF of the re-aligned optics has an 80% encircled energy diameter of <30-m.

Keeping the instrument in good alignment is also critical. In particular, controlling flexure is critical for science operations. See section 3.2.5 for a description of our planned flexure compensation system for the instrument. We have done extensive simulations of the optical configurations inherent in the flexure compensation system. In particular, we have evaluated the image quality as a function of collimator and camera primary tip-tilt angles expected to be necessary for flexure compensation. We find that the image quality remains essentially unchanged over the full range of image motion expected during long (>4 hour) exposures, and even from horizon-to-zenith pointing.

2.10 Additional Tasks

There are three important tasks yet to be completed for MODS: scattered light analysis, the design of the baffle system, and the design of the calibration system. We have obtained the *LightTools* software package, and plan to analyze the scattered light in the instrument. The results of this analysis should help to define the baffle system for the instrument. Preliminary results suggest that baffles close to the camera and around the grating are particularly important. The requirements for the calibration system are to provide accurate flat fields and wavelength comparison sources. We are currently developing more specific requirements for these functions.

3 Mechanical Design

3.1 Overview

This section describes the mechanical design of the MODS spectrograph.

3.1.1 Mechanical Engineering Strategy

The optical and mechanical designs of MODS are treated as a coupled problem in which the instrument is designed from the inside out, starting with optics and mechanisms and then designing the structure around them. This close-coupling design strategy has served us well in previous instrument projects.

For MODS, the basic design roadmap is as follows:

- The optical design is done in Code V. This produces a set of files with the optical prescription for the system.
- The optical design data are imported into Mechanical Desktop and a 3D parametric model is constructed that locates the optical elements & optical beam paths in space.
- Optical supports are then designed and built around the optics, and the impact on location of the optics relative to the instrument volume feeds back into the optical design (e.g., it introduces constraints on camera-collimator angles, how the two optical paths are folded into space, etc.)

Once the optical design and basic layout of the optics in space converged, the design process shifted into the design of mechanisms and the overall instrument support structure:

- Mechanisms (filter wheels, actuators, etc.) are built around the optics.
- The instrument structure is then built around the mechanisms.
- The instrument structure is constrained on the outside by instrument envelope at the LBT direct Gregorian focus.

As before, this is an iterative process with detailed structural and thermal modeling as the design proceeds.

A key outcome of this design process is the development of a “mechanical model” that in effect defines the “instrument”. The instrument model serves a number of different roles in the MODS project:

- Forms the basis for a detailed Finite Element Analysis (FEA) of the system mechanical and thermal performance. FEA modeling is performed to ensure that the design meets or exceeds the scientific requirements for MODS.
- The model can be translated into Computer Numerically Controlled (CNC) machining instructions for the fabrication of instrument components, either in-house or by outside vendors.

- The model is used to generate part drawings for all optical and mechanical components of MODS, and will be used to generate the final set of engineering drawings delivered to the LBT project with the spectrograph.
- The model is used to perform the essential mass and moment calculations to ensure that MODS will work within the mechanical and space constraints of the LBT and not impact the overall performance of the telescope.

3.1.2 Scope of this section

The mechanical design described below will concentrate on the following areas, in order. A number of subsystems are not yet designed at this time (e.g., the cross-disperser changer mechanism) and will not be discussed here:

1. MODS Optical Spectrograph overview
2. Telescope Interface
3. Structural Design
4. Optics Support Design
5. Camera Structure
6. Primary Structure
7. Flexure Compensation System
8. Spectrograph Mechanisms
9. Detector Mechanical & Thermal Systems

For MODS we are following the same basic design strategy that we have used for our previous facility-class instruments. We are also drawing upon a 10-year heritage of mechanical designs, allowing us to reuse and adapt existing designs in addition to new mechanisms and systems needed for MODS. Our modular approach and design and fabrication strategy have been very successful, and adopting them here will greatly reduce our development time.

3.2 MODS Mechanical Design

3.2.1 Instrument Mass & Telescope Interface

MODS is designed to work at the *f*/15 direct Gregorian focus behind each of the primary mirrors of the LBT.

The available volume behind the primary mirror defines the instrument envelope. This volume has the shape of a roughly cylindrical envelope extending about 3-meters behind the direct Gregorian rotator's mounting surface and is approximately 2.5-meters in diameter. The instrument can also extend up to a meter into the back of the primary mirror cell. This gives us plenty of room for MODS. A 3D model of MODS is shown in Figure 3.1.

The instrument weight limits are as follows:

- Mass must be less than 3500 kg. The current MODS mass estimate is ~2000 kg.

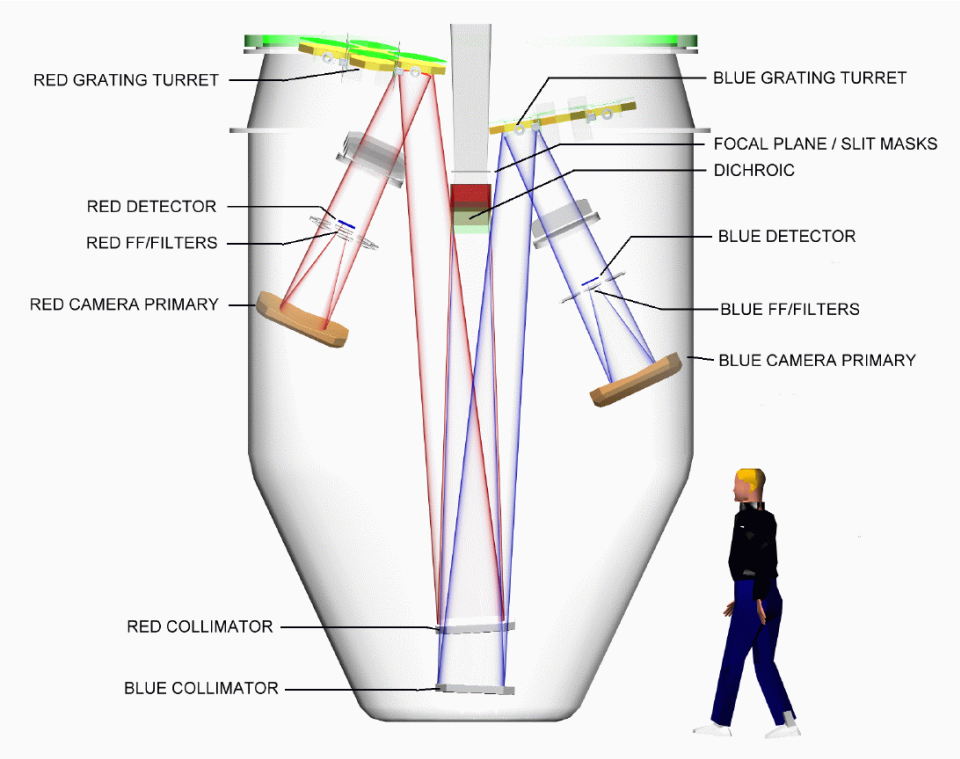

Figure 3.1: 3D Model of MODS

- Moment must be less than 3500 Kg-meters.

The instrument will be mounted to the Gregorian focus rotator using:

- 6-point ball-in-cone semi-kinematic mounts
- Automatic clamping.

The instrument will be balanced and cabled to permit rotation through about 360-degrees.

3.2.2 Optics Support System

MODS will have large (up to 400mm) optics with stringent support requirements. The largest optics will be supported on bonded flexible couplings ("flexures"). These flexures decouple the bending moments that would otherwise distort the mirrors. The advantages of this approach are:

- No stick-slip, friction, or hysteresis
- Predictable performance.

An example of one of the mirror mounting flexures with an Invar support is shown in Figure 3.2 (the flexure shown is approximately 2 inches long).

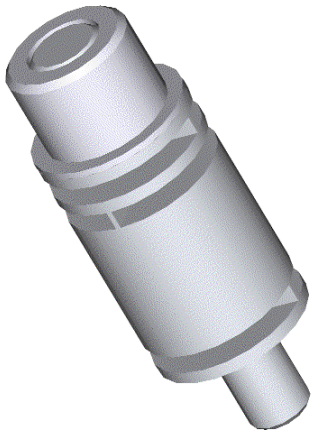

Figure 3.2: Mirror mounting flexure

The gratings will be replicated onto solid Zerodur, and will be permanently mounted on flexures in individual grating cells. Each cell will permit adjustment in tip, tilt, piston and groove rotation.

The large camera corrector lenses will be mounted on blade flexures bonded to the edges of the lens. This will fix the camera corrector relative to the cell; so all alignment will be done using the camera structure proper. We have extensive experience using blade flexures for lens mounts in both free-air and cryogenic instruments and understand their performance very well.

The Camera and Collimator mirrors are large optics with special support requirements, but have the advantage of being able to be supported from behind. We are having these mirrors fabricated from Hextek honeycomb structured blanks. This offers us a number of advantages:

- Low weight of the optics.
- High stiffness-to-weight ratio of the honeycomb blanks allows efficient use of a 3-point support system.
- Mounting bosses will be manufactured into the blanks at the center-of-gravity, giving no parasitic moments.

Figure 3.3 shows a half-symmetry FEA of the camera primary mirror when pointing at the Zenith. Zenith-to-Horizon image distortion due to the mirror supports (both collimator and camera primary) is summarized in Table 3.1. The linear sum given in the table represents the worst-case scenario, and assumes that all errors add, and that all mirrors are at zenith at the same time. Note that the largest distortion is 1.39μm, much smaller than a single CCD pixel (15μm), and well within specifications. Deformation of the mirrors due to the supports yields two effects:

- Relative image motion due to tilting (distortion) of the mirrors.
- Increase in the image spot size on the detector.

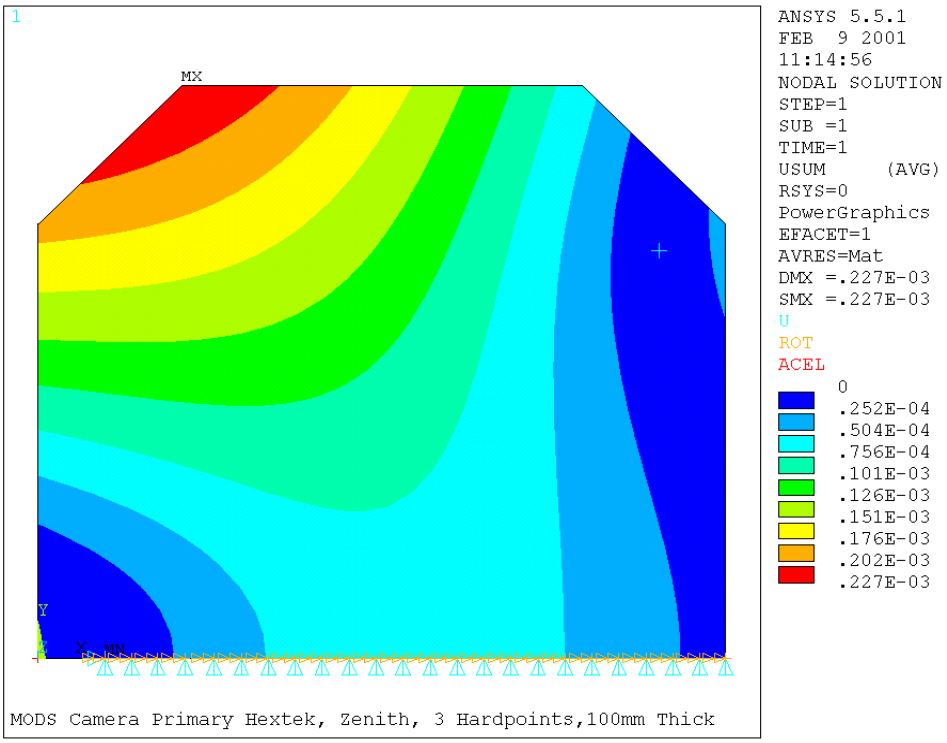

Figure 3.3: MODS Primary Camera Distortion

Table 3.1: Image Degradation due to the Mirror Supports

Image Scale ("/pixel) 0.125

Pixel Size (μm) 15

	Field Center		Field Edge		Field Corner	
	Distortion	Spot Size	Distortion	Spot Size	Distortion	Spot Size
	(μm)	(μm)	(μm)	(μm)	(μm)	(μm)
Collimator Mirror	0.00	0.23	0.25	0.18	0.69	0.10
Grating	0.06	0.15	0.00	0.27	0.00	0.27
Camera Primary Mirror	0.00	0.50	0.60	0.25	0.70	0.40
Totals (μm at CCD)	**0.060**	**0.880**	**0.850**	**0.700**	**1.390**	**0.770**

3.2.3 Camera Structure

The structure of the MODS cameras is shown in Figure 3.4. Alignment of the camera primary mirror and corrector lens is critical to achieving the optical performance, and we have adopted an open design using adjustable invar trusses. The virtues of this design are as follows:

- Camera focus will be insensitive to temperature (athermalized structure).
- Very stiff and lightweight structure, giving less than 15 microns of image motion from zenith to horizon (roughly 1 pixel).
- Corrector/Primary/Detector alignment is accomplished by changing the lengths of the trusses.
- Camera is a module mounted from the middle bulkhead, so it can be aligned and tested on the bench before integration into the instrument.

The MODS Red camera is shown in Figure 3.4 (for scale, the detector is ~125 mm wide). The blue camera will be essentially identical in appearance.

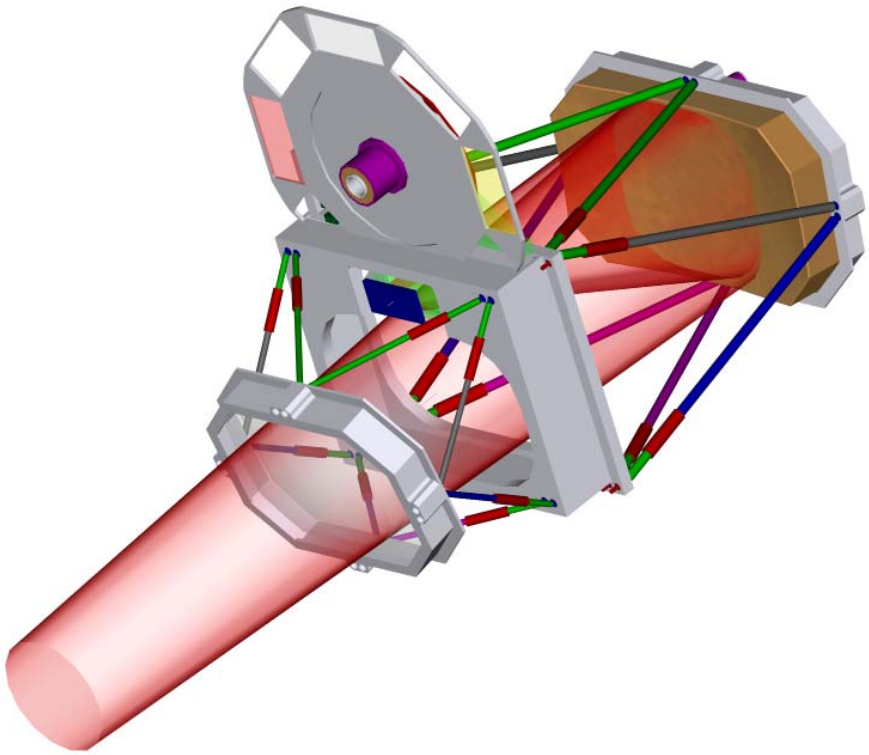

Figure 3.4: MODS Camera Structure

3.2.4 Primary Structure

The MODS primary structure is a welded steel structure. This offers the following advantages:

- Low structure CTE

- Excellent stiffness
- Inexpensive

We will use low-hysteresis welded joints wherever possible. The structure will be subjected to a complete opto-mechanical analysis to ensure optical alignment and to predict the range and character of the image motion.

3.2.5 Flexure Compensation System (FCS)

From a simple scaling analysis it is clear that passive control of flexure in a structure the size and complexity of MODS is extremely difficult. Our flexure goal is 0.1 pixels (1.5μm) at the detector in 1 hour of exposure. The primary structure is expected to flex an amount that translates to 20-40 μm in a 1-hour exposure. MODS will therefore require some kind of active flexure compensation system (FCS) to meet the flexure specification.

We plan to build a closed-loop active FCS for MODS. An open-loop FCS would use a look-up table (like a telescope pointing model) to correct for previously mapped flexure. This approach, however, has the following disadvantages:

- Must build an accurate pointing model
- Changes in the instrument configuration can affect the pointing model
- Cannot compensate for hysteresis in the structure.
- Difficult to compensate for temperature gradients in the structure.

A closed-loop FCS addresses many of these issues, in particular

- Can compensate for elastic flexure, hysteresis, “ticks & clicks”, and temperature effects.
- System should be robust and require little maintenance.
- Initial costs are offset by improved performance and reduced operational support needs (e.g., time to build and update detailed instrument pointing maps for all configurations).

The closed-loop FCS concept is as follows:

- Use an infrared (λ=1.5μm) reference beam to measure the image motion. This would be an IR laser originating at the instrument focal plane (slit plane).
- IR beam shares all key optical elements as the optical “science” beam.
- Use a ~1.5cm diameter IR “bypass grating” located in the center of the “science grating” (a location shadowed by the secondary mirror). The location in the secondary “shadow” means we get no throughput penalty in the science beam. This grating would be a coarse-ruled grating that would give many spots from many orders (50-100 spots).

- An IR detector in the camera focal plane measures the spot centroids, and then passes any image motion information to the FCS. The FCS uses these data to null image motion by tipping and tilting the camera primary mirror.

The FCS can operate at any science grating tilt angle as there will always be at least one laser spot on the IR detector at all possible grating tilts. Use of a 1.5μm IR laser (standard for fiber communications applications) avoids contamination of the science detector with scattered light.

In essence, the proposed FCS will replicate the system known to work well for telescopes. Although telescopes are often pointed in open loop with corrections derived from a software model, no telescope relies on this model for accurate tracking or precision pointing. All modern telescopes employ guide cameras and target acquisition systems (typically sensitive cameras at a focal plane position offset from the science field or which use a different wavelength than the science light) to finely hone the pointing and tracking of the telescope. No single exposure longer than ~1 minute is typically attempted without the prior acquisition of a guide star. As MODS is larger and more complex than many professional telescopes, a similar philosophy should be applied; the infrared laser functions as the guide star to compensate for the flexure of the instrument.

A prototype FCS based on off-the-shelf components (IR laser and detectors) is currently under development.

3.3 Instrument Mechanisms

MODS has a large number (~30) of mechanisms. The design of these mechanisms will be similar to many others we have successfully deployed in other instruments (often with more exacting requirements). The main mechanism classes are as follows, in order from the entrance of the instrument:

- Focal Plane Slit-Mask Cassette
- Acquisition and Guiding Stage
- Dichroic Changer
- Collimator Focus (and tip/tilt active alignment/FCS system)
- Grating Select and Tilt
- Camera Shutter
- Camera Primary Focus/tip/tilt
- Filter Wheel

Systems not yet designed but for which space is provided are:

- Atmospheric Dispersion Corrector (ADC) Prisms
- Calibration system.
- Cross-disperser change mechanism (space left, but not part of the baseline instrument)

In general, our mechanisms share a number of common properties:

- Use stepper motors as the prime movers
- Payload position is maintained by the mechanism when power to the motor is off.
    - Use detented wheels, brakes, or screw drives as required.
    - This minimizes heat dissipation from the motors.
- Limit switches, proximity sensors, encoders, etc. provide position feedback.

3.3.1 Focal Plane Slit-Mask Cassette

Each MODS spectrograph can have up to 25 slit masks stored on the telescope in a cassette mechanism. This mechanism has the following functions:

- Select a mask from the storage cassette.
- Insert or retract a mask into the focal plane

Figure 3.5 shows the design of the slit-mask cassette system.

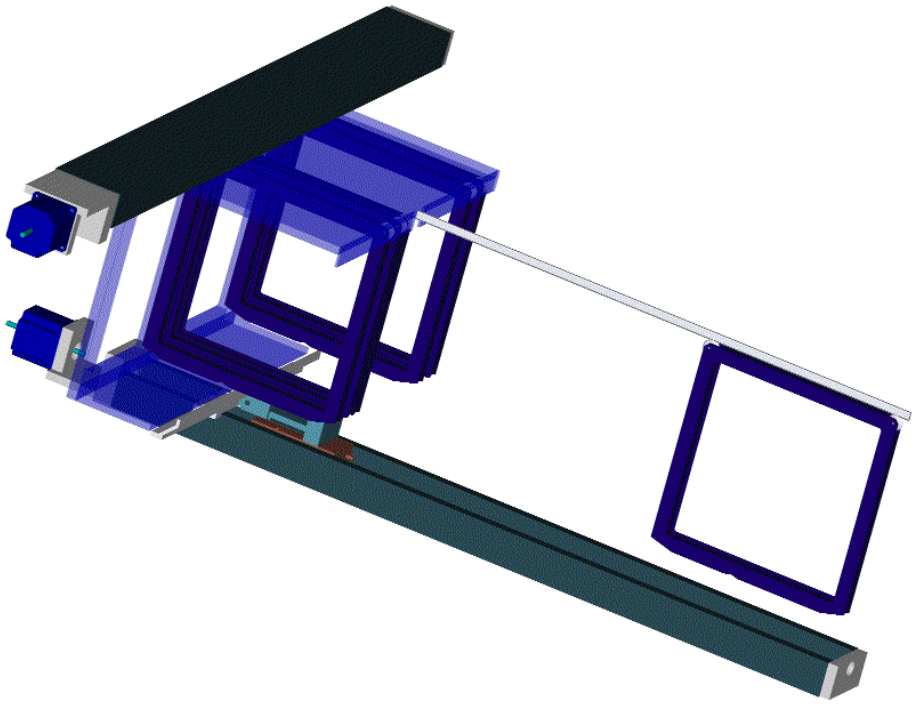

Figure 3.5: Slit Mask Cassette Mechanism

Masks include facility long-slit masks and custom multislit masks. The latter are laser machined on-site, using MODS project-provided software. Because of the curved *f*/15 Gregorian focal plane, the masks must be spherical in shape (~1.2 cm of "sag" corner-to-center). Our current design calls for mask substrates made of a carbon fiber laminate:

- Similar to the material being used by the GMOS spectrograph on Gemini North.

- 150-200μm thickness

Mask fabrication system will be a laser machine. We are working with the LUCIFER team to define a common mask-making machine for both instruments.

3.3.2 Acquisition and Guide Stage

MODS will need its own Acquisition and Guiding (A&G) system because the instrument intrudes deeply into the direct Gregorian focus volume and we cannot simultaneously accommodate the current Potsdam AGW system. We will, however, in all likelihood use the same cameras and wavefront sensors as the AGW at the other foci.

The basic properties of the MODS A&G system are as follows:

- X-Y stage to move a 1-square arcminute pickoff mirror around the focal plane.
- Can scan both the science field and an off-axis guide field.
- Stage carries the acquisition CCD camera, optics, and filters.

We currently are exploring guide cameras located behind and in front of the slit plane and expect to ultimately deploy guide/acquisition capabilities in both locations.

3.3.3 Dichroic Changer

MODS has three basic modes:

1. Red+Blue Dual Channel (imaging & spectroscopy) using a dichroic beam splitter.
2. Red-Channel Only (imaging & spectroscopy) using a red (silvered) flat mirror
3. Blue-Channel Only (imaging & spectroscopy) using an open position.

We accomplish this by using a 3-position detented rotary drum located below the slit plane and field lens:

- Dichroic position for dual-beam mode.
- Silver-coated flat mirror for red-only mode
- “open” position for blue-only mode

The blue collimator mirror is tilted to compensate for image shifts between these modes. Code V analysis shows that aberrations are small.

3.3.4 Collimator Focus

The collimator mirror cell is mounted on three linear actuators that allow a full range of focus, tip, and tilt adjustment:

- Actuators translate the collimator cell.
- 50mm travel using 3 identical linear actuators

Different spectrograph positions will require different camera/collimator focus combinations. These may be calibrated in advance and incorporated into instrument setup scripts.

3.3.5 Grating Select and Tilt

Each channel of MODS (Red & Blue) has a 4-position rotary grating select and tilt mechanism. A rendering of this system is shown in Figure 3.6. The features of this mechanism are as follows:

- 4-position rotary indexing turret carrying up to 3 gratings plus an imaging flat.
- Tangential detent docks the turret.
- Identical select mechanism used for the blue and red channels.
- Need a cable wrap or slip ring to get signals and power into the turret.

Each grating has an independent tilt mechanism featuring:

- Worm gear drive to tilt the grating via a semi-circular worm gear.
- Pre-loaded Teflon cone bearings for the tilt axis, with friction maintaining the grating tilt during observations.
- The grating is balanced around the tilt axis

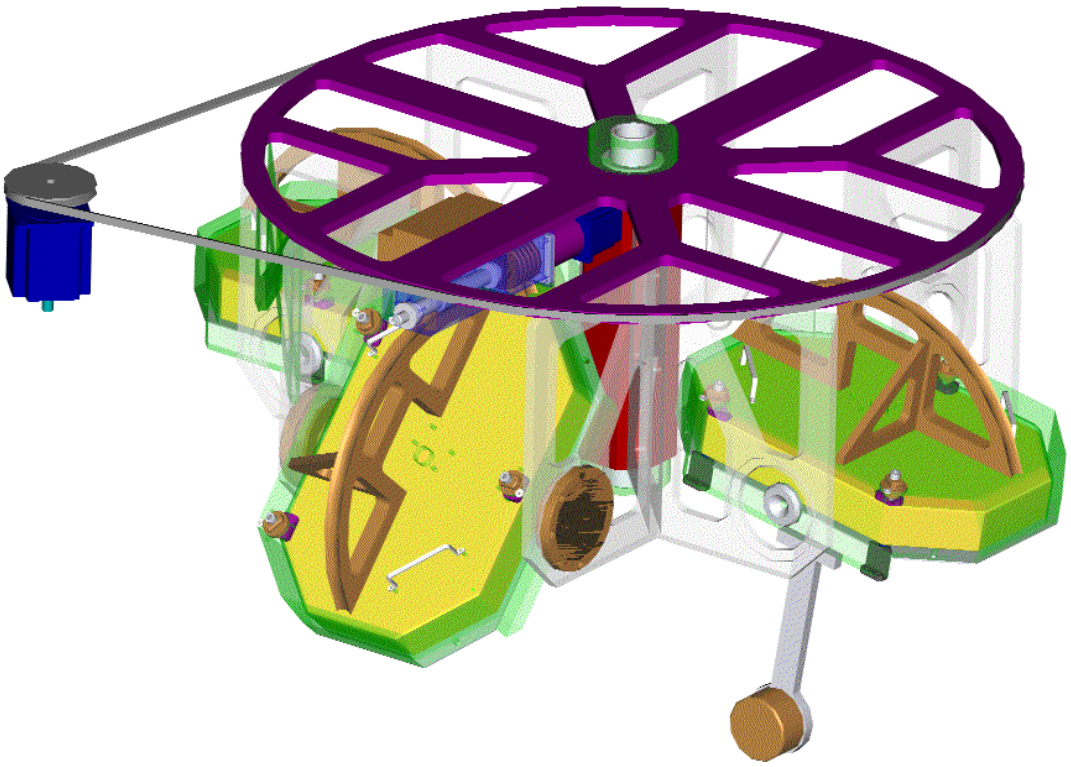

Figure 3.6: Grating Turret

3.3.6 Camera Primary Focus/Tip/Tilt Actuators

The camera primary mirror cell needs to be adjusted for focus and tip/tilt. A diagram of the actuator system is shown in Figure 3.7. The actuators are stepper-motor driven differential screws. The system has the following features:

- Identical actuators at each of the three camera mirror hardpoints.
- Coupled to the mirror through flexures
- Used for focus as well as alignment and active flexure compensation.
- Position resolution: ~0.3μm
- Range of motion: ~3mm
- Diaphragm flexures used for linear guides

During flexure compensation, the actuators are controlled by the FCS, which effectively steers the camera primary to "guide" the IR laser spot on the reference location (see §3.2.5).

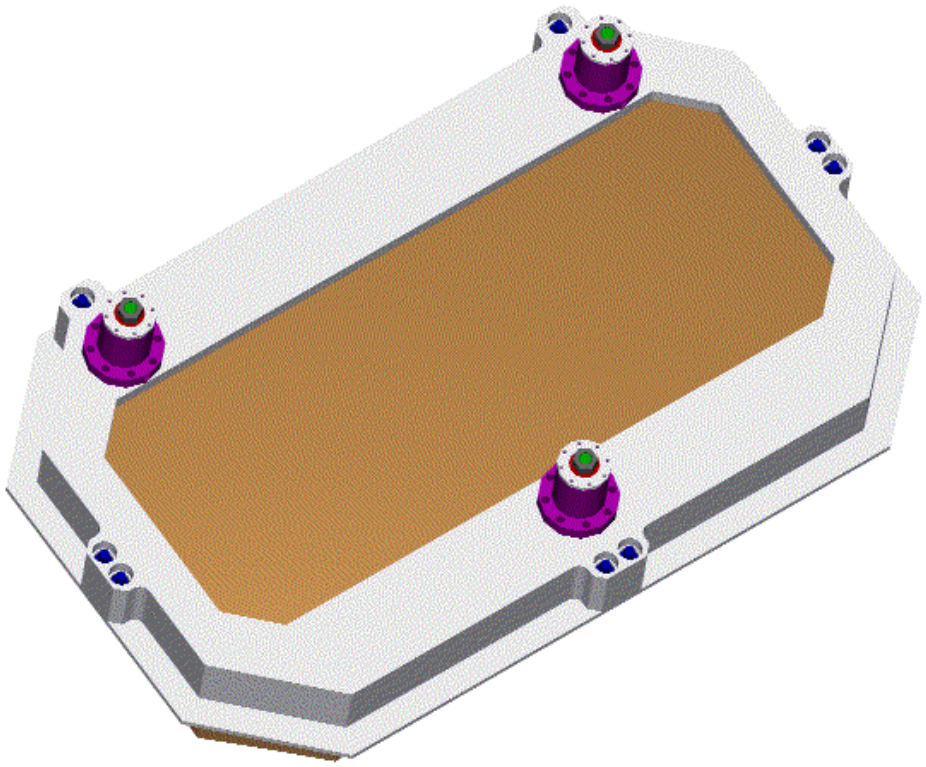

Figure 3.7: Camera Primary Focus/Tip/Tilt Actuator System

3.3.7 Filter Wheel

Each detector (red and blue) has a dedicated filter wheel located in front of the dewar window.

- 8 positions: 7 facility or user filters plus a reserved open position.
- Detented rotary wheel
- Mounted to the camera middle bulkhead.
- Accessible via access ports for inserting filters while on the telescope.

Filters are rectangular, approximately 184×88mm in size. A diagram of the filter wheel is shown in Figure 3.8.

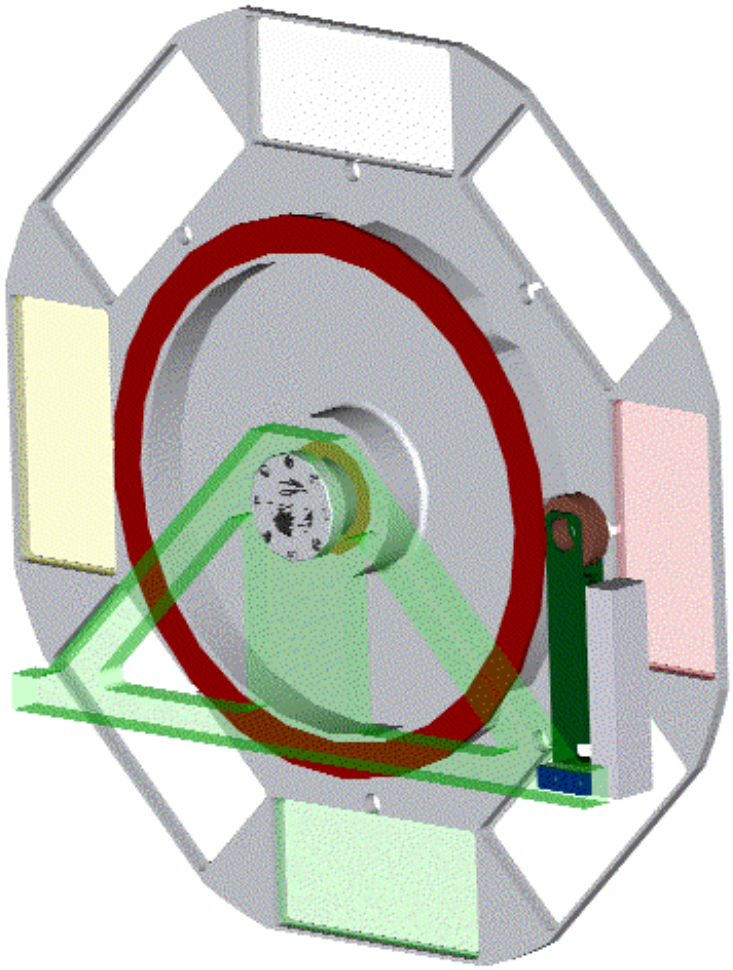

Figure 3.8: Filter Wheel Assembly

3.3.8 Detector Mechanical & Thermal

The CCD detectors are enclosed in side-looking dewars attached to the camera middle bulkhead behind the filter wheel. The detectors will be cooled with liquid nitrogen (LN_2). The dewar design parameters are as follows:

- Hold-time goal: 36-hours
- Expected thermal load: ~10 Watts
- 5 liters/day of LN_2

- Field flattener lens is the vacuum window of the dewar (distortion due to the inside-to-outside pressure differential does not affect the performance and has been analyzed with FEA and Code V).

The dewars are modules that can be separated from the cameras and operated on the bench. The location of the dewar relative to the MODS camera is shown in Figure 3.9.

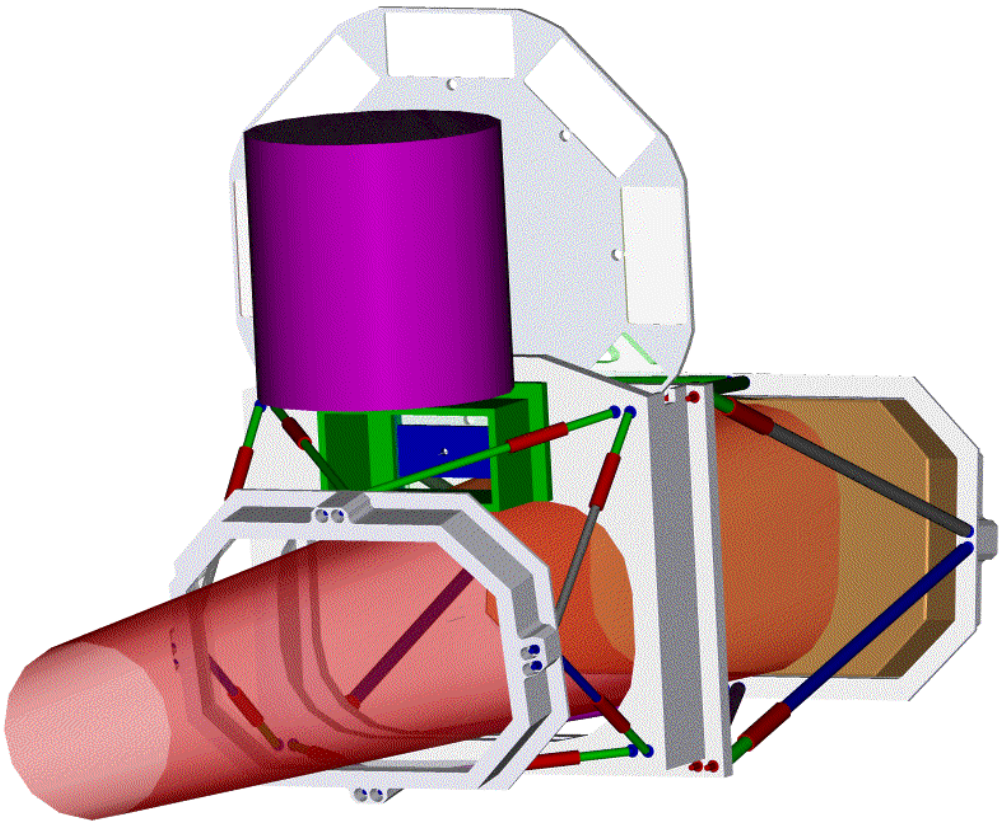

Figure 3.9: MODS Dewar (conceptual)

4 Instrument Mechanism Controls

4.1 Overview

MODS will have a number of internal mechanisms operated by motors and actuators. The instrument control system handles positioning of the mechanisms, reads and reports the encoder positions. The basic control issues are as follows:

- Stepper motor and actuator control for individual mechanisms.
- Mechanism position feedback to the control system.

Each full MODS spectrometer has a number of remotely operated mechanisms:

- One full MODS: 34 mechanisms
- One Phase 1 (first-light) MODS: 10 mechanisms

In designing the mechanism control system for MODS, we need to satisfy these basic requirements:

- Mechanism operation must have no negative effect on the science detector (i.e., we can take data while moving a mechanism without parasitic noise on the images).
- Ability to simultaneously move more than one mechanism.
- System must be able to handle a wide variety of mechanism types transparently.
- Use the same drive family for all similar mechanisms.

In this section we describe the mechanism control system we will employ in MODS.

4.2 Instrument Control on Existing OSU Instruments

MODS instrument control will build upon the basic instrument control system that we have been using in our facility instruments since 1992. We have built and deployed 6 instruments with multiple remotely operated mechanisms: IFPS, CCDS, OSIRIS, TIFKAM, ANDICAM, and DANDICAM. The most complex of these instruments (OSIRIS) has 9 mechanisms. These are summarized in Table 4.1

Our standard image control package consists of the following components:

- An instrument electronics box designed in-house & mounted outboard on the instrument.
- Commercial single-board microcomputer embedded running the control software.
- In-house designed and built driver/encoder boards for each mechanism.

We have developed a number of instrument mechanism families that have been used in our instruments with minor variations; for example, all of our cryogenic instruments (OSIRIS, TIFKAM, ANDICAM, and DANDICAM) use the same basic filter wheel mechanism and control system. In the ANDICAM and DANDICAM, we also routinely

move up to 4 mechanisms during integration with no effect on the image noise characteristics.

Table 4.1: Mechanisms in previous OSU instruments

Instrument	N_{mech}	Mechanisms
CCD Spectrometer (CCDS)	6	Filter & prefilter select sliders Slit Width adjust Grating tilt Collimator focus CCD shutter
Imaging Fabry-Perot Spectrometer (IFPS)	7	Filter select wheel & wheel tilt Lamp select Focal plane slider Camera focus UV blocking filter flip CCD shutter
OSIRIS Infrared imager/spectrometer	9	Focal plane mask/slit select wheel Filter & Pre-Filter select wheels Camera select & focus Grating select & tilt Pupil Mask X & Y position
TIFKAM Infrared imager/spectrometer	7	Focal plane mask/slit select wheel Filter & Grism select wheels Camera select & focus Pupil Mask X & Y position
ANDICAM & DANDICAM 2-channel CCD & IR imagers	6	CCD filter select wheel CCD shutter IR filter select wheel IR tip/tilt mirror (3 actuators)

4.3 MODS Control Systems

MODS mechanisms fall into two basic categories:

1. Indexed mechanisms that are typically set once and then not moved during an integration
2. Actively controlled systems that may be operated during an integration either in open- or closed-loop.

Indexed mechanisms in MODS include the filter wheels, grating select and tilt systems, slit mask select/deploy, and the dichroic/folding-flat select mechanism. Active mechanisms are those associated with camera and collimator focus and alignment, and the real-time Flexure Compensation System (FCS) on each channel of MODS.

4.3.1 Indexed Mechanism Controller

The basic control architecture for indexed mechanisms is shown in Figure 4.1. The mechanism control computer will be an embedded system (e.g., our current generation

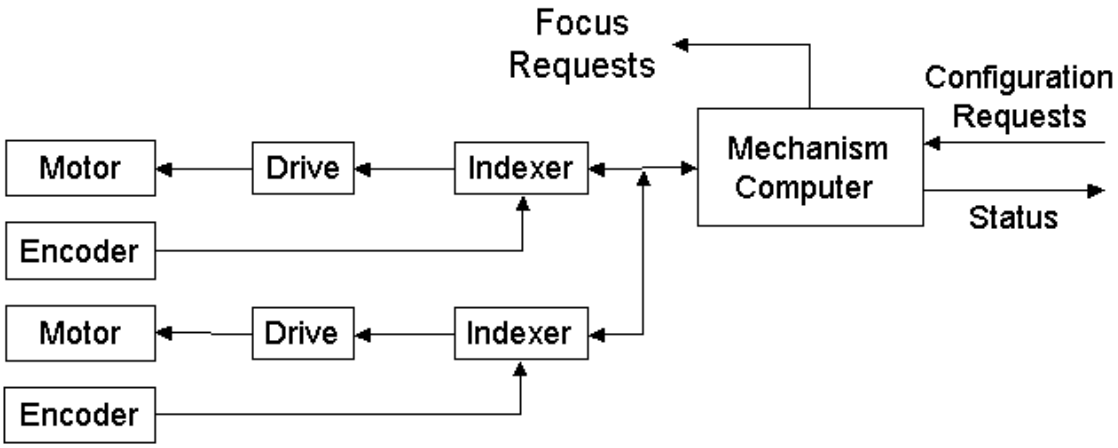

Figure 4.1: Basic mechanism control architecture for indexed mechanisms.

instruments use a single-board x86 processor computer running compiled BASIC code stored on flash RAM) integrated with the instrument motor control package. The mechanism computer software services configuration requests from the user (issued via the high-level data-taking software described in §6.3), and returns position status information or an error message. The interface provides low-level commands (e.g., "move motor X so many steps", "read encoder Y", etc.), and high-level commands that handle the various low-level move-and-sense operations necessary to make a mechanism setting (e.g., "select filter position 1", "what is the red grating tilt?" etc.). It also maintains a table of the status of each mechanism that may be queried to get a snapshot of the current instrument mechanism configuration. Low-level configuration request validation is also performed by this system (e.g., it returns an error if an out-of-range position is requested). Each mechanism motion is controlled by a dedicated stepper motor driven and drive.

Given the complexity of MODS and the time it takes to change the configuration of the instrument, we will be making a departure from our previous "one mechanism at a time" model and provide the capability to move non-conflicting mechanisms in parallel. This would allow, for example, commanding the system to select a new grating and tilt, refocus the camera, and select a new filter simultaneously.

4.3.2 Flexure Control System Controller

The FCS requires a set of active controls to steer the camera primary mirror in tip, tilt, and focus (piston) in response to feedback from the reference laser position and temperature sensors. Because it is vested with real-time requirements, the FCS has its own dedicated control computer connected to the general instrument mechanism computer.

Requests for focus changes, which use the same actuators as the FCS, are routed to the FCS computer for servicing. This avoids control conflicts between the different controllers. The basic architecture of the FCS is shown in Figure 4.2. The precise architecture of this system (e.g., DOS vs. Linux) is to be determined by which FCS scheme we ultimately adopt. The functional block diagram shows a reasonable sketch of what types of inputs and outputs we can expect.

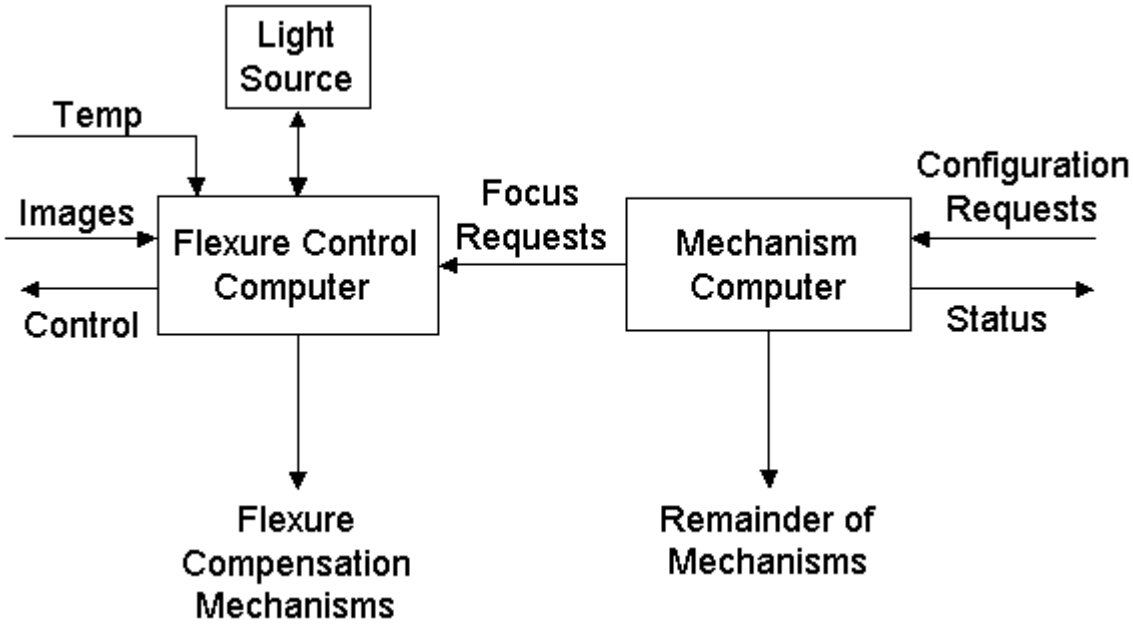

Figure 4.2: Basic architecture of the FCS for MODS. The Mechanism Computer at right is the same as in Figure 4.1.

5 Detectors

5.1 Introduction

The MODS detectors will be used at the focal plane of the spectrograph camera described in section 2. The camera illuminates a detector of up to ~123 mm long in the dispersion direction and ~43 mm in the direction along the slit. This corresponds to a detector comprised of roughly 8K×3K 15 μm pixels. The camera is a Maksutov-Schmidt design that would normally have a trapped focus; that is, the focal surface would be in the incoming beam. However, MODS uses a de-centered design. Only a sub-aperture of the parent camera is used. If the sub-aperture is sufficiently off-axis the detector does not vignette the incoming beam. As the sub-aperture is moved farther from the optical axis of the parent camera, more room is available to mount the detector, but at the expense of degraded image quality. We have determined that an optimal location for the detector, one which leaves sufficient room for mounting the CCD and which does not vignette the incoming beam and which produces good image quality, allows for 22 mm of mounting room for a 62 mm wide detector.

Figure 3.9 (§3.3.8) shows the configuration of the camera and the location of the detector. In the figure the light from the grating enters from the left. The beam expands as it approaches the camera primary (on the right) because of the finite field angle required for the dispersion from the grating. The detector is the blue rectangle above the incoming beam about half way between the corrector (not shown) and the primary mirror. The large octagonal structure above the beam is the filter wheel and the cylindrical purple space shows the volume available for the cryogen reservoir.

5.2 Detector Selection

5.2.1 The Ideal Detector for MODS

As discussed in section 5.1, the ideal detector for MODS would have a format large enough to allow observations at all possible wavelengths simultaneously with moderate spectroscopic resolution and read noise low enough to allow for digital beam combination to exploit the full aperture of the LBT. Shown in Figure 5.1 is what we consider to be the optimal detector format. The full area illuminated by the camera is covered (even though not all of that area will be used in all observing modes). The main detector area is divided into four horizontal strips with the left and right halves begin mirror images of each other. The detector is divided in the vertical direction, making the horizontal strips, to allow for the possibility of split frame transfer. In the split frame transfer mode the Image sections labeled AI, BI, CI and DI would be used to collect the light. When the exposure is complete the charge can quickly (about 1 second) be transferred to the corresponding Storage sections AS, BS, CS and DS. Splitting the frame transfer and reading out from both sides of the detector allows for fewer transfers, on average, between pixel and the output amplifier and increases the locations where it is easy to implement output amplifiers. A new exposure can then begin while the data is read from the storage sections. Since it is desirable to avoid having to trade off readout speed for noise, multiple amplifiers are provided at each corner of the detector.

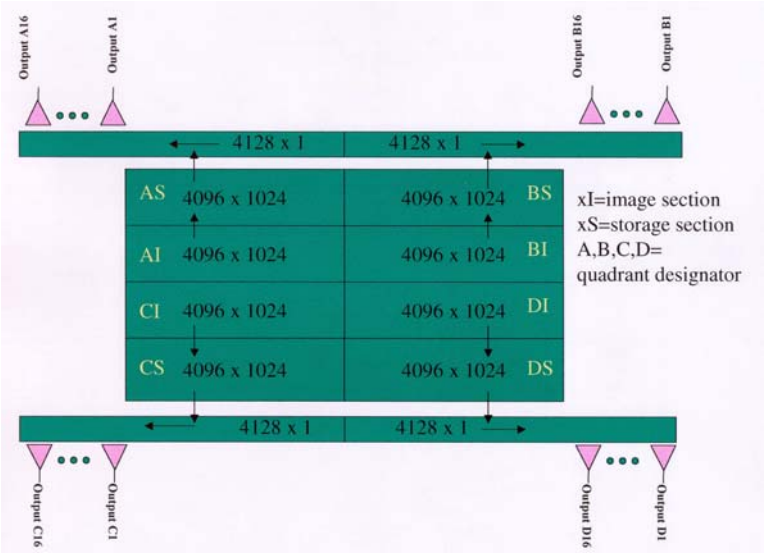

Figure 5.1: Optimal MODS Detector Format

All 64 outputs should be floating gate skipper structures. A single reset clock can be used for all 16 amplifiers in a quadrant as well as a single connection for all sixteen-output drains. One phase of the vertical clocks can be common to all eight vertical sections with out loss of flexibility. The total number of vertical clocks would then be 17. One phase can be common to all four serial registers for nine total clocks. The skipper structures require an additional 5 clocks. This ideal 4K×8K could be a single detector or a 1×2 array of 4K×4K devices. The single detector can be fabricated on 6-inch wafers but at the cost of having only one device per wafer. Forming the detector from two 4K×4K devices has the advantage of a better probable yield but at the expense of a gap between the two devices.

The frame transfer architecture allows an exposure to begin while the previous exposure is being read. This allows for relatively long read times and the consequent reduction in read noise without compromising observing efficiency. Of course, the storage sections must be masked to prevent stray light from contaminating the image during readout. Since the mask must be removed to use the full height of the detector it will be located a small distance away from the detector surface and will therefore be slightly out of focus. A small buffer zone must be defined between the image and storage areas to allow for the blurry edge of the mask

In imaging mode only the central 2880×2880 pixels will be used. Frame transfer will not be needed in this mode due to the relatively high sky background in all imaging applications. In the 6′ long slit mode or in the largest area multislit mode, a 2880×8192 pixel area of the detector will be used. Frame transfer will not be possible in this mode, since the remaining detector area is not large enough.

In the mode where the slit height or the distribution of multislits is limited to 4′ a 1920×8192 pixel section of the detector will be illuminated. When frame transfer is desired the remainder of the device will be divided into two 128×8192 buffer areas and two 960×8192 storage areas. Note that, in order to shift the image to the storage area, the

used image area will be clocked in the vertical direction 128 times more that the number of rows. In addition to leaving the image in the correct position on the detector for readout any reasonable amount of deferred charge will be removed from the image area. Figure 5.2 shows a schematic representation of the device in this mode.

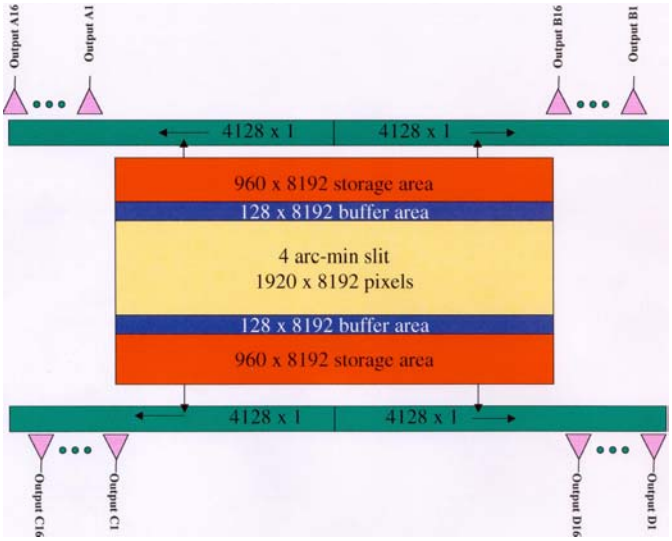

Figure 5.2: Frame-transfer CCD layout.

The MODS detectors must be very low noise (~1 electron RMS) if they are not going to limit the signal to noise in some applications. The situation that demands the lowest read noise is high-resolution spectroscopy of faint sources through small apertures. Even if only some of the adaptive optics schemes now proposed are implemented there will be times that observations will be appropriate with effective apertures having only 0.1 arcsec^2. At moderate and high resolution the sky will only contribute only a few detected photons in 1000 seconds. Detected signal-to-noise can be increased, up to a point, by increasing the electronic integration time on each pixel. However, when the frequencies included in the integral begin including the low frequency, 1/f, noise present in all detectors, the resulting signal-to-noise stops increasing. Skipper amplifiers avoid this problem by modulating the signal with a carrier above the 1/f corner and integrating by synchronous detection. With skipper amplifiers the signal-to-noise increases as the square root of the integration time.

Janesic et al have reported the signal-to-noise gains of skipper amplifiers. Their system operated with a read noise of less than one electron RMS. Geary and Luppino have designed and built a device with 8 skipper amplifiers distributed along a serial register. We operate this device in the lab using our standard controller architecture. We have confirmed multi-output mode operation and measured noise reduction from multiple non-destructive reads of the device. Further measurements and device characterization tests are underway.

5.2.2 Choices for MODS Detectors

The ideal MODS detector with large format, skipper amplifiers, and frame transfer, does not currently exist. If the budget of the project allows, we will pursue the option of

creating a new CCD mask set that defines the ideal detector and organize "foundry runs" to produce the required raw devices. The wafers containing the raw devices can then be probed and graded; suitable wafers can be processed into finished devices. If designed properly, these devices will be well-suited to many astronomical and other low noise applications, so we anticipate that part of the costs of this approach could be shared among various interested parties. Note that Mike Lesser (Steward Observatory) and Richard Bredthauer have expressed interest in designing a CCD like the one described here. Mitel Semiconductor has a 6-inch wafer CCD production line that can produce the required wafers.

If the budget is too tightly constrained or if custom devices are unobtainable on the timescale required for the project, several acceptable options exist. For example, several manufacturers currently make 2K×4K devices that can be used in pairs for a nearly contiguous 2K×8K detector. Both SITe and Marconi make devices in this format that have good quantum efficiency and low read noise. Furthermore, two of the 4K×4K devices now being fabricated at Mitel could be mounted in a common package with a relatively small gap. The resulting 4K×8K device, while not having skippers or frame transfer, would cover the entire focal surface of the MODS optical design.

5.2.3 CCD Anti-Reflection Coatings and Material Choices

The dual-beam approach we have adopted for MODS allows for a choice of CCD anti-reflection coatings that can be optimized for a more restricted wavelength than is often possible. For example, a variety of CCD anti-reflection coatings exist for the blue channel CCDs. Some examples are shown in Figure 5.3, which shows measured quantum efficiency curves for CCDs coated by M. Lesser. Note that all are equivalent at 500 nm.

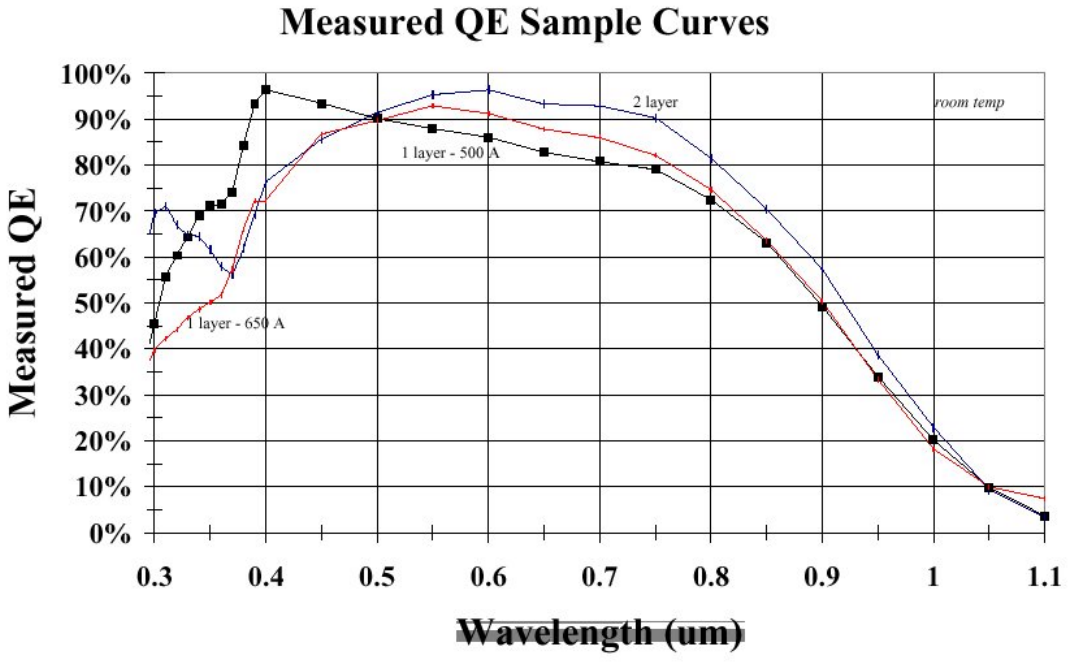

Figure 5.3: Possible AR choices for MODS CCDs.

Furthermore, except for the relatively rapid drop in quantum efficiency in the ultraviolet, a simple single layer (50 nm) coating gives very good performance. Since the blue channel should be rarely used for observations beyond 550 nm, the somewhat degraded performance of this coating in the red is unimportant. We plan to work with Mike Lesser to define coatings for the MODS CCDs that will optimize performance in each channel.

Figure 5.4 shows the quantum efficiency of high resistivity devices currently being produced by LBNL. If this technology can be applied to large format CCDs and if the "cosmic ray" event detection rate is acceptable, then these sorts of devices offer the possibility of unprecedented quantum efficiency in the red. We plan to fully investigate the use of such new technologies for MODS as appropriate.

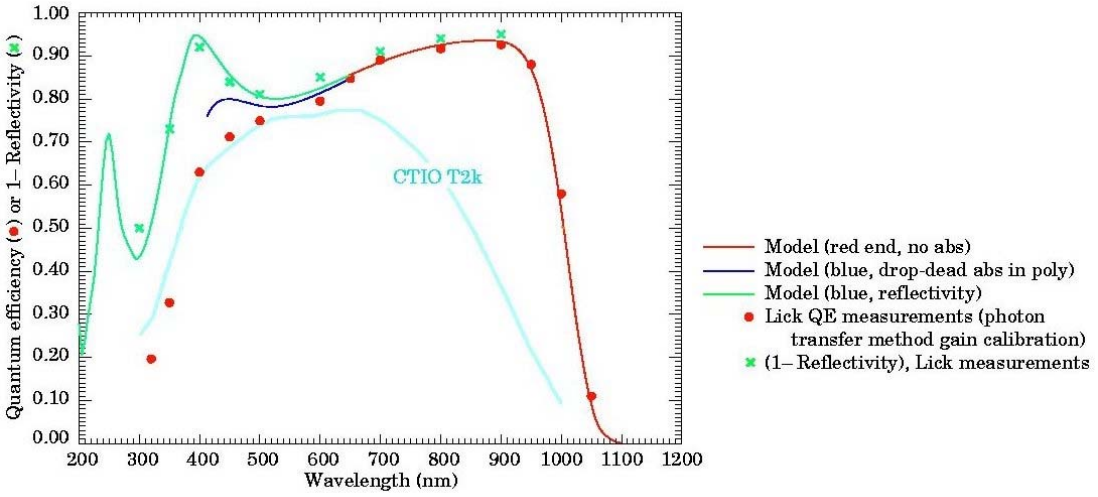

Figure 5.4: Quantum efficiency curves for LBNL red-sensitive CCDs.

5.3 Description of CCD Controller

The electronics for the MODS detectors will be the latest implementation of the ICIMACS system described in section 6. There are roughly 15 implementations of this system in use around the world and it has proven to be flexible and reliable. Requirements for the system pertinent to MODS include:

- *Very low system noise:* demonstrated electronics system read noises <1 e^- are required to not compromise the best-anticipated detector characteristics.
- *Adaptive binning in both axes:* variations in seeing and/or science requirements indicate that flexible binning arrangements for the system CCDs should be available.
- *Rapid read out times:* efficient use of telescope time requires rapid acquisition and calibration exposures. This is also required by some types of science observations.
- *Flexible controller configuration control:* the detector control electronics must be capable of exploiting many current and future CCD characteristics, including

region-of-interest, frame transfer, use of skipper amplifiers, read out through a large number of amplifiers (>32), etc.

Our standard detector controller system meets all these requirements. We currently operate many varieties of detectors with a standard controller architecture, including 1024×11024 HgCdTe HAWAII arrays, 1024×1024 InSb ALADDIN arrays, SITe 2048×2048 and 2048×4096 CCDs, and Loral/Lesser 2048×2048 CCDs. These detectors read out through as many as 32 amplifiers, have measured system noises <1 e^-, and include provision of variable read out configurations (i.e. allow for focus frames, region-of-interest, binning, etc.). We have also operated devices with skipper amplifiers using our controller architecture in the lab. For comparison, we estimate that we could read a 2880×8196 section of a CCD at read noise <5 e^- in ~30 seconds (assuming 8 amplifiers are available); similar performance has been demonstrated on several CCDs. Furthermore, our detector controller systems have operated for ~10,000 observing nights, with an uptime record of >99.9%.

The philosophy of the detector controller system rests on the reality that despite advances in digital signal processing, the analog circuits that amplify and define the bandwidth of the low level signals from astronomical detectors are a critical element in obtaining the best possible signal-to-noise ratio. Also, substantial experience with debugging and maintaining detector systems at remote locations guides the choice of architecture and hardware. For example, for improved modularity, flexibility in component selection, and to support our grounding strategy, we do not include any electronics components in the detector dewar. In addition, all circuits that connect to the detectors are located on a single board, the Clock-Bias-Board, which has a very robust ground plane. All connections between the Clock-Bias-Board and the detector dewar are made with a cable having miniature coaxial cables with an overall shield. The coaxial cables provide clean connection for the clock, bias, and signal connections to the detector. The shields for the clock and bias connections are connected at both the Clock-Bias-Board and the dewar end, and, in addition to shielding their respective signals, form a ground connection that has very low impedance at all important frequencies.

More details of our detector controller architecture are available if requested. However, we feel confident that control of the CCDs for MODS should not pose a major difficulty.

We do intend to incorporate several hardware improvements to the detector control system for MODS. These include

- *1 GHz fiber connections:* the faster link will eliminate the 5 Mpixel/sec limit of the current 120 MHz fiber link and provide better optical power budgeting. Performance monitoring will also be included.
- *PCI bus sequencer*: will allow the use of modern motherboards and deeper and wider pattern memory, and eliminate the bottleneck caused by the relatively slow ISA DMA transfer.
- *Use of largest available ALTERA device*: allows more options and flexibility in configuring read-out schemes

- *Switch to Flex Circuit for Thermal Break from Room Temperature:* much lower fabrication costs, more flexible detector shorting, and more consistent performance
- *Repackage Post Amplifiers using surface mount devices*
- *ADC for every channel:* upgrade to one ADC per channel using low-cost devices

Note that we currently intend to implement all these changes to our standard controller in an imaging system for the MDM Observatory. This will allow us the opportunity to test all these changes on a CCD system under actual observing conditions.

6 Data Acquisition & Instrument Control Software

6.1 Overview

The software to control the MODS instrument and acquire data falls into two basic categories:

Low-level Software to control hardware-level tasks:

- Real-time instrument mechanism control (grating, filters, etc.).
- CCD detector control, exposure timing, and data buffering for raw images.
- Coordination of autonomous and semi-autonomous instrument subsystems that have their own processors and associated software.
- Provide the interface to observatory subsystems, specifically the Telescope Control System (TCS), Guiding & Acquisition systems at each Gregorian Focus, and any Adaptive Optics (AO) and related systems (e.g., secondary mirror figure and focus, AO enable/disable, etc.).

High-level Software used by observers:

- Observing applications (data-taking program, data logging, etc.)
- Observing preparation & advance planning tools.
- Applications to enable remote and queue/service observing modes.

Each of these software categories will be discussed below. For MODS we will draw extensively upon our existing data-taking software, allowing us to concentrate our development efforts on those areas that are unique to the MODS instrument and the LBT observatory system.

6.2 Low-Level Software

The low-level software is used to control instrument mechanisms, operate the CCD controllers, receive and buffer images from the CCDs, assemble FITS headers, and deliver a FITS format image to disk. In addition it must provide entry points for the user interface layers and any other observatory systems that need information about the instrument status, and provide logging & instrument diagnostic functions.

6.2.1 Low-Level Software Heritage

Our current low-level system is ICIMACS (**I**nstrument **C**ontrol & **IM**age **AC**quisition **S**ystem), and has been used in all instruments built and deployed by OSU since 1992. ICIMACS is not a single program but rather it is a collection of autonomous systems (usually built around DOS PCs) that communicate via a uniform asynchronous messaging protocol. ICIMACS offers a simple, human-readable ASCII command syntax, and provides a bare-bones command line interface (no scripting). The primary mode of communication between ICIMACS processes is via serial (RS232) interfaces, although socket interfaces have been used in some configurations. All high-level

programs that interact with the low-level systems communicate via the ICIMACS messaging protocol. This protocol is described in a separate document.

We expect that DOS will remain available and useful for a long time to come. Far from being obsolete, DOS is found on virtually every desktop machine (do a search for "command.com" on any Windows 95/98/2000 PC and execute it). For us, DOS is particularly appropriate to the instrument computers in MODS, which, despite their physical resemblance to desktop PCs, have more in common with embedded systems: they run a single real-time program that performs the same set of activities continuously for the entire life of the instrument. In the embedded systems world, DOS remains popular for its small footprint, meager system requirements, and exclusive real-time tasking.

The current implementation of ICIMACS is written in BASIC on DOS PCs. Table 6.1 gives a summary of the instruments using our ICIMACS-based data-taking systems that have been deployed at various observatories.

Table 6.1: ICIMACS Deployment History

Site	Telescope(s)	Instruments	Detector(s)
Lowell	1.8-m & 1.1-m	CCD Imager	SITe 2048^2 CCD
KPNO	4-m & 2.1-m	TIFKAM	512×1024 InSb
MDM	2.4-m & 1.3-m	CCD Spectrograph	Loral 1200×800 CCD
		TIFKAM	512×1024 InSb
CTIO	YALO 1-m	ANDICAM	Loral 2048^2 CCD Hawaii 1024^2 HgCdTe
	4-m & 1.5-m	OSIRIS	Hawaii 1024^2 HgCdTe
SAAO	1-m	DANDICAM	Loral 2048^2 CCD Hawaii 1024^2 HgCdTe
Wise	1-m	CCD Imager	SITe 2048×4096 CCD
MSU	various	CCD Imager	Thomson 2048^2 CCD

The MODS low-level system will most closely resemble the ANDICAM and DANDICAM systems. These are dual-channel simultaneous CCD and IR imagers currently deployed at the 1-m YALO telescope (CTIO) and the 1-m Elizabeth telescope (SAAO), respectively. The data-taking system for the ANDICAMs operate the CCD and IR array cameras asynchronously: each detector has its own control computer, called the "IC" and "IR" respectively, running as part of an ICIMACS system.

Synchronization of CCD and IR data-acquisition is done at the user-interface level: we do not attempt to enforce hardware synchronization. This gives us flexibility in designing observing experiments. We can also operate instrument mechanisms during data acquisition, which permits us to dither short IR images using an internal IR tip/tilt while simultaneously acquiring a single long-exposure CCD image. The software to coordinate

these operations is vested in the user interface layer rather than at low levels, and is controlled using observing templates built by the observer with either external programs or a web-based form interface (the latter particularly used for YALO which is operated in a queue-scheduled mode). The system has proven very robust and reliable in nearly 2 years of continuous operations with the ANDICAM at CTIO.

MODS will reuse proven solutions refined in 2 years of continuous science operations with the ANDICAM at CTIO, where we take 1–2GB of CCD and IR imaging for various projects (in queue/service mode) every clear night except Christmas and New Years.

We will prototype key MODS software using these existing 2-channel instruments as a model. We have already begun this effort in the lab by converting the laboratory ANDICAM system to readout two 4K×8K CCDs (the arrays are "phantoms" that read noise from the sequencer electronics). We are using this system to determine the MODS data-transfer requirements, array software synchronization issues, etc. In general, if we had to deploy MODS today, we have the basic low-level software infrastructure already in place, if perhaps not optimized for MODS or the LBT environment. We need to address various issues with our current system, and the MODS project affords an opportunity to make a number of much-needed evolutionary changes, as will be described.

6.2.2 Example: The ANDICAM Data-Taking System

The layout of the current ANDICAM data-taking system is as follows. There are four basic layers shown in the block diagram below (Fig 1):

Detector Control PCs (IC & IR):

- Provide Real-time array control for each detector (1 computer per detector system)
- Assemble the exposure parameters, instrument state, and telescope pointing and timing information into FITS header records.
- Write the raw data onto transfer disks for storage on the observer workstation.

Instrument Mechanism Controller (IE):

- Controls instrument mechanisms (two filter wheels and a tip/tilt mirror for internal dithering of IR images).
- Replies to queries about the instrument configuration by other ICIMACS processes (e.g., IC, IR, WC, etc.)

ICIMACS Instrument "server" PC (WC):

- Coordinates the activities of the IC, IR, and IE computers.
- Buffers the incoming FITS images from each detector onto a data-transfer disk for storage on the observer's Unix workstation.
- Serves as the interface point for the YALO 1-meter Telescope Control System, here a PC/TCS system built by Dave Harvey, by filtering communications from

the PC/TCS into ICIMACS protocol format for the IC and IR, and for the user-interface layers.

Observer Workstation (Sparc 5/170 running Solaris 2.6):

- Runs the *Prospero* data-taking package. This is where the observer types data-taking and instrument configuration commands, and provides the primary user interface into the ANDICAM.
- Runs the *ariel* ICIMACS interface daemon that brokers communications between the Unix workstation and the DOS PCs (WC, IC, and IR).
- Runs the *caliban* data-transfer daemon that transfers FITS images from the WC computer and writes them onto the Unix workstation's raw data disks. The caliban daemon also performs real-time data logging functions.

A functional block diagram of the current ANDICAM data-taking system, showing how the elements all fit together, is shown in Figure 6.1.

As listed in Table 6.1 above, our ICIMACS/Prospero system is being used to control facility-class instruments at 6 observatories located on 4 continents. MODS will mostly require another, modified, implementation of our existing system, not a completely new development effort.

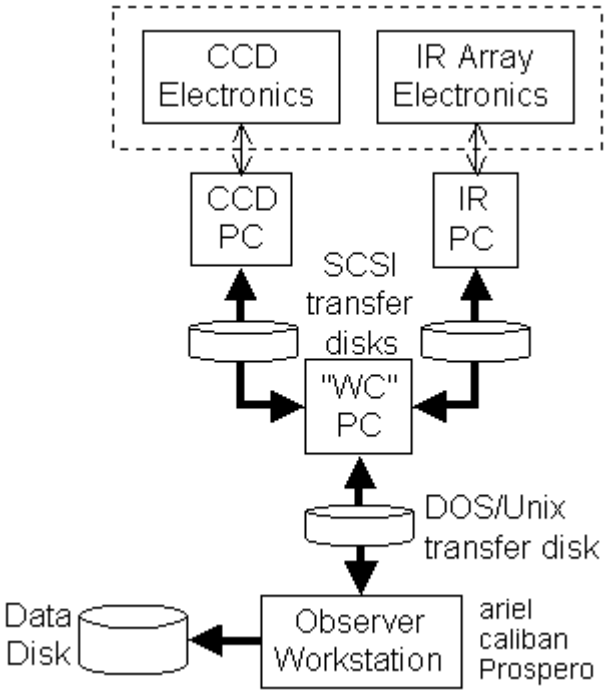

Figure 6.1: Functional Block diagram of the ICIMACS architecture for the ANDICAM.

6.2.3 ISIS: an Integrated Science Instrument Server

One of the least satisfactory aspects of our current data-taking system is the PC/Unix interface. Currently the functions at the coordination and control layers are split between

two machines: a DOS PC (called for historical reasons the "WC" as its first function was as the observer's "workstation" in the FORTH-based system that preceded ICIMACS), and Unix workstation running a pair of daemons ("ariel" and "caliban") that provide the entry points for the user interface. Unnecessary redundancy of function, synchronization issues, and ugly kludges in the basic interface have been problems for years. We have identified a path for eliminating these problems by developing an improved "instrument server" architecture that will merge the two existing systems into a single "integrated" system named ISIS (Integrated Science Instrument Server).

ISIS will be a common instrument server environment for all of our instruments, not just MODS, with these principal functions:

- Communications interface and low-level system coordination functions currently performed by the WC and ariel systems.
- Raw data storage and logging of images coming from detectors.
- Interface between the instrument systems and the observatory system.

As presently conceived, ISIS will be a PC running Linux, using modified versions of existing programs as well as a new "isis" server program that will replace the "wc.exe" and "ariel" programs. A functional block diagram of the ISIS system for MODS is shown in Figure 6.2.

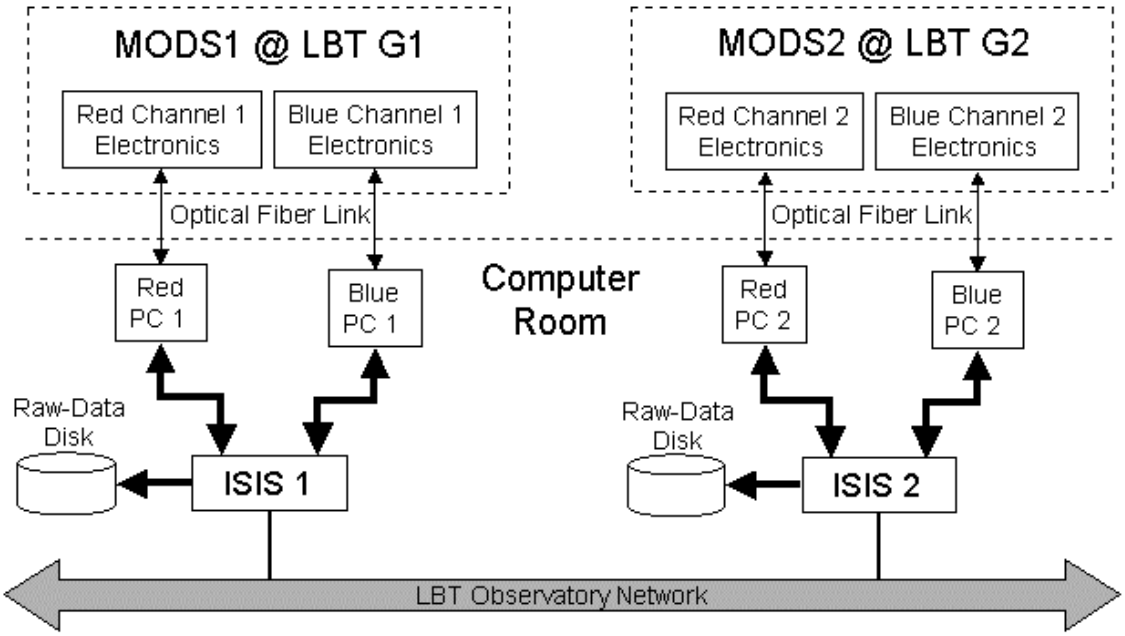

Figure 6.2: ISIS and ICIMACS layout for the low-level MODS system at the LBT

ISIS will provide the main entry point of MODS into the LBT Observatory system. Specifically, ISIS will provide the main interface point between MODS and

- the LBT TCS, Guider, and AO systems (as required)

- observing applications running on the observing workstation or remote clients will connect to ISIS to operate the instrument
- engineering applications, including those running on other machines, will interface to MODS via ISIS using tools (or interface specifications) provided by the MODS project.

The goal of the ISIS development is to make our existing instrument control and data acquisition architecture more open, allowing us the flexibility to develop new tools for observing and engineering functions without having to rewrite and recompile the low-level systems.

6.3 High-Level Software

The high-level software's primary responsibility is to provide a seamless interface into the MODS system for observers and operators. There are three basic tools needed:

1. Observing Interface: what the observer uses to take data and setup the instrument.
2. Engineering Interface: to provide access to low-level instrument functions for maintenance and troubleshooting.
3. Observing Preparation: tools to assist in observing planning and execution with MODS.

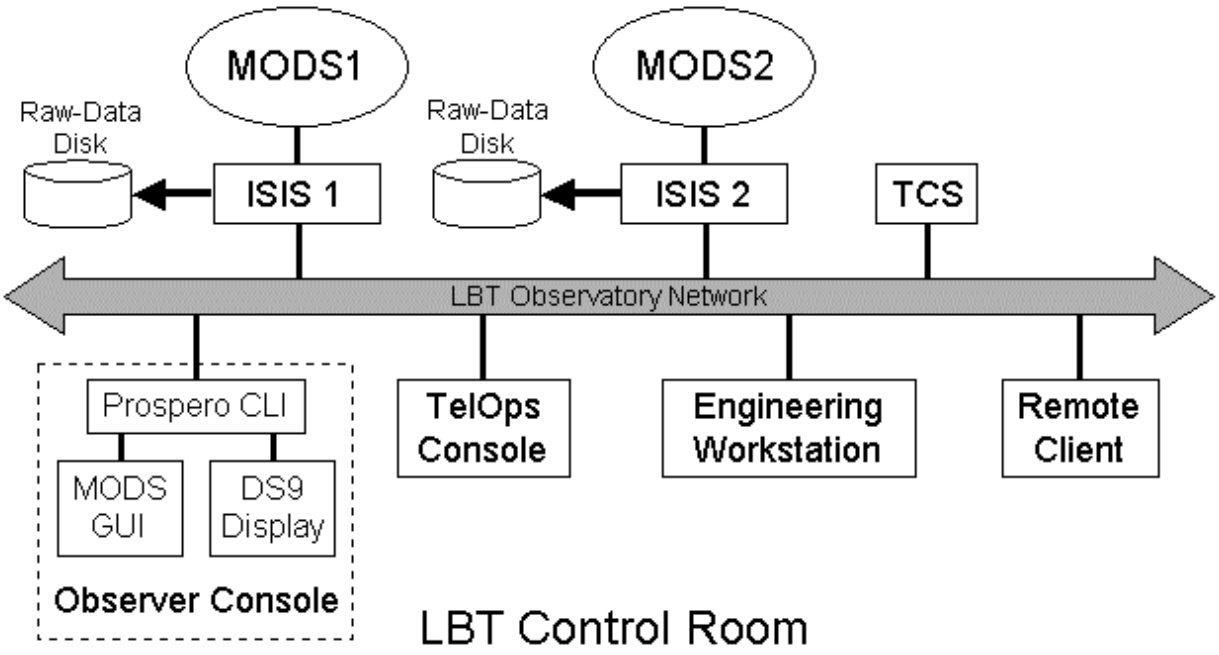

Figure 6.3: User interface layers for MODS, shown relative to the ISIS/ICIMACS system in Fig 6.2

The observing interface runs on the observer's workstation and provides commands for instrument control and data acquisition, as well as providing simple interaction with the telescope and related subsystems (e.g., query current telescope position, command small offsets or pointings, etc.). This application should provide, at a minimum:

- Command-line, scripting, and graphical user interfaces to MODS and related systems.
- Observing setup & execution utilities for local & remote operations.

The Engineering interfaces are applications designed to run on the TelOps console or an engineering workstation or laptop computer. These applications should provide at a minimum:

- Access to low-level instrument diagnostics and runtime logs.
- Access to low-level functions (CCDs, motors) for maintenance and troubleshooting.

Observing preparation applications should be portable so as to be easily installed on the observer's home computers and work the same as programs installed on the mountain. These include:

- Exposure time calculators
- Instrument setup and visualization tools
- Programs (web-based?) for preparing and submitting remote or queue/service mode observing instructions.

The basic User Software Architecture is shown in Figure 6.3, displaying how the interface layers map into the "ISIS" low-level architecture described above.

The high-level software development will consist of 3 main elements: the *XProspero* GUI, the *icsh* low-level ICIMACS command shell (an engineering application), and the *MODSView* instrument visualization tool, each described below.

6.3.1 *XProspero*: The Observer's view of MODS

The user interface for MODS should provide the following functions:

- Acquire data & execute observing scripts.
- Configure the instrument & telescope for an observation.
- Manage data acquisition in each of the red & blue channels in 2 MODS.

The MODS user-interface will be the based on the OSU *Prospero* package that has been in use for the past 9 years with all OSU-built instruments. Prospero uses the successful command-line and scripting model employed by the Vista and IRAF data-analysis packages, and was originally built on the Vista command and script parser. Prospero provides the observer with a rich, fully documented data-taking command set. Because we need to support a wide range of instruments at (currently) 6 different observatory sites, Prospero is designed to be auto-configuring. When Prospero starts, it asks for the instrument identity and loads an external "instrument configuration file" describing the instrument. Adapting Prospero to a new instrument is straightforward and very rapid: we need to write a new instrument configuration file for that instrument, and will have to add a small amount of low-level code to deal with idiosyncratic features of either the instrument or its observatory site. Our typical development time is 1 month from the

point we first get our hands on the instrument to a working field installation of the complete system. From our perspective MODS offers new mechanisms and features that will require a few software modifications to Prospero, but nothing major.

In a departure from previous practice, we will bow to the zeitgeist and develop a Graphical User Interface (GUI) for MODS: *XProspero*. XProspero will be a Tcl/Tk application layered on the current Prospero command-line package, modeled on the Keck dashboard UI used by ESI & DEIMOS. This approach allows us to retain the powerful Prospero command-line and command-scripting interfaces, while providing a GUI layer for the observer that provides full access to the Prospero command suite (including direct contact with ISIS and selected LBT TCS functions).

The features of the XProspero GUI will include:

- Graphical instrument configuration & status map.
- Full control of detector configuration & readout.
- Tools to setup & execute observations (single or dual).
- Tools to load & execute observing scripts written in the Prospero command language.

Modifications to Prospero to open its architecture to a GUI layer are straightforward and are being prototyped at this writing. This strategy lets us reap the benefits of our 9-year investment in Prospero by providing it with a new (arguably more fashionable) interface layer rather than scrapping it and starting over. To start on a new completely GUI-based data-taking system to replace rather than augment Prospero is impossible given our human resources and the project schedule.

6.3.2 *icsh*: an *ICIMACS* command shell

One of the problems of working with the current version of the ICIMACS system is that it practically requires you to be sitting at one of the DOS PC keyboards to have full access to the lowest-level commands. The current WC/ariel system has a closed architecture, and getting into the PCs from the Unix side, especially remotely over the Internet for troubleshooting, has been extremely difficult.

The ISIS architecture described in section 6.3.1 is designed from the start as an open architecture, and we are developing a Unix command shell, *icsh*, to provide a convenient low-level entry point into the ISIS/ICIMACS system for engineering and diagnostic work. The icsh program is being written in ANSI-C using the GNU *readline* and *history* utilities to provide a tcsh-like command environment. The engineering-level user will be able to interact with all instrument subsystems by typing ICIMACS-protocol commands and receiving the same responses they should see were they sitting at the consoles for each of the individual instrument PCs. We do this sort of thing in our current system in a rather roundabout way, but icsh will formalize the interface into a single, consistent tool.

6.3.3 *MODSView*: a *MODS* Visualization Tool

MODSView is a visualization tool that we originally developed to give us a better idea of how the MODS focal plane and offset guiding regions map onto the sky. It quickly

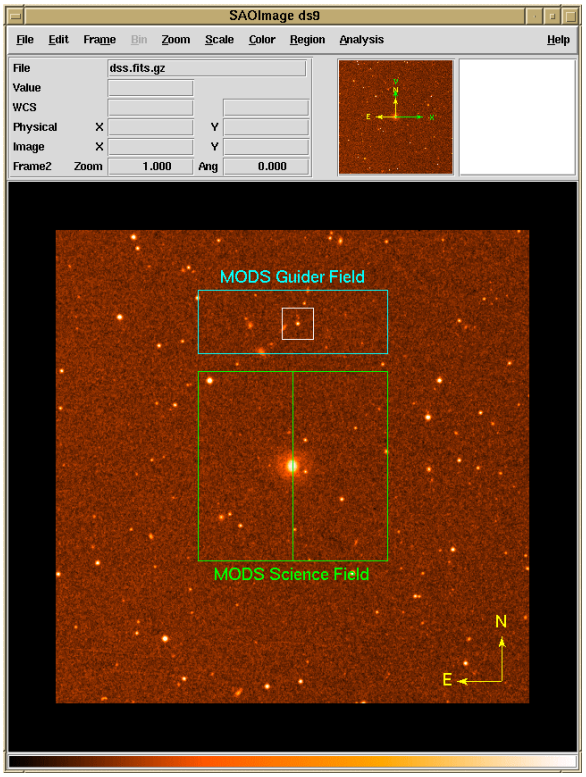

Figure 6.4: MODSView screenshot for a long-slit acquisition of a Seyfert galaxy with MODS.

became clear that a more advanced version of this program would be very useful for observing planning and for acquisition and guiding at the telescope, especially the identification and acquisition of suitable offset guide stars for a field. Our intention is to make MODSView available as a standalone package to member institutions as well as maintaining a "real-time" version on the mountain.

Given the celestial coordinates of the target and the instrument position angle, MODSView loads a Digitized Sky Survey (DSS) image of the field into DS9 and draws the MODS instrument and offset-guide fields over the image. In this view the observer can quickly identify potential guide-stars, as well as identify all objects falling within the instrument FOV. For observing planning, this lets the observer choose the optimal choice of position angles and guide stars in advance, reducing setup time at the telescope.

At the telescope, MODSView would read the telescope pointing and instrument rotation parameters from the TCS and show a DSS view of the sky as seen by MODS after target acquisition. This gives the observer or telescope operator (for remote or queue/service modes) a quick-look verification of the instrument position relative to the proposed target, and provides interactive tools for selecting guide stars after target centering and peak-up. MODSView will communicate with the LBT TCS and the MODS A&G system via ISIS to automate guide-star acquisition.

6.4 Development and Implementation

In building the MODS control system, we will build upon our successful 9-year heritage of operating a variety of sophisticated facility-class instruments with our ICIMACS/Prospero system. The basic software infrastructure is already in place except

for two new evolutionary elements (ISIS and the XProspero GUI), and MODS can be viewed, to first order, as yet another ICIMACS/Prospero instrument not as a completely new development project. This allows us to concentrate our limited programming resources and efforts on those aspects that will be unique to the MODS project. Development and implementation of the low- and high-level systems will proceed in parallel.

6.4.1 Low-Level Software

The primary task is to adapt ICIMACS for MODS architecture and to develop the ISIS system.

A prototype ISIS will be developed before actual work begins on the MODS hardware, and will be deployed at MDM for testing and evaluation with current instruments. Our intention is to make ISIS the model for all OSU instruments, not just MODS, so that when the MODS system begins to come together we will be applying a field-tested and proven ISIS, not a new development that has never seen starlight.

Specific Milestones:

- Adapt ICIMACS for MODS, including possible extensions of the protocol to make it easier to integrate four detector systems, and new readout modes.
- Develop and deploy a prototype ISIS system merging the current WC PC and ariel functions into a single Unix system. The first ISIS will be deployed at MDM for testing with our CCD spectrometer and TIFKAM IR imager spectrometer. The second phase will be to adapt ISIS to operate the ANDICAM at CTIO to acid-test coordinated 2-channel operations required for MODS.
- Adapt our current lab ANDICAM simulator into a MODS simulator to investigate raw-data transport & bandwidth issues (e.g., to see if we can keep using our current transfer-disk system, or to explore other options like a dedicated private gigabit network, etc.). This is already in progress.
- Implement & test instrument control modules in parallel with MODS fabrication.

6.4.2 High-Level Software

The main development task for the high-level software is to open the Prospero architecture to permit addition of a Tcl/Tk-based GUI. This is a new area for us, but we have the benefit of numerous examples, in particular we are in contact with De Clarke at Lick Observatory and are preparing to prototype a GUI based on their "dashboard" approach for Keck instruments (ESI and DEIMOS).

Specific milestones:

- Develop the prototype *XProspero* "dashboard" GUI.
- Extend the Prospero command set for MODS.
- Develop the *MODSView* program for observing planning and data-acquisition/guiding setup.

- Implement & test engineering applications (e.g., *icsh*) in parallel with MODS fabrication.
- Integrate the high- and low-level systems during MODS integration at OSU.
- Deploy with the Phase I instrument.

Other high-level software we will need for observing preparation is a tool for creating multiobject masks. For this we are investigating using the VIRMOS "mmu" software developed for the ESO VLT. This system is also used by other MOS spectrographs, and provides generic tools for translating astrometric positions of objects (either in absolute FK5 coordinates or image coordinates from frames taken through the instrument) into the (x,y) coordinates of slits to be machined into the mask substrate.

6.4.3 Coding Standards

Our group embraces the Open Source/Open Standards that have emerged in the software community. This is nothing more than a common-sense approach to software development in resource- and cost constrained circumstances. In particular, we shall

- Use public domain code as much as possible.
- Develop and maintain all of our source code in the public domain.
- Make extensive use of internal documentation and source control.

Pursuant to this, we are currently evaluating a number of public-domain software packages and utility libraries for our system. In particular, we are evaluating these software packages:

- Tcl/Tk for GUI development.
- cfitsio libraries for FITS support.
- SAOImage DS9 for image display.
- XPA messaging system for interprocess communication and access point services

The SAO XPA system is very promising, and is undergoing testing now, whereas we have already adopted the other packages. XPA offers a very simple and clean way to open our system architecture in a networked environment without having to re-invent socket-layer communications software. The support from SAO's High-Energy Astrophysics Division (who wrote XPA and SAOImage) has been terrific.

6.4.4 Software Testing & Acceptance

We intend to deploy a prototype ISIS & XProspero GUI at MDM and YALO 1-m (ANDICAM) for use in actual observing. We have chose to do this because:

- Many MDM interface issues are similar to those we face at LBT.
- ANDICAM will be an acid test of full 2-channel operation with the ISIS and XProspero systems.
- Observers break programs in ways we could never imagine because in general they refuse to read the manuals or use online help utilities.

MODS-specific system deployment will be used for all pre-commissioning activities at OSU as the MODS assembly, integration, and testing proceeds. We will deploy the full ISIS/Prospero system at LBT during commissioning.

6.4.5 Documentation

We follow the principle that you document as you go:

- Existing modules will have documentation adapted from the original system.
- New modules will be documented during alpha testing.

Specific deliverables with our system include:

- Low-level system technical manuals.
- Observer's manual.
- Observer's quick-reference card.

All of our documentation will be written in HTML, and we will develop indexing & search tools to accompany it. Hardcopy versions of the HTML documents (if such are required) will be generated using Adobe Acrobat, and bound in heavy-duty, 3-ring, vinyl-covered binders (e.g., National Brands model number 67-982 or equivalent).

6.4.6 Human Resources

While the software development work described above looks like a lot of work (and it is), we emphasize that most of the pieces already exist in our current system. Indeed, we could run MODS today with our existing system. Much of what we are doing is adding features to existing programs specific to MODS (e.g., a GUI interface and a new socket communications layer), adding LBT interface code (all TBD at this point since the LBT Project Office has not yet provided us with anything in this regard), and moving ahead on new versions of code already in the works but at low priority (e.g., ariel is already being recast as "ISIS", taking on formally functions it already possesses "informally" in versions not deployed in the field).

The primary human resource needs are the low-level programming tasks specific to MODS being undertaken by Jerry Mason, who is assigned full-time to instrumentation programming tasks. Given past experience, we do not anticipate any short falls in resources for programming. Modifications to Prospero for MODS are minor (adding a couple of new mechanism types to an existing internal data structure and building the necessary command hooks into existing command subroutines).

7 Project Management

7.1 Introduction

The MODS project is not the first instrument built by the OSU Astronomy instrumentation group. However, it is the largest instrument we have ever attempted. Nonetheless, given our stable instrument culture (the same people have been working together for roughly 10 years) and high level of previous success, we are confident of our abilities to complete the instrument on time and within the allotted budget. Indeed, many of the mechanisms and sub-systems that will be found in MODS will strongly resemble similar systems in our other instruments. We acknowledge that additional management is required for MODS compared to our other efforts, however, and explain our approach to project management (some of which is mandated by funding agencies and the LBT) in this section.

7.2 Staffing

The current OSU team dedicated to building MODS includes:

- P. Osmer-Department Chair and Principal Investigator; science requirements and overall responsibility
- D. L. DePoy-Co-PI and project manager; science requirements and organization
- R. W. Pogge-Project Scientist; science requirements and software development
- B. Atwood-Instrument Scientist; all aspects of instrument design and detectors
- T. O'Brien-Senior Mechanical Engineer; mechanical design, analysis, assembly, and test
- P. Byard-Optical Designer; optical design and oversight of optics fabrication
- D. Pappalardo-Electronics Engineer; electronics design, analysis, assembly, and test
- J. Mason-Software Engineer; low-level software and computer systems
- M. Derwent-Mechanical Engineer; mechanical design, analysis, assembly, and test
- D. Weinberg-Very Smart Astronomer; science requirements
- S. R. Belville-Mechanical Designer
- D. Steinbrecher-Machinist
- D. Brewer-Machinist and Welder
- E. Teiga-Electronics Technician

We expect to make additional hires for the project as needed. This team has been together since approximately 1990 (D. Pappalardo was hired in 1997; M. Derwent in 2001) and has been responsible for the design and construction of all OSU astronomical instrumentation.

7.3 Project Reviews and Risk Management

7.3.1 Periodic Review Plan

We review MODS progress in two ways: weekly team meetings and major design reviews. The weekly team meetings are attended by all MODS team members, including project scientists, engineers, graduate students, and technical staff. Occasionally, other interested parties also attend (typically other LBT partner representatives or potential instrument users). Generally, these meetings last approximately one hour, during which many kinds of MODS issues are discussed. Recently, for example, we have discussed the field and use of the ADC and a possible low-resolution mode of operation. Notes describing the discussions are available at http://www.astronomy.ohio-state.edu/LBT/MODS/Reports/index.html for each meeting (occasionally the discussions are not appropriate for general distribution, such as when we discuss major vendor selection; we do not report these discussions on the web). These meetings offer a rapid and flexible way to make decisions regarding MODS specifications, to monitor MODS progress, and to quickly identify aspects of the project that have encountered unanticipated difficulties. They also serve as an open forum to the LBT community on the decisions we have made regarding the instrument and we encourage feedback from potential users.

We are also committed to two types of more major design reviews. The first are yearly NSF-mandated progress reviews. These reviews will take the form of a meeting at which we will present annual progress reports to NSF staff and appointed outside reviewers. We will include at each presentation a program plan for the coming year showing planned activities and expected distribution of funds. These progress reviews will be held in May or June.

We are also subject to a series of LBT project-mandated reviews. These reviews follow the NASA/ESA formula of Conceptual/Preliminary/Final Design Review process. A meeting was help in March 1999 that was functionally the Conceptual Design Review for the project. At this meeting, in which 8 interested members of the LBT-partner communities participated, we received valuable input that helped to shape the design parameters for the instrument. The written record that came from that meeting is available in the Appendices of this document.

This document is the primary source of Preliminary Design Review materials. As mandated by LBT we provide this document to describe our work to date and demonstrate how our design and efforts map onto the science goals we have for the instrument. We seek meaningful input from the PDR review committee on any aspect of the design presented here or on issues that deserve additional attention.

7.3.2 Risk Management

In a project of this scale, the leading source of potential cost overruns is increased labor costs due to delays in fabrication, testing, or software development. All of our instrumentation staff (machinists, draftsmen, programmers, electronics fabrication, engineers, and scientists) are permanent salaried employees of the Ohio State University.

In the event of unforeseen delays, the Department agrees to cover any additional labor costs.

Detectors are another common risk factor in instrument development. MODS has been designed to permit the use of two 2K×4K 15μm pixel format CCDS; these devices have emerged as the workhorse CCD in ground-based astronomy. Nearly all large-instrument projects are using some variant of this detector. In addition, we have no extraordinary detector requirements, so detector procurement should not be a risk factor in this instrument. The aspheric surfaces required on the collimators, rear surface of the corrector plates and camera mirrors are all relatively mild by today's standards. Several different manufacturers can supply the sizes and materials required for the optics.

7.4 Fabrication & Assembly Strategies

7.4.1 Fabrication Strategy

7.4.1.1 Optical Fabrication

All of the optical fabrication work will be completed by outside sources. We have received bids on all of the optical components for MODS from multiple vendors. In particular, four different manufacturers have bid on the fabrication of the aspheric corrector singlet lens and the off-axis paraboloidal collimator mirrors.

7.4.1.2 Mechanical Fabrication

The Astronomy Department has a well-equipped machine shop that will do much of the mechanical fabrication for MODS using our CNC lathe and mill and specialized welding equipment. Some pieces of the instrument are inappropriate for our shop, such as the large support structure. For these pieces of the instrument we will contract to qualified vendors. For example, we may contract with the shop currently building the wind-bracing and secondary support structures for the LBT to fabricate the MODS support structure. In the past we have used outside vendors with great success and have experience with several in the central US that could provide useful services to the project.

7.4.1.3 Electronics Fabrication

Electronics and electrical fabrication for MODS is somewhat less extensive than the mechanical sub-systems. We expect that existing staff will do most of the required work.

7.4.1.4 Software Fabrication

Software for MODS will draw from legacy code in use on other OSU instruments. In particular, we have control and interface software for an optical spectrograph in operation at the MDM Observatory and for dual-channel (optical/infrared) imagers at Cerro Tololo Inter-American Observatory and South African Astronomical Observatory. The functionality available between these two instruments closely overlaps that needed to operate MODS. We believe that building the software for MODS will be a straightforward combination of these existing tools. We have connected our instruments to a wide variety of telescope interfaces (e.g. MDM, KPNO, CTIO, Lowell Observatory, and SAAO), so interfacing it to the LBT system should pose no special challenges.

We currently anticipate creating the MODS software with existing staff. We will re-evaluate software staffing needs as necessary and make additional hires as needed.

7.4.2 Assembly Strategies

MODS will be completely assembled in Columbus in the "high bay" area in the basement of McPherson Lab. Both internally and externally fabricated sub-systems will be gathered and integrated on the instrument structure as they become available. As each sub-system is assembled it will be tested in accordance with our quality assurance program (see below). No additional staffing or resources (space or equipment) are currently anticipated for assembly of the instrument.

Detailed assembly procedures cannot be defined until the instrument has a more advanced design. However, our modular philosophy will allow assembly procedures to be developed for each mechanism, optical assembly, and electronics sub-assembly well before the instrument undergoes final integration. This will streamline the documentation process (see below) and leave only the high-level assembly procedures for the end of the project.

7.5 Testing Program

MODS will be thoroughly tested in Columbus prior to shipment to the LBT. Each individual sub-system of the instrument will be tested as it is assembled and each implementation of the instrument checked comprehensively before deployment to Mt. Graham. All of these tests will be documented (see below).

7.5.1 Mechanical Testing

Mechanical testing will be conducted on several levels to insure reliable long-term operation of the instrument. In particular, individual mechanisms will begin testing for functionality, durability, and reliability immediately after they are fabricated and assembled. This will identify any deficiencies early in the program and allow any necessary re-work or re-design to proceed well before system integration begins. As each mechanism is tested and qualified, the next one fabricated will enter the testing process. This serial process of mechanism testing will result in a complete set of well-tested modules ready for high-level system integration, which is a key advantage of our standard modular approach.

Inspection and testing methodology will be modeled after that used by the FAA for aircraft modifications and maintenance. Every assembly or component will have a separate inspection; wherever possible the inspection will be performed by a person not involved in the fabrication.

The final level of testing will be with the fully assembled instrument (initially with reduced set of capabilities) using the instrument control electronics and instrument control software. This will allow testing of all high-level functions, instrument initialization routines, fault trapping and recovery, etc. At this point, simulated faults such as open wires, malfunctioning limit switches, stalled motors, etc. will be conducted as time permits to test instrument control software in as many states as possible.

The crucial flexure compensation system will also be thoroughly tested in the lab. We plan to build a telescope simulator that will allow the instrument to be moved through the full range of altitude and azimuth angles expected on the LBT. This will allow us to completely characterize and debug the flexure compensation system before deployment.

7.5.2 Electronics Testing

Our standard modular approach to the instrument electronics will allow us to test all components and sub-systems as they are fabricated or acquired and before system integration begins. We typically maintain an electronics package that simulates the functionality of the instrument electronics, for example, so each board or module can be tested while driving actual mechanisms.

The detector electronics will be tested separately before system integration. The ability to test the detector system independently of the instrument is essential to maintain the project schedule (see below). We currently anticipate obtaining a CCD similar to those that will be used in MODS and using it as an imaging system at our 2.4m and 1.3m telescopes in Arizona. This will allow us to gain valuable experience with the CCDs, characterize their performance, reliability, etc. under actual observing conditions.

7.5.3 Final System Testing

The final demonstration of MODS as a successful scientific instrument can only come as the result of a series of successful astronomical observations. Therefore, part of the test of the instrument will consist of a short but demanding series of scientifically useful observations. Some of these projects may be as described in section 1. The observations conducted with MODS will be reduced and analyzed by the project scientists to determine the scientific capabilities and performance of the instrument and ensure that it satisfies the project requirements.

7.6 Documentation

7.6.1 Fabrication and Testing Records

All assemblies within the instrument will be assigned a unique number and wherever possible assemblies will be indelibly marked with this number. Where more that one copy of an assembly is made, they will be assigned a sequential serial number. All assemblies and fabricated components will be based on detailed construction drawings that will clearly show the assembly number.

All steps in production and testing will be recorded in a notebook associated with an assembly or in the general notebook maintained by the personnel performing the fabrication or test. All assembly, disassembly, and re-assembly steps will be recorded in a notebook as well. The notebook will record the date, personnel involved, assembly numbers and serial numbers, and discrepancies observed. All testing and retesting will be recorded in a notebook. Test data will include a description of the test setup, personnel participating, and test outcome. Tests will be divided into initial functional checks with subsequent checks against each of the design requirements.

We believe that National Brand Computation Notebook Model 43-648 (75 sheets, 4×4 Quad ruled) and Boorum & Pease No.21 Columnar Book (when used with European style pagination) are acceptable units for the record keeping.

7.6.2 Documentation Provided to LBT

We have deployed instruments to many remote locations, as observing conditions are generally poor in Ohio. We generally prefer that the on-site observatory support staff provide the first line of instrument maintenance, problem identification, and repair. Therefore, we will provide a complete set of maintenance and operation data and procedures for the instrument in the form of manuals. These manuals will contain information sufficient to enable LBT Project personnel to perform all expected instrument operating and maintenance functions. The manuals will include discussion of all anticipated normal and emergency operating and maintenance procedures, spare parts, warranties, wiring diagrams, inspection procedures, performance curves, shop drawings, product data, future maintenance procedures, points of contact for additional information (such as names, addresses, telephone numbers, and e-mail addresses of persons fully acquainted with the instrument), and any other pertinent information. The manuals will include separate sections devoted to each major component of the instrument and will be organized into elements of manageable size, which will be adequately labeled and identified. We anticipate that much of the manual material will be in the form of PDF-format files that will be written onto a CD (or comparable media). Some of the manual material will necessarily be provided in heavy-duty, 3-ring, vinyl-covered binders (National Brands model number 67-982, for example, which is available in a wide range of colors and sizes and which has proven to be rugged and reliable in use on other mountain-top environments).

7.7 Budget

7.7.1 Project Cost Estimate

A total project cost estimate and expenditure plan will be available at the PDR meeting on June 11.

7.7.2 Tracking and Reporting

MODS is funded by a complex set of sources. These sources include the U.S. National Science Foundation, the state of Ohio Board of Regents for higher education, the Ohio State University Office of Research, the OSU College of Mathematical and Physical Sciences, and the OSU Astronomy Department. Furthermore, the instrument comprises a part of our capital contribution to the telescope construction. Therefore, we have a wide variety of requirements for tracking and reporting project effort and expenditures.

Within Ohio State, the Astronomy Department is managing the utilization of funds within the budgetary guidelines and procedures established by the College of Mathematical and Physical Sciences and the Office of Research. This also includes the submission of matching fund requests to the Ohio Board of Regents. The Astronomy Department front-office staff in conjunction with the PI and Co-PI typically handles the formal paperwork required.

We expect to write a contract with the LBT Project office for the construction of MODS after the conclusion of the PDR. This contract will likely include provision and specification of tracking effort and expenditures to meet LBT Project standards. We expect that this will involve at least quarterly effort and expenditure assessments.

7.8 Schedule

We have developed a detailed work breakdown structure for MODS that includes 568 separate tasks that must be performed to complete the instrument. These have been assigned effort estimates and specific human resources and have been scheduled and balanced against all on-going OSU operations and projects. Note these estimates for MODS are based on our experience building a large number of instruments for 2-4m class telescopes.

We expect to deliver the first full two-channel MODS to the LBT in mid-2005. However, since first-light for the telescope is expected in 2003, we will install a one-channel version of MODS (a "first-light" configuration that includes the red channel with a simplified slit mechanism) during second-quarter 2004. Thus, we will begin pursuing our science goals as soon as possible. Note that this "phased-deployment" of the instrument is consistent with our long-term goal of providing two complete two-channel MODS (one for each primary mirror of the LBT).

The full project schedule and Gantt chart will be available at the PDR on June 11.

Appendix A: Optical Prescription

This section gives the complete optical prescription for the red and blue channel optics for MODS. The descriptions are in the form of Code-V "sequence" (.seq) files. These files are available on the web at http://www.astronomy.ohio-state.edu/LBT/MODS/Data/ as files mods_red_v7glb.seq and mods_blue_v7glb.1.seq, respectively.

MODS Red Channel Optical Prescription

```
!file name: mods_red_v7glb.seq
!revised 11/14/00
!revised 01/10/01 changed rear radius of field lens to move stop image
between grating
!and corrector. There is no penalty in the error function and the
footprint on the camera
!mirror now agrees with the older values.
!_____________________________________________________________________

                        MODS RED SPECTROGRAPH
!_ ____________________________________________________________________
!
!BK7 Camera with filter in place. The error function of this camera is
119 for a 4 arc
!minute slit height with the slit in the center of the field.
!
! All surfaces up to and including the grating are specified in global
coordinates with
! respect to the vertex of the telescope focal surface.
RDM;LEN       "VERSION: 8.50       LENS VERSION: 50       Creation
Date: 16-Oct-2000"
TITLE 'MODS_red_v7glb'
EPD   8408.0
DIM   M
WL    1022.22179954 893.167368547 764.112937554 636.504491195
508.896044836
REF   3
WTW   0 0 80 0 0
INI   'PLB'

! The field angles and vignetting factors are for a centered 4 arc-min
high slit

XAN   -0.0333333333333 -0.0166666666667 0.0 0.0166666666667
0.0333333333333
YAN   0.0 0.0 0.0 0.0 0.0
WTF   1.0 1.0 1.0 1.0 1.0
!These are the vignetting factors for the secondary diameter above
VUY          0.01513       0.01515       0.01515       0.01515
0.01513
VLY          0.01513       0.01515       0.01515       0.01515
0.01513
VUX          0.01618       0.01568       0.01515       0.01459
0.01400
VLX          0.01400       0.01459       0.01515       0.01568
0.01618
```

```
!
SO    0.0 0.1e21
S     0.0 10663.69                          !position of secondary
S     -19200.004 -10663.69 REFL             !telescope primary
  CON
  K   -1.0
  CIR OBS 444.5
  CUM 0.0; THM 750.0
S     1974.2416 10663.69 REFL               !telescope secondary
  STO
  CON
  K   -0.7328021
  CUM 0.0; THM 300.0
S     -19200.0 3049.33                      !surface of primary
S     1014.0 0.0                            !telescope focal surface
S     500.0 6.0 SILICA_SPECIAL              !front surface of field lens
      GLB G5
  XDE 0.0; YDE 0.0; ZDE 65
  ADE 0.0; BDE 0.0; CDE 0.0
S     521.0 269.0                    !rear surface of field lens
S     0.0 0.0 REFL                          !front surface of dichroic
      GLB G5
  XDE 0.0; YDE 0.0; ZDE 275
  ADE 0.0; BDE 35.0; CDE 0.0
  CUM 0.0; THM 25.0
S     0.0 -310.0                            !dummy surface to realign
chief ray
  ADE 0.0; BDE 35.0; CDE 0.0
S     0.0 0.0 REFL                          !fold mirror
      GLB G5
  XDE 291.3047; YDE 0.0; ZDE 168.9738
  ADE 0.0; BDE 32; CDE 0.0
  CUM 0.0; THM 30.0
S     0.0 0.0                               !dummy surface to realign
chief ray
  ADE 0.0; BDE -38.0; CDE 0.0
S     0.0 2870.644615                       !dummy surface to locate
vertex of collimator
  ADE -6.855431; BDE 0.0; CDE 0.0
S     -6900.0 0.0 REFL                      !collimator mirror
      GLB G5
  XDE 589.2235; YDE -342.6532; ZDE 3003.4814
  ADE -5.7312; BDE -5.9702; CDE -0.5981
  CON
  K   -1.0
!  ADE 1.15543; BDE 0.0; CDE 0.0
  REX EDG 206.0; REY EDG 206.0
  ADY EDG 314.0
  CUM 0.0; THM 100.0
S     0.0 -3600.0                           !dummy surface to align chief
ray
  XDE 0.0; YDE 343.502466; ZDE -8.55028528369
S     0.0 0.0 REFL                          !location of grating (global
coordinates)
  GRT
  K   0.0; IC Yes
  A   0.0; B 0.0; C 0.0; D 0.0
```

```
  GRO -1; GRS 0.0030303030303
  GRX 0.0; GRY 1.0; GRZ 0.0
  GLB G5
  XDE 217.45843; YDE 357.55118; ZDE -533.62667
  ADE 16.8872882382; BDE -5.74303787383; CDE 1.74001099192
  REX EDG 153.0; REY EDG 204.0
  CUM 0.0; THM 30.0
S     0.0 0.0
  GLB G5                                  !dummy surface at front of
camera lens (global)
  XDE 286.05109; YDE 653.84151; ZDE 118.9889          !global position
w.r.t. slit center
  ADE 24.4183; BDE -5.4667; CDE 2.4766

!_____________________________________________________________________

!                       MODS RED CAMERA SECTION SEQUENTIAL FILE
!_____________________________________________________________________

! The first surface of each refractive surface is located globally with
respect to the surface preceding the camera
! section (S16 above for the red camera)
!
S     1235.946 40.0 BK7_SCHOTT                  !front of corrector
lens
  XDE 220.0; YDE 0.0; ZDE 0.0
S     1283.338 1032.524                         !rear (aspheric surface
of corrector lens)
  ASP
  K   0.0
  IC  Yes; CUF 0.0
  A   0.153297630669e-9; B 0.760658037634e-16; C 0.150995730012e-21; D&
   -0.658170470821e-28
S     -1525.0 -684.969 REFL                     !camera mirror
      GLB G16
      XDE 3.541; YDE 0.0; ZDE 1057.093
      ADE 0.0; BDE 8.159; CDE 0.0
      THM 80
!
S     0.0 -6.0 BK7_SCHOTT                       !filter front
      GLB G16
      XDE 220; YDE 0.0; ZDE 387.555
!
S     0.0 -2.0                                  !filter rear
S     -260.778 -25.0 BK7_SCHOTT                 !field flattener front
      GLB G16
      XDE 220; YDE 0.0; ZDE 379.555

!
S     0.0 -37.275                               !field flattener rear
S    0.0 0.0                                    !focal surface
      GLB G16
      XDE 220; YDE 0.0; ZDE 317.28
SI

ZOO   5
ZOO   WTW W1 0 80 0 0 0
```

```
ZOO    WTW W2  0  0  80  0  0
ZOO    WTW W3  80  0  0  0  0
ZOO    WTW W4  0  0  0  80  0
ZOO    WTW W5  0  0  0  0  80
ZOO    REF  3  1  2  4  5
GO
```

MODS Blue Channel Optical Prescription

```
!file: mods_blue_v7glb
!revised 11/14/00
!revised 1/31/00 position of field lens corrected to agree with red
channel
RDM;LEN       "VERSION: 8.50       LENS VERSION: 50       Creation
Date: 27-Oct-2000"
TITLE 'MODS bluechannel'
!_____________________________________________________________________

!                       MODS BLUE SPECTROGRAPH
!_____________________________________________________________________
!
!Fused Silica Camera with filter in place. and dichroic substrate in
place. Error
!function is dependent on whether dichroic is in or out.
EPD   8408.0 !diameter of primary mirror NB used diameter is less
DIM   M
WL    642.758576347 565.799121337 488.839666327 412.679255855
336.518845383
REF   3
WTW   0 0 80 0 0
INI   'PLB'
XAN   -0.0333333333333 -0.0166666666667 0.0 0.0166666666667
0.0333333333333 !Field values for a 4 arc-min slit
YAN   0.0 0.0 0.0 0.0 0.0
WTF   1.0 1.0 1.0 1.0 1.0
!These are the vignetting factors for the secondary diameter of 457 mm
calculated
!for a 4 arc-min slit height.
VUY          0.01513       0.01515       0.01515       0.01515
0.01513
VLY          0.01513       0.01515       0.01515       0.01515
0.01513
VUX          0.01618       0.01568       0.01515       0.01459
0.01400
VLX          0.01400       0.01459       0.01515       0.01568
0.01618
!
SO    0.0 0.1e21
S     0.0 10663.69
S     -19200.004 -10663.69 REFL                !Telescope Primary
  CON
  K   -1.0
  CIR OBS 444.5
  CUM 0.0; THM 750.0
S     1974.2416 10663.69 REFL                  !Telescope secondary
  STO
  CON
  K   -0.7328021
  CIR EDG 457.1                                !size of secondary for
f/15 @ focus
  CUM 0.0; THM 300.0
S     -19200.0 3049.33
S     1014.0 0.0                               !focal surface
```

```
S     500.0 6.0 SILICA_SPECIAL
      GLB G5                                    !location for front of
field lens
      XDE 0.0; YDE 0.0; ZDE 65.0
      ADE 0.0; BDE 0.0; CDE 0.0
S     521.00 269.0                              !rear of field lens

S     0.0 25.0 SILICA_SPECIAL                   !dichroic substrate
      GLB G5
      XDE 0.0; YDE 0.0; ZDE 275.0
      ADE 0.0; BDE 35.0; CDE 0.0
S     0.0 0.0                                   !rear surface of
dichroic

S     -6900.0 0.0 REFL                          !collimator
      GLB G5
  XDE 0.0; YDE 342.6532; ZDE 3445.77            !Value of zde with
dichroic
  ADE 5.70; BDE 0.0; CDE 0.0
  CON
  K   -1.0
  CUM 0.0; THM 100.0
S     0.0 0.0 REFL                              !grating
  GRT
  K   0.0; IC Yes
  A   0.0; B 0.0; C 0.0; D 0.0
  GRO 1; GRS 0.00181818181818
  GRX 0.0; GRY 1.0; GRZ 0.0
  GLB G5
  XDE 0.0; YDE -357.5510; ZDE -123.3558
  ADE -17.3; BDE 0.0; CDE 0.0
  CUM 0.0; THM 30.0
S     0.0 0.0                                   !dummy surface locating
camera (S10)
  GLB G5
  XDE 0.0; YDE -653.8413; ZDE 532.8646          !global position w.r.t.
slit center
  ADE -24.299999; BDE 0.0; CDE 0.0
!
!_____________________________________________________________________

!                      MODS BLUE CAMERA SECTION SEQUENTIAL FILE
!_____________________________________________________________________
!
! The first surface of each refractive surface is located globally with
respect to the surface preceding the camera
! section (S12 above for the blue camera)
!
S     2105.27833 40.0 SILICA_SPECIAL            !front of corrector
lens
      GLB G12
      XDE 220.0; YDE 0.0; ZDE 0.0
!
S     2406.55412 1147.0876                      !rear of corrector lens
(aspheric surface)
  ASP
  k  0.0
```

```
  A 0.156138556515e-9; B 0.258524237673e-16; C 0.388025729601e-21; D&
   -0.739378606444e-27
!
S     -1525.0 -691.750992 REFL                  !camera mirror
      GLB G12
      XDE 6.454; YDE 0.0; ZDE 1172.0825
      ADE 0.0; BDE 8.04; CDE 0.0
      THM 80
!
S     0.0 -6.0 SILICA_SPECIAL                   !filter front
      GLB G12
      XDE 220; YDE 0.0; ZDE 495.3366
!
S     0.0 -2                                    !filter rear
!
S     -244.34593 -25.0 SILICA_SPECIAL           !field flattener front
      GLB G12
      XDE 220; YDE 0.0; ZDE 487.3366
!
S     0.0 -26.8672044                           !field flattener rear
S     0.0 0.0
      GLB G12                                   !focal surface
      XDE 220; YDE 0.0; ZDE 435.469
!
SI    0.0 0.0
ZOO   5
ZOO   WTW W1 0 80 0 0 0
ZOO   WTW W2 0 0 80 0 0
ZOO   WTW W3 80 0 0 0 0
ZOO   WTW W4 0 0 0 80 0
ZOO   WTW W5 0 0 0 0 80
ZOO   REF 3 1 2 4 5
GO
```

Appendix B: Optics Bid Package

The following pages contain copies of the optics bid package for all of the MODS optics (both red and blue channels), including scanned/reduced copies of the optics drawings. We sent this package to 18 optics manufacturers. We received at least partial responses from 8 manufacturers to this package; 5 for the large optics including the camera correctors. Selection of manufacturers is currently in progress and a report will be given (if desired) at the PDR on 2001 June 11.

The following specifications and drawings are for optical components we need for a large astronomical spectrograph under construction at The Ohio State University. Two identical copies of the instrument will become part of the instrument complement for the Large Binocular Telescope (LBT). The LBT is scheduled for first light in 2003.

There are 7 items for which we request bids.

Qty	Part#	Description	Price	Delivery
2	FIELD_LENS_R1.dwg	Field lens		
4	COLLIMATOR_Rl.dwg	Collimator Mirror		
2	RED_CORRECTOR_Rl.dwg	Red Camera Corrector		
2	BLUE_CORRECTOR_R1.dwg	Blue Camera Corrector		
4	CAMIERA_PRIMARY_R1.dwg	Camera Primary Mirror		
2	RED_FLATTENER_R1.dwg	Red Camera Field-flattener		
2	BLUE_FLATTENER_R1.dwg	Blue Camera Field flattener		

Notes

Please consider the following comments:

1. Detailed optical specifications and tolerances for each item are included in the accompanying sheets and attached drawings.
2. We will provide BK7 Material for RED_CORRECTOR_Rl.dwg
3. We will provide Fused Silica material for BLUE_CORRECTOR_R1.dwg
4. We will provide 4 Hextek Blanks for COLLIMATOR_R1.dwg
5. We will provide 4 Hextek Blanks for CAMERA_PRIMARY_R1.dwg
6. All Items are to be quoted uncoated
7. Explanatory note on the surface error tolerances:

   The surface error tolerances for each item have been derived using structure function arguments considering the encircled energy requirements in the final image. These tolerances are expressed as maximum allowable rms surface deviations for given scale length. The surface deviation tolerances are expressed in units of wavelength (X) for a test wavelength of 633 nm.

8. Test data for each item for customer verification will be required. Please include a description of the test data to be provided with all bids.

Item 1: MODS SPECTROGRAPH FIELD LENS

Number of pieces to quote:	Quantity 2
Description:	Meniscus field lens
Material:	**UV-grade fused silica** (BPFS Coming #7980, Grade 0C)
Size:	Square, sides=230 mm, Center thickness 6 mm.
Surfaces:	both surfaces spherical
Coating:	uncoated
Drawing:	Attached drawing FIELD_LENS_R1.dwg

SPECIFICATION OF MAXIMUM SURFACE FIGURE ERRORS

The specification for the surface figure is specified as RMS values at 5 different scales as follows:

SCALE in mm	RMS error @ λ=633nm
<10	λ/10
10-25	λ/4
25-50	λ/4
50-100	λ/2
100 > 230	λ/2

Item 2:MODS SPECTROGRAPH COLLIMATOR MIRROR

Number of pieces to quote:	Quantity 4
Description:	Off-axis Paraboloid
Material:	**Hextek Substrates provided by Ohio State Refer to COLLIMATOR_BLANK_Rl.dwg**
Finished Size:	Square 490 mm by 490 mm. per drawing
Surface:	parabolic
Coating:	uncoated
Drawing:	Attached drawing COLL1MATOR_R1.dwg

SPECIFICATION OF MAX1MUM SURFACE FIGURE ERRORS

The specification for the surface figure is specified as RMS values at 5 different scales as follows:

SCALE in mm	RMS error @ λ=633nm
<10	λ/20
10-25	λ/20
25-50	λ/8
50-100	λ/3
100 > 230	λ/2

Item 3: MODS SPECTROGRAPH RED CAMERA CORRECTOR

Number of pieces to quote:	Quantity 2
Description:	**Decentered** meniscus Schmidt corrector lens
Material:	**BK7 Blank to be provided by Ohio State** **Refer to RED_CORR_SUBSTRATE_Rl.dwg**
Size:	Rectangular 440 mm x 320 mm.
Surfaces:	Surface 1 portion of decentered sphere Surface 2 portion of decentered asphere
Coating:	uncoated
Drawing:	Attached drawing RED-CORRECTOR-R1.dwg

1. DESCRIPTION OF ASPHERIC SURFACE

The sag z measured in a direction perpendicular to the vertex of the parent asphere to the surface as a function of distance y measured tangentially from the vertex of the parent asphere is described by the following expression.

$$z = \frac{cy^2}{1+\left[1-(1+K)c^2y^2\right]^{1/2}} + Ay^4 + By^6 + Cy^8 + Dy^{10}$$

where: the vertex radius r = 1283.338 mm, c= 1/r = .000779218

K=0
A=+0. 15329763067E-09
B=+0.76065803763E-16
C= +0.150995730OIE-21
D= -0.65817047082E-28

2. SPECIFICATION OF MAXIMUM SURFACE FIGURE ERRORS

The specification for the surface figure is specified as RMS values at 5 different scales as follows:

Convex spherical surface S1

SCALE in mm.	RMS error @ λ=633nm
<10	λ/10
10-25	λ/5
25-50	λ/4
50-100	λ/2
100 > 230	λ

Concave aspheric surface S2

SCALE in mm.	RMS error @ λ=633nm
<10	λ/5
10-25	λ/3
25-50	λ/2
50-100	1.3λ
100 > 230	2.4λ

Item 4: MODS SPECTROGRAPH BLUE CANMRA CORRECTOR

Number of pieces to quote:	Quantity 2
Description:	**Decentered** meniscus Schmidt corrector lens
Material:	**Fused Silica Blank to be provided Ohio State Refer to BLUE_CORR_SUBSTRATE_Rl.dwg**
Size:	Rectangular 440 mm x 320 mm.
Surfaces:	Surface 1 portion of decentered sphere Surface 2 portion of decentered asphere
Coating:	uncoated
Drawing:	Attached drawing BLUE_CORRECTOR_RI.dwg

1. DESCRIPTION OF ASPHERIC SURFACE

The sag z measured in a direction perpendicular to the vertex of the parent asphere to the surface as a function of distance y measured tangentially from the vertex of the parent asphere is described by the following expression:

$$z = \frac{cy^2}{1+\left[1-(1+K)c^2y^2\right]^{1/2}} + Ay^4 + By^6 + Cy^8 + Dy^{10}$$

where: the vertex radius r = 2406.554 mm, c = 1/r =0.0004155319

K=0

A=+0.15613855651E-09

B=+0.25852423767E-16

C=+0.38802572960E-21

D= -0.73937860644E-27

2. SPECIFICATION OF MAXIMUM SURFACE FIGURE ERRORS

The specification for the surface figure is specified as RMS, values at 5 different scales as follows:

Convex spherical surface S1

SCALE in mm.	RMS error @ λ=633 nm
<10	λ/10
10-25	λ/5
25-50	λ/4
50-100	λ/2
100 > 230	λ

Concave aspheric surface S2

SCALE in mm.	RMS error @ λ=633nm
<10	λ/5
10-25	λ/3
25-50	λ/2
50-100	1.3λ
100 > 230	2.4λ

Item 5: MODS SPECTROGRAPH CAMERA PRIMARY MIRROR

Number of pieces to quote:	Quantity: 4
Description:	Spherical Schmidt camera mirror
Material:	**Hextek Substrates provided by Ohio State** **Refer to CAMERA_PRIMARY_BLANK_Rl.dwg**
Size:	Rectangular 620 mm by 360 mm per drawing
Surface:	Spherical
Coating:	uncoated
Drawing:	Attached drawing CAMERA_PR1MARY_R1.dwg

SPECIFICATION OF MAXIMUM SURFACE FIGURE ERRORS

The specification for the surface figure is specified as RMS values at 5 different scales as follows:

SCALE in mm.	RMS error @ λ=633nm
<10	λ/20
10-25	λ/20
25-50	λ/8
50-100	λ/3
100 > 230	λ/2

Item 6: MODS SPECTROGRAPH RED CAMERA FLATTENER

Number of Pieces to quote:	Quantity 2
Description:	Section of plano-convex field flattener
Material:	BK7 (Schott BK7 Class H4 BO or better)
Size:	Rectangular 175 mm by 116 mm per drawing
Surfaces:	Surface 1 spherical Surface 2 plano
Coating:	uncoated
Drawing:	Attached drawing RED_FLATTENER_R1.dwg

SPECIFICATION OF MAXIMUM SURFACE FIGURE ERRORS

The specification for the surface figure is specified as RMS values at 5 different scales as follows:

SCALE in mm.	RMS error @ λ=633nm
<10	λ/10
10-25	λ/4
25-50	λ/4
50-100	λ/2
100 > 230	λ/2

Item 7: MODS SPECTROGRAPH BLUE CAMERA FIELD FLATTENER

Number of pieces to quote:	Quantity 2
Description:	Section of plano convex field flattener
Material:	UV grade fused silica (BPFS Coming #7980, Grade OC)
Size:	Rectangular 175 mm by 116 mm per drawing
Surfaces:	Surface 1 spherical Surface 2 plano
Coating:	uncoated
Drawing:	Attached drawing BLUE_FLATTENER_R1.dwg

SPECIFICATION OF MAXIMUM SURFACE FIGURE ERRORS

The specification for the surface figure is specified as RMS values at 5 different scales as follows:

SCALE in mm.	RMS error @ λ=633nm
<10	λ/10
10-25	λ/4
25-50	λ/4
50-100	λ/2
100 > 230	λ/2

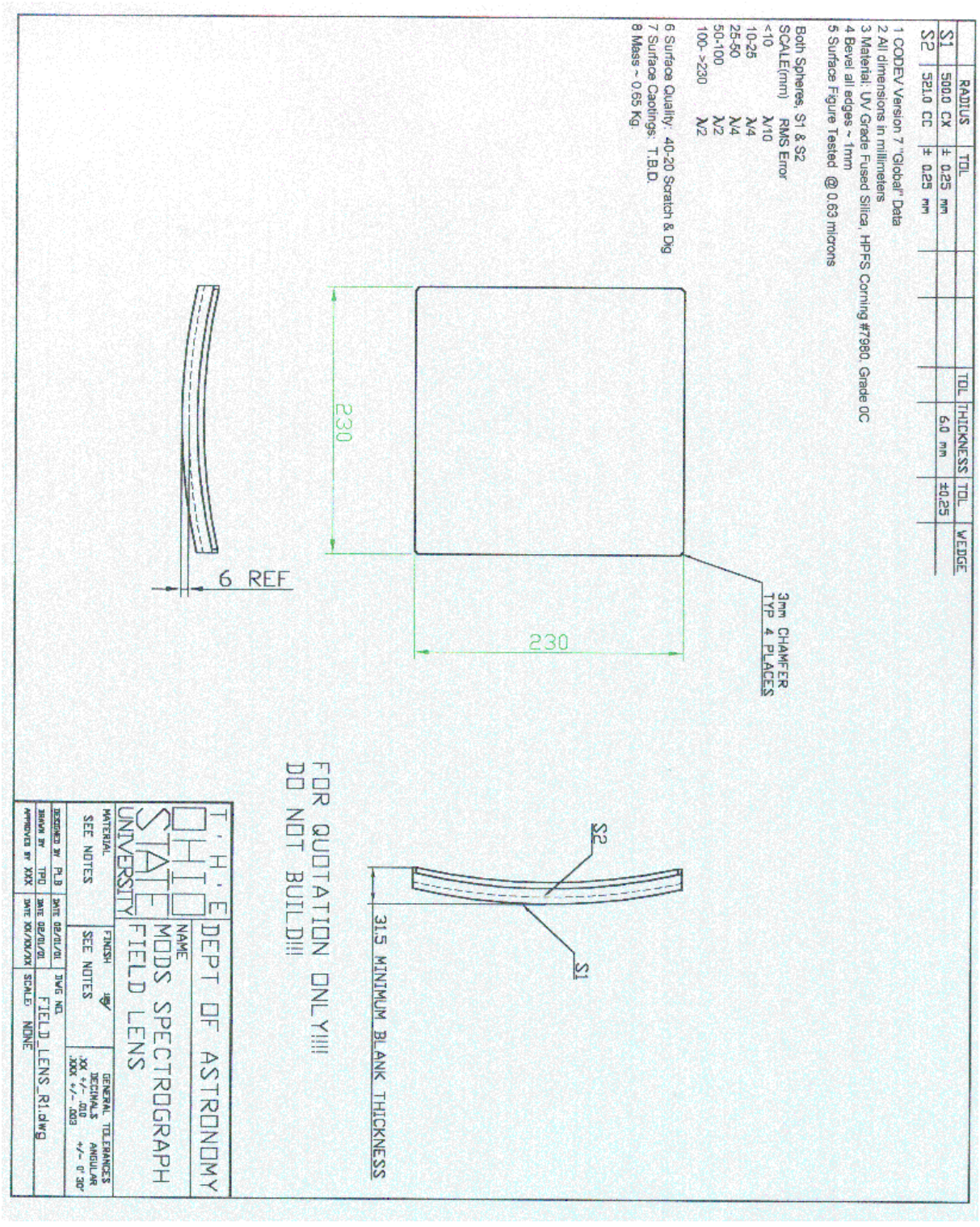
RADIUS TOL
S1 500.0 CX ± 0.25 mm
S2 521.0 CC ± 0.25 mm
TOL THICKNESS TOL WEDGE
6.0 mm ±0.25
1 CODEV Version 7 "Global" Data
2 All dimensions in millimeters
3 Material: UV Grade Fused Silica, HPFS Corning #7980, Grade 0C
4 Bevel all edges ~ 1mm
5 Surface Figure Tested @ 0.63 microns
Both Spheres, S1 & S2
SCALE(mm) RMS Error
<10 λ/10
10-25 λ/4
25-50 λ/4
50-100 λ/2
100->230 λ/2
6 Surface Quality: 40-20 Scratch & Dig
7 Surface Caotings: T.B.D.
8 Mass ~ 0.65 Kg.
6 REF
230
230
3mm CHAMFER TYP 4 PLACES
S2
S1
31.5 MINIMUM BLANK THICKNESS
FOR QUOTATION ONLY!!!!
DO NOT BUILD!!!
T.H.E. OHIO STATE UNIVERSITY
DEPT OF ASTRONOMY
NAME
MODS SPECTROGRAPH FIELD LENS
MATERIAL
SEE NOTES
FINISH
SEE NOTES
GENERAL TOLERANCES
DECIMALS
ANGULAR
DESIGNED BY PLB DATE 02/01/01
DRAWN BY TPO DATE 02/01/01
APPROVED BY XXX DATE XX/XX/XX
DWG NO. FIELD_LENS_R1.dwg
SCALE: NONE

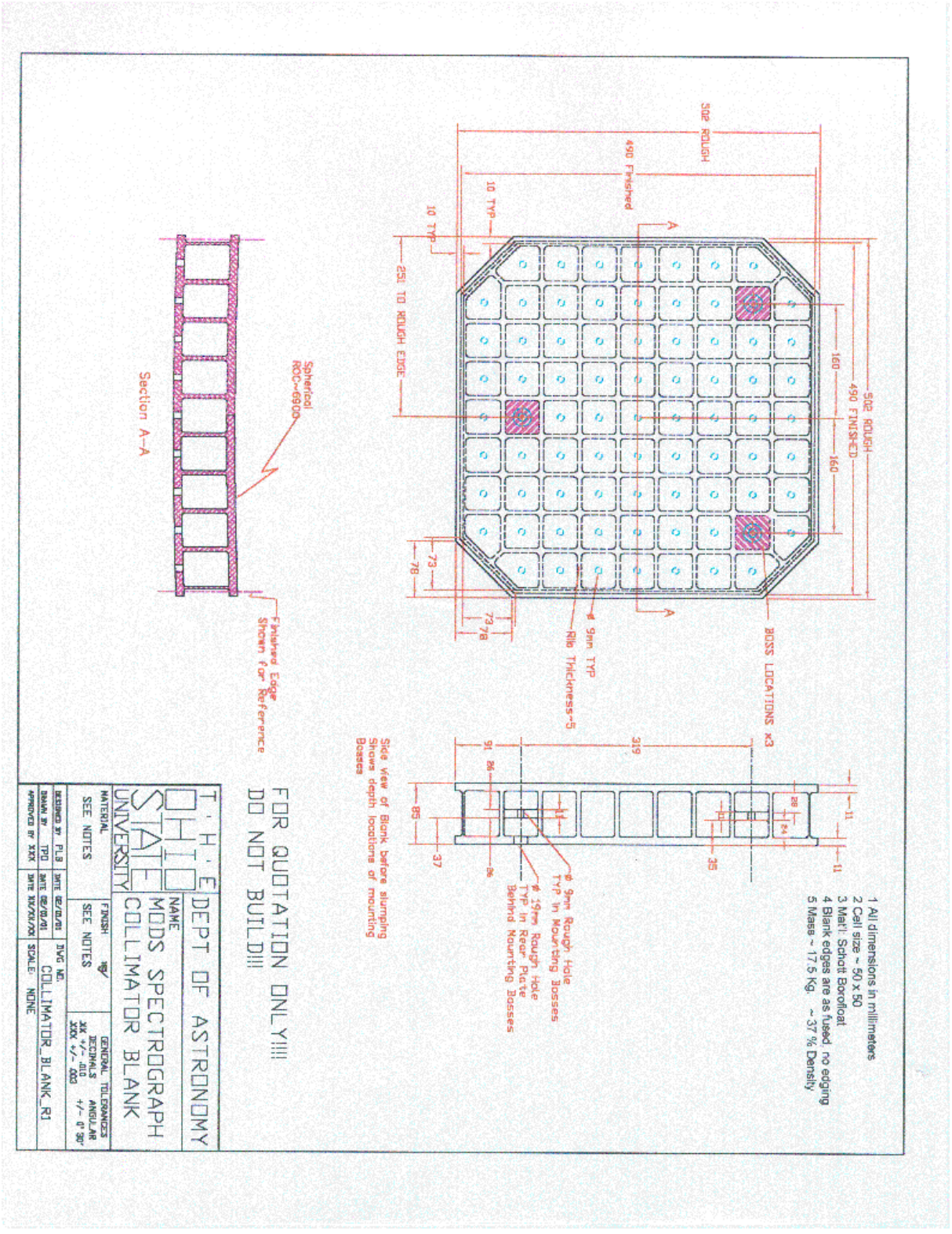
1 All dimensions in millimeters
2 Cell size ~ 50 x 50
3 Matl: Schott Borofloat
4 Blank edges are as fused, no edging
5 Mass ~ 17.5 kg. ~ 37 % Density
502 ROUGH
490 FINISHED
160
160
502 ROUGH
490 Finished
10 TYP
10 TYP
251 TO ROUGH EDGE
73
78
73
78
9mm TYP
Rib Thickness=5
BOSS LOCATIONS x3
Section A-A
Spherical ROC=6900
Finished Edge Shown for Reference
Side view of Blank before slumping
Shows depth locations of mounting Bosses
319
91
86
85
37
35
11
11
28
84
86
Ø 9mm Rough Hole TYP in Mounting Bosses
Ø 19mm Rough Hole TYP in Rear Plate Behind Mounting Bosses
FOR QUOTATION ONLY!!!!
DO NOT BUILD!!!
THE OHIO STATE UNIVERSITY
DEPT OF ASTRONOMY
NAME
MODS SPECTROGRAPH
COLLIMATOR BLANK
MATERIAL
SEE NOTES
FINISH
SEE NOTES
GENERAL TOLERANCES
DECIMALS
ANGULAR
DESIGNED BY PLB
DRAWN BY
APPROVED BY XXX
DATE 02/05/01
DATE 02/05/01
DATE XX/XX/XX
DWG NO.
COLLIMATOR_BLANK_R1
SCALE: NONE

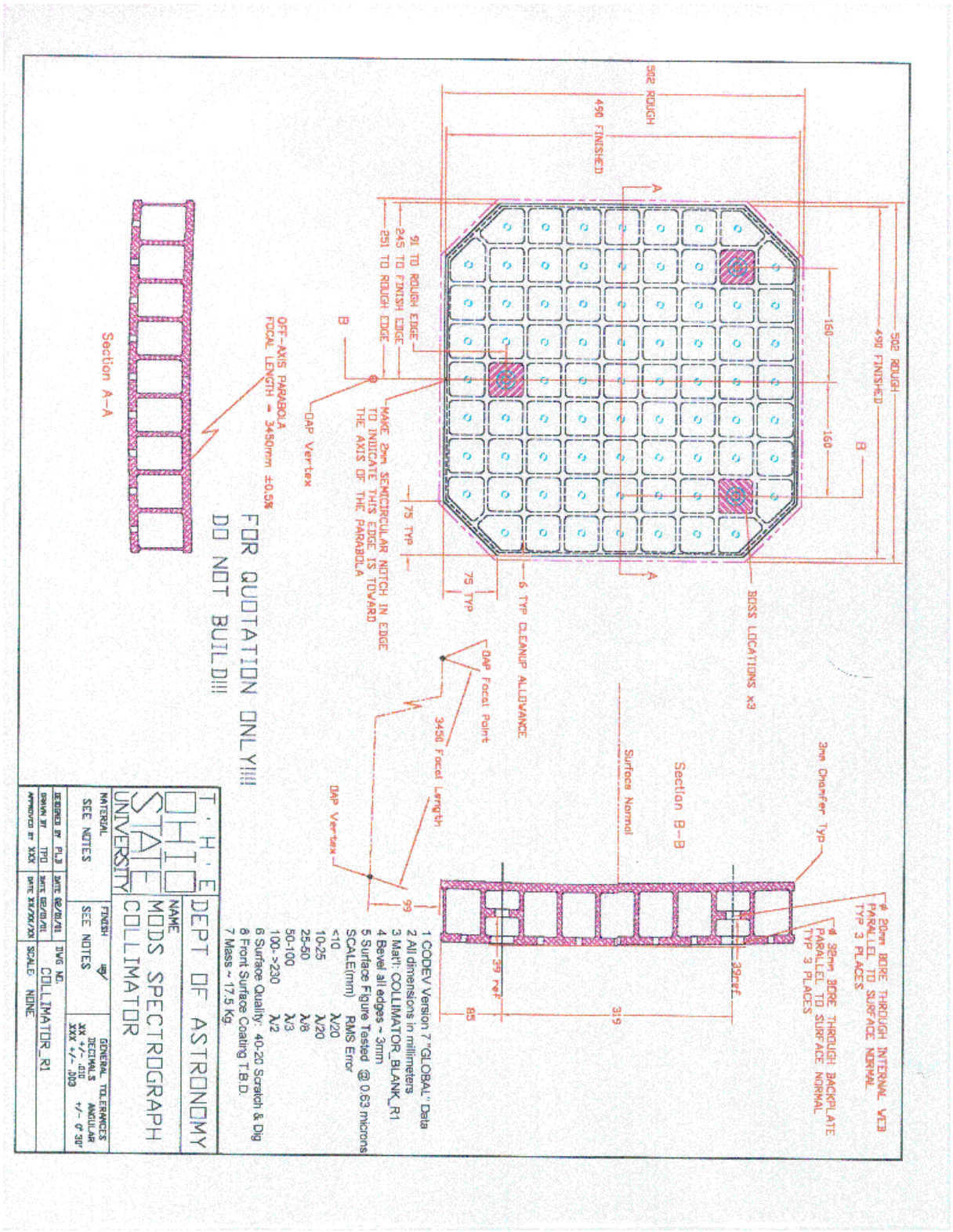
502 ROUGH
490 FINISHED
160
160
B
A
A
BOSS LOCATIONS x3
6 TYP CLEANUP ALLOWANCE
75 TYP
75 TYP
91 TO ROUGH EDGE
245 TO FINISH EDGE
251 TO ROUGH EDGE
MAKE 2mm SEMICIRCULAR NOTCH IN EDGE TO INDICATE THIS EDGE IS TOWARD THE AXIS OF THE PARABOLA
B
DAP Vertex
OFF-AXIS PARABOLA
FOCAL LENGTH = 3450mm ±0.5%
Section A-A
DAP Focal Point
3450 Focal Length
DAP Vertex
99
Surface Normal
Section B-B
3mm Chamfer Typ
Ø 20mm BORE THROUGH INTERNAL WEB PARALLEL TO SURFACE NORMAL TYP 3 PLACES
Ø 32mm BORE THROUGH BACKPLATE PARALLEL TO SURFACE NORMAL TYP 3 PLACES
32ref
39 ref
85
319
1 CODEV Version 7 "GLOBAL" Data
2 All dimensions in millimeters
3 Matl: COLLIMATOR_BLANK_R1
4 Bevel all edges ~ 3mm
5 Surface Figure Tested @ 0.63 microns
SCALE(mm) RMS Error
<10 λ/20
10-25 λ/20
25-50 λ/8
50-100 λ/3
100->230 λ/2
6 Surface Quality: 40-20 Scratch & Dig
8 Front Surface Coating T.B.D.
7 Mass ~ 17.5 Kg.
FOR QUOTATION ONLY!!!!
DO NOT BUILD!!!
T. H. E
OHIO
STATE
UNIVERSITY
DEPT OF ASTRONOMY
NAME
MODS SPECTROGRAPH
COLLIMATOR
MATERIAL
SEE NOTES
FINISH
SEE NOTES
GENERAL TOLERANCES
DECIMALS
ANGULAR
DESIGNED BY PLB
DRAWN BY TPO
APPROVED BY XXX
DWG NO.
COLLIMATOR_R1
SCALE NONE

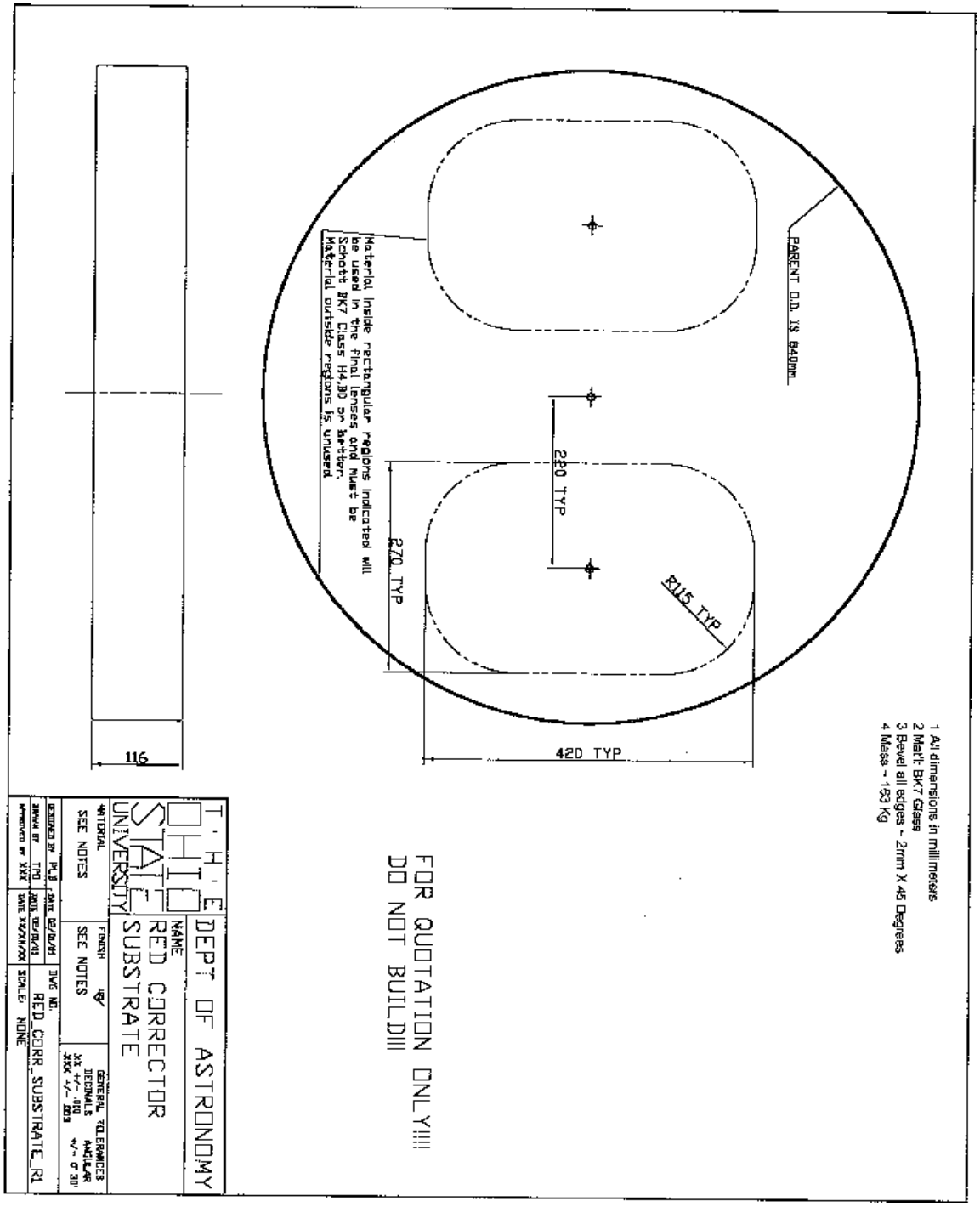
1 All dimensions in millimeters
2 Mat'l: BK7 Glass
3 Bevel all edges ~ 2mm X 45 Degrees
4 Mass ~ 153 Kg
PARENT O.D. IS 840mm
220 TYP
270 TYP
R115 TYP
420 TYP
Material inside rectangular regions indicated will be used in the final lenses and must be Schott BK7 Class H4,BD or better.
Material outside regions is unused.
116
FOR QUOTATION ONLY!!!!
DO NOT BUILD!!!
THE OHIO STATE UNIVERSITY
DEPT OF ASTRONOMY
NAME
RED CORRECTOR SUBSTRATE
MATERIAL
SEE NOTES
FINISH
SEE NOTES
GENERAL TOLERANCES
DECIMALS
ANGULAR
DWG NO.
RED_CORR_SUBSTRATE_R1
SCALE: NONE

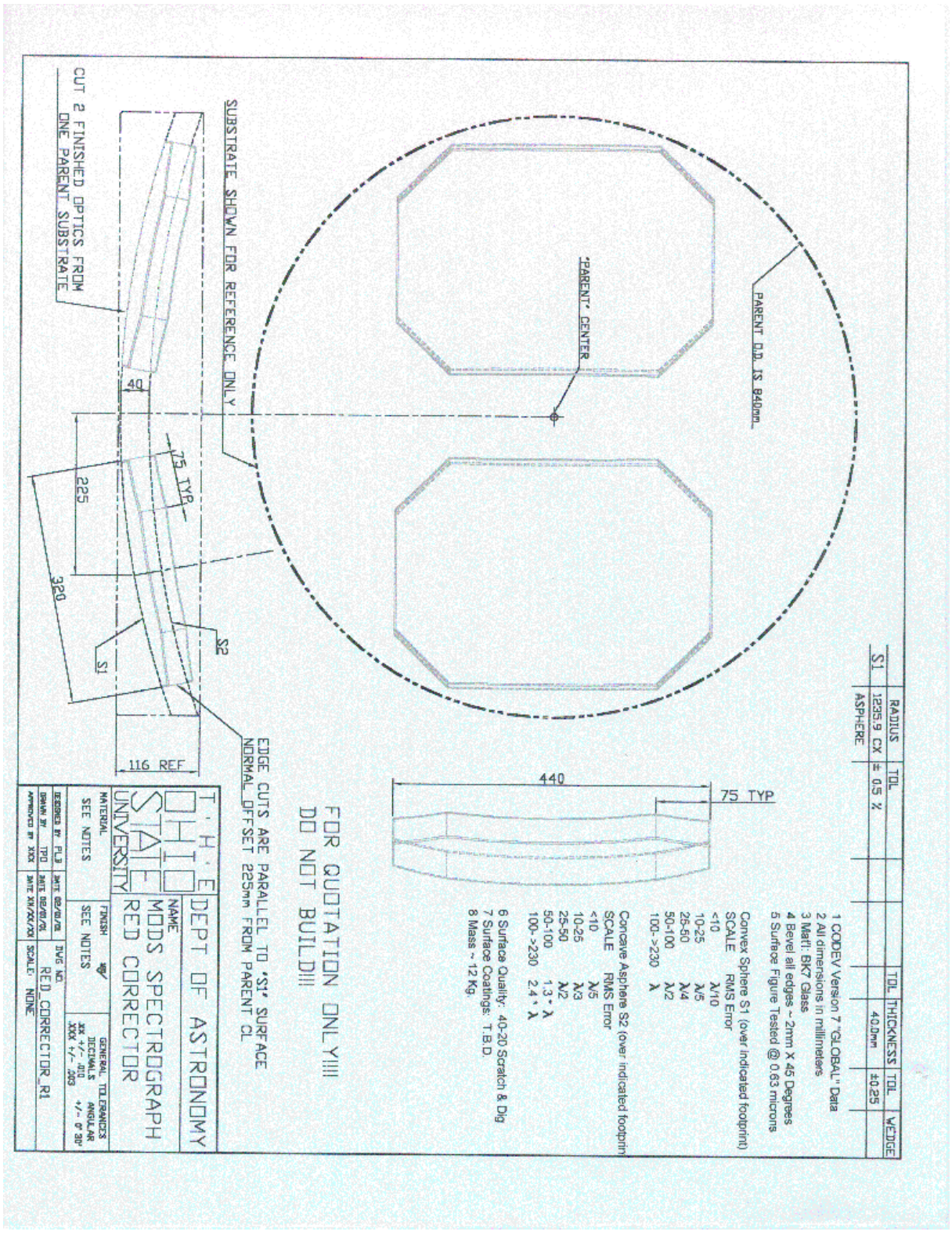
S1
RADIUS
TOL
THICKNESS
TOL
WEDGE
1235.9 CX
± 0.5 %
40.0mm
±0.25
ASPHERE
1 CODEV Version 7 "GLOBAL" Data
2 All dimensions in millimeters
3 Matl: BK7 Glass
4 Bevel all edges ~ 2mm X 45 Degrees
5 Surface Figure Tested @ 0.63 microns
Convex Sphere S1 (over indicated footprint)
SCALE RMS Error
<10 λ/10
10-25 λ/5
25-50 λ/4
50-100 λ/2
100-->230 λ
Concave Asphere S2 (over indicated footprint)
SCALE RMS Error
<10 λ/5
10-25 λ/3
25-50 λ/2
50-100 1.3 * λ
100->230 2.4 * λ
6 Surface Quality: 40-20 Scratch & Dig
7 Surface Coatings: T.B.D.
8 Mass ~ 12 Kg.
PARENT O.D. IS 840mm
'PARENT' CENTER
SUBSTRATE SHOWN FOR REFERENCE ONLY
CUT 2 FINISHED OPTICS FROM ONE PARENT SUBSTRATE
40
75 TYP
225
320
S1
S2
116 REF
440
75 TYP
EDGE CUTS ARE PARALLEL TO 'S1' SURFACE
NORMAL OFFSET 225mm FROM PARENT CL
FOR QUOTATION ONLY!!!!
DO NOT BUILD!!!
THE OHIO STATE UNIVERSITY
DEPT OF ASTRONOMY
NAME
MODS SPECTROGRAPH
RED CORRECTOR
MATERIAL
SEE NOTES
FINISH
SEE NOTES
GENERAL TOLERANCES
DECIMALS ANGULAR
XX +/- .01 +/- 0° 30'
XXX +/- .005
DESIGNED BY: PLB
DRAWN BY: TPD
APPROVED BY: XXX
DATE 02/01/01
DATE 02/01/01
DATE XX/XX/XXX
DWG NO.
RED_CORRECTOR_R1
SCALE: NONE

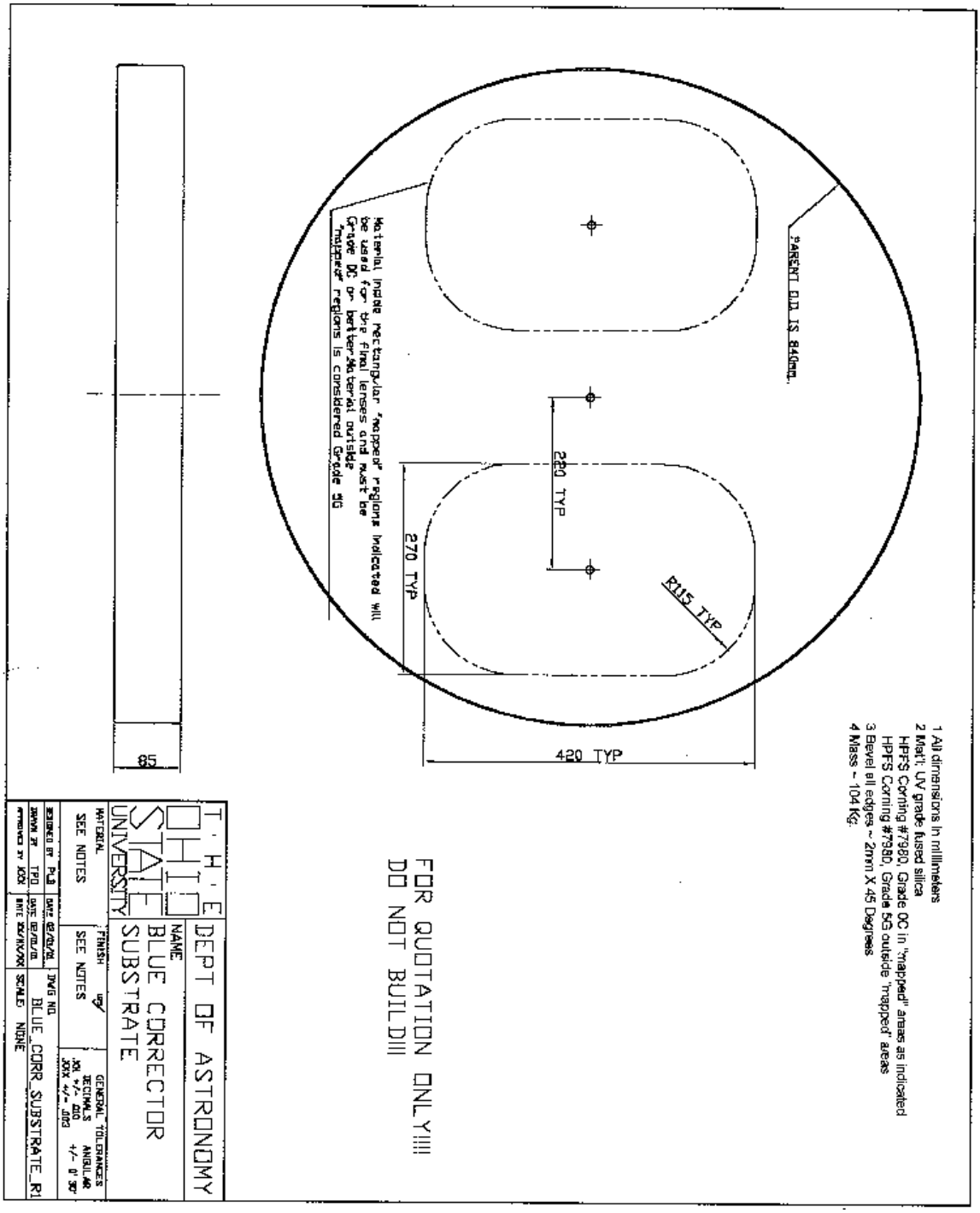
1 All dimensions in millimeters
2 Mat'l: UV grade fused silica
HPFS Corning #7980, Grade 0C in "mapped" areas as indicated
HPFS Corning #7980, Grade 5G outside "mapped" areas
3 Bevel all edges ~ 2mm X 45 Degrees
4 Mass ~ 104 Kg.
PARENT O.D. IS 840mm.
Material inside rectangular "mapped" regions indicated will be used for the final lenses and must be Grade 0C or better. Material outside "mapped" regions is considered Grade 5G
280 TYP
270 TYP
R115 TYP
420 TYP
85
FOR QUOTATION ONLY!!!!
DO NOT BUILD!!!
THE OHIO STATE UNIVERSITY
DEPT OF ASTRONOMY
NAME
BLUE CORRECTOR SUBSTRATE
MATERIAL
SEE NOTES
FINISH
SEE NOTES
GENERAL TOLERANCES
DECIMALS
.XX +/- .010
.XXX +/- .003
ANGULAR
+/- 0° 30'
DRAWN JR
CHECKED PJB
APPROVED JK TPD
DATE 02/01/01
DATE 02/01/01
DATE XX/XX/XX
DWG NO.
BLUE_CORR_SUBSTRATE_R1
SCALE NONE

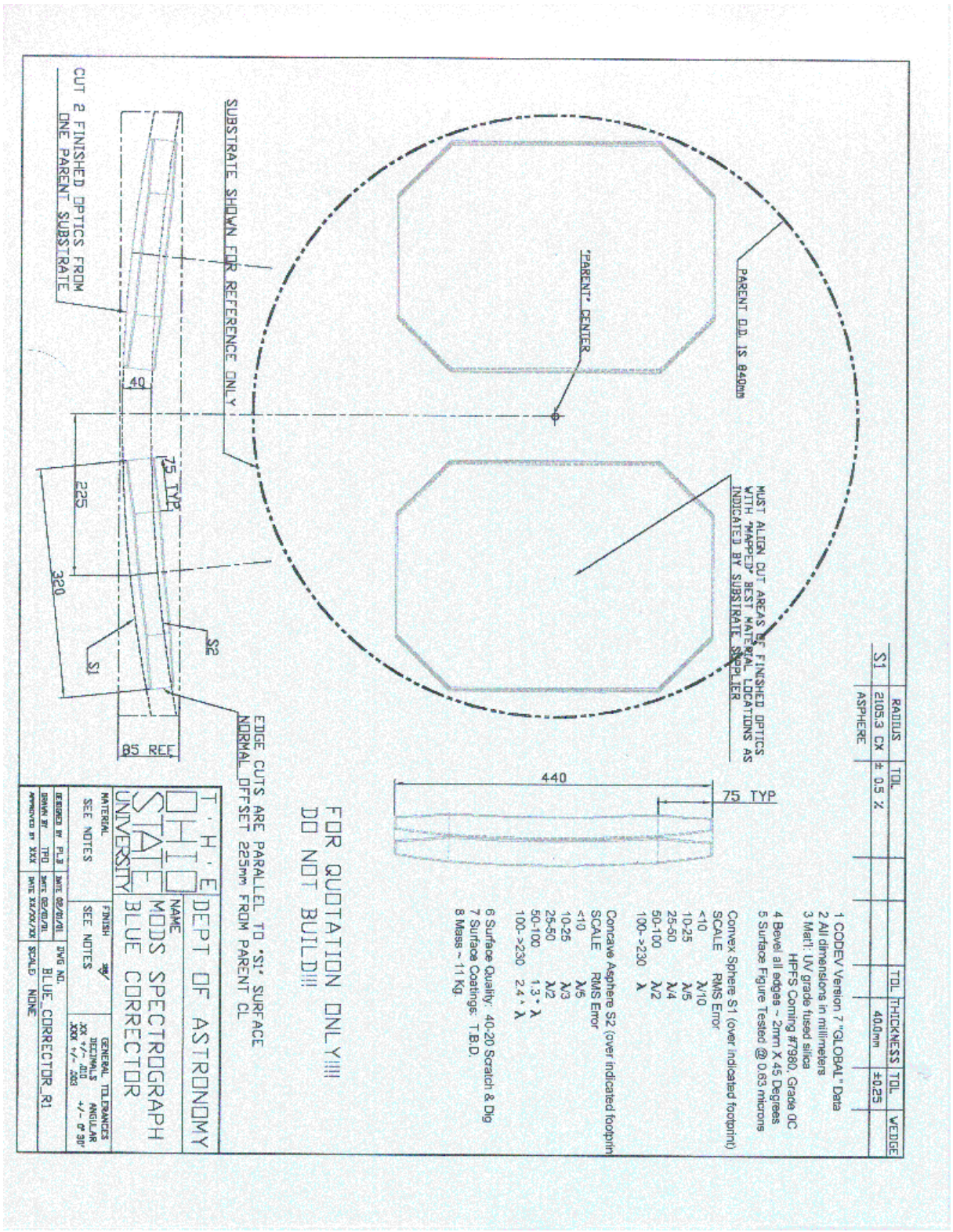
S1
RADIUS
2105.3 CX
ASPHERE
TOL
± 0.5 %
THICKNESS TOL
40.0mm ±0.25
WEDGE
1 CODEV Version 7 "GLOBAL" Data
2 All dimensions in millimeters
3 Matl: UV grade fused silica
HPFS Corning #7980, Grade 0C
4 Bevel all edges ~ 2mm X 45 Degrees
5 Surface Figure Tested @ 0.63 microns
Convex Sphere S1 (over indicated footprint)
SCALE RMS Error
<10 λ/10
10-25 λ/5
25-50 λ/4
50-100 λ/2
100->230 λ
Concave Asphere S2 (over indicated footprint)
SCALE RMS Error
<10 λ/5
10-25 λ/3
25-50 λ/2
50-100 1.3 * λ
100->230 2.4 * λ
6 Surface Quality: 40-20 Scratch & Dig
7 Surface Coatings: T.B.D.
8 Mass ~ 11 Kg.
440
75 TYP
FOR QUOTATION ONLY!!!!
DO NOT BUILD!!!
EDGE CUTS ARE PARALLEL TO "S1" SURFACE
NORMAL OFFSET 225mm FROM PARENT CL
SUBSTRATE SHOWN FOR REFERENCE ONLY
CUT 2 FINISHED OPTICS FROM
ONE PARENT SUBSTRATE
MUST ALIGN CUT AREAS OF FINISHED OPTICS
WITH "MAPPED" BEST MATERIAL LOCATIONS AS
INDICATED BY SUBSTRATE SUPPLIER
"PARENT" CENTER
PARENT O.D. IS 840mm
40
75 TYP
225
320
S1
S2
85 REF
T. H. E. OHIO STATE UNIVERSITY
DEPT OF ASTRONOMY
NAME
MODS SPECTROGRAPH
BLUE CORRECTOR
MATERIAL
SEE NOTES
FINISH
SEE NOTES
GENERAL TOLERANCES
DECIMALS
.XX +/- .010
.XXX +/- .003
ANGULAR
+/- 0° 30'
DESIGNED BY FLB
DRAWN BY TPD
APPROVED BY XXX
DATE 02/01/01
DATE 02/01/01
DATE XX/XX/XX
DWG NO.
BLUE_CORRECTOR_R1
SCALE NONE

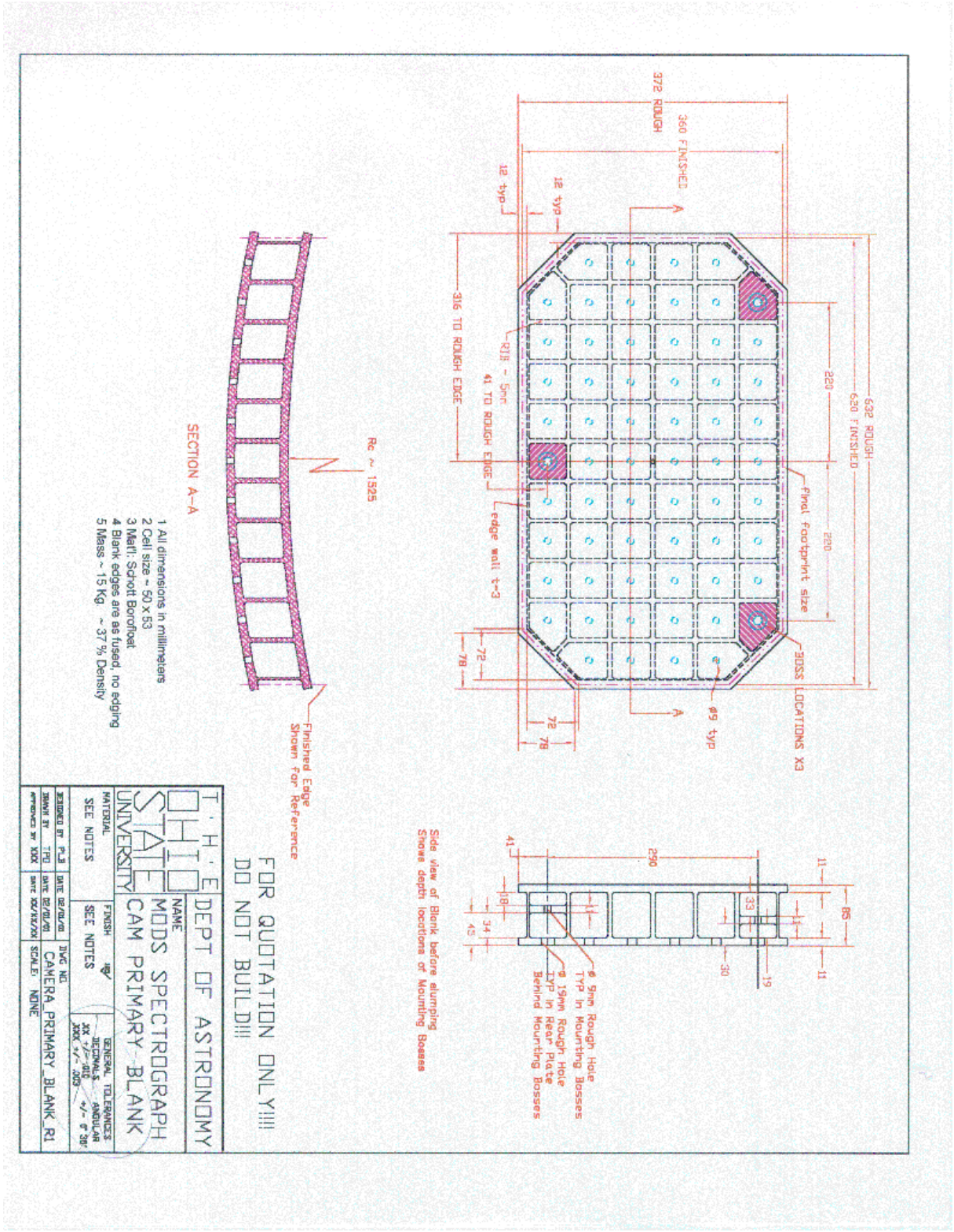
632 ROUGH
620 FINISHED
220
280
final footprint size
BOSS LOCATIONS X3
372 ROUGH
360 FINISHED
12 typ
12 typ
316 TO ROUGH EDGE
41 TO ROUGH EDGE
edge wall t~3
72
78
72
78
Ø9 typ
Rc ~ 1525
Finished Edge
Shown For Reference
SECTION A-A
1 All dimensions in millimeters
2 Cell size ~ 50 x 53
3 Melt: Schott Borofloat
4 Blank edges are as fused, no edging
5 Mass ~ 15 Kg. ~37 % Density
Side view of Blank before slumping
Shows depth locations of Mounting Bosses
41
290
11
65
33
11
11
8
34
45
30
19
Ø 9mm Rough Hole
TYP In Mounting Bosses
Ø 19mm Rough Hole
TYP In Rear Plate
Behind Mounting Bosses
FOR QUOTATION ONLY!!!!
DO NOT BUILD!!!
THE OHIO STATE UNIVERSITY
DEPT OF ASTRONOMY
NAME
MODS SPECTROGRAPH
CAM PRIMARY BLANK
MATERIAL
SEE NOTES
FINISH
SEE NOTES
GENERAL TOLERANCES
DECIMALS
ANGULAR
DWG NO
CAMERA_PRIMARY_BLANK_R1
SCALE: NONE

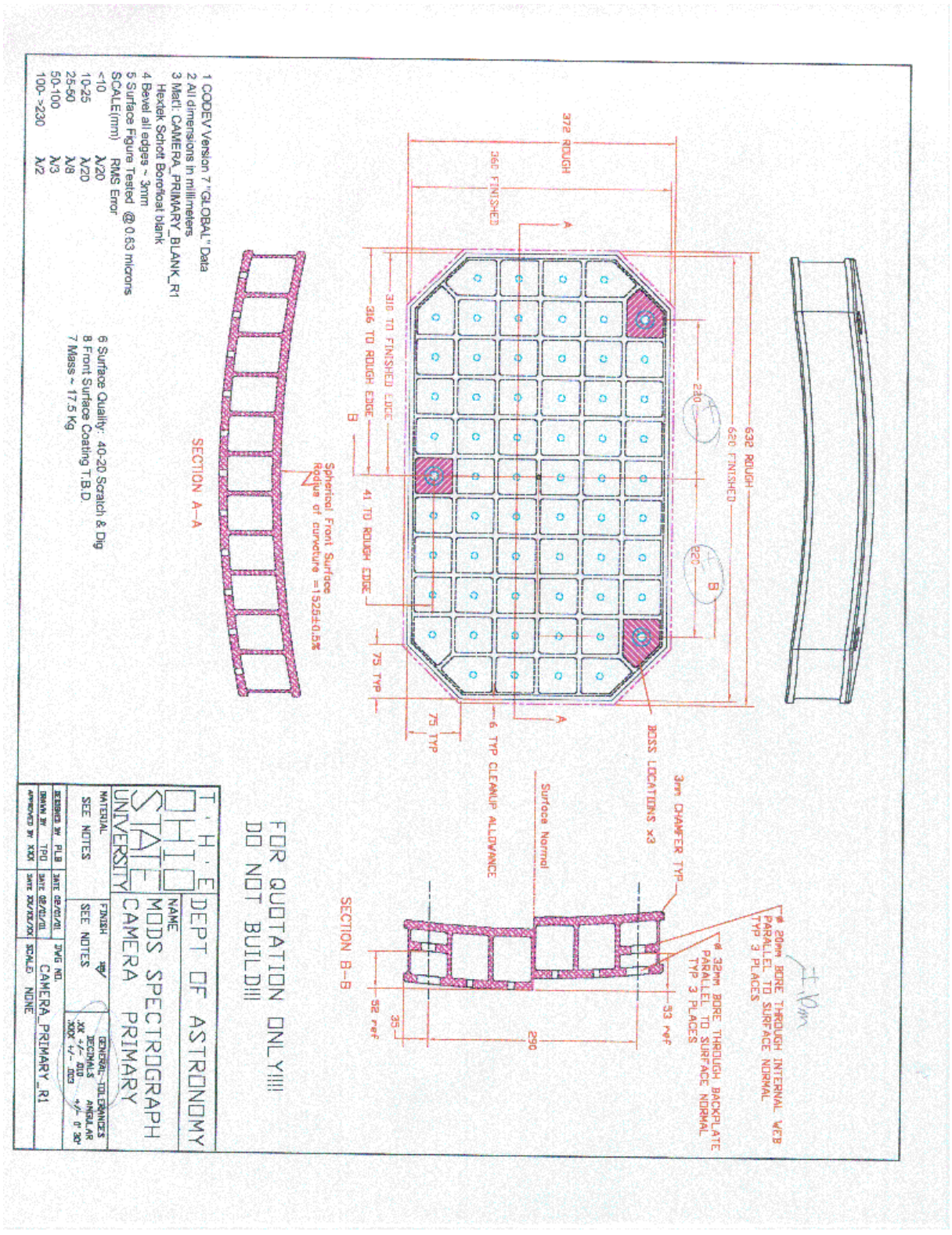
1 CODEV Version 7 "GLOBAL" Data
2 All dimensions in millimeters
3 Matl: CAMERA_PRIMARY_BLANK_R1
Hextek Schott Borofloat blank
4 Bevel all edges ~ 3mm
5 Surface Figure Tested @ 0.63 microns
SCALE(mm) RMS Error
<10 λ/20
10-25 λ/20
25-50 λ/8
50-100 λ/3
100- >230 λ/2
6 Surface Quality: 40-20 Scratch & Dig
8 Front Surface Coating T.B.D.
7 Mass ~ 17.5 Kg
SECTION A-A
Spherical Front Surface
Radius of curvature =1525±0.5%
372 ROUGH
366 FINISHED
316 TO FINISHED EDGE
316 TO ROUGH EDGE
41 TO ROUGH EDGE
75 TYP
75 TYP
632 ROUGH
620 FINISHED
230
220
6 TYP CLEANUP ALLOWANCE
BOSS LOCATIONS x3
3mm CHAMFER TYP.
Surface Normal
SECTION B-B
Ø 20mm BORE THROUGH INTERNAL WEB
PARALLEL TO SURFACE NORMAL
TYP 3 PLACES
Ø 32mm BORE THROUGH BACKPLATE
PARALLEL TO SURFACE NORMAL
TYP 3 PLACES
33 ref
290
35
52 ref
FOR QUOTATION ONLY!!!!
DO NOT BUILD!!!
THE OHIO STATE UNIVERSITY
DEPT OF ASTRONOMY
NAME
MODS SPECTROGRAPH
CAMERA PRIMARY
MATERIAL
SEE NOTES
FINISH
SEE NOTES
GENERAL - TOLERANCES
DECIMALS
ANGULAR
DRWG NO.
CAMERA_PRIMARY_R1
SCALE: NONE
DESIGNED BY: PLB
DRAWN BY: TPO
APPROVED BY: XXX
DATE: 02/01/01
DATE: 02/01/01
DATE: XX/XX/XX

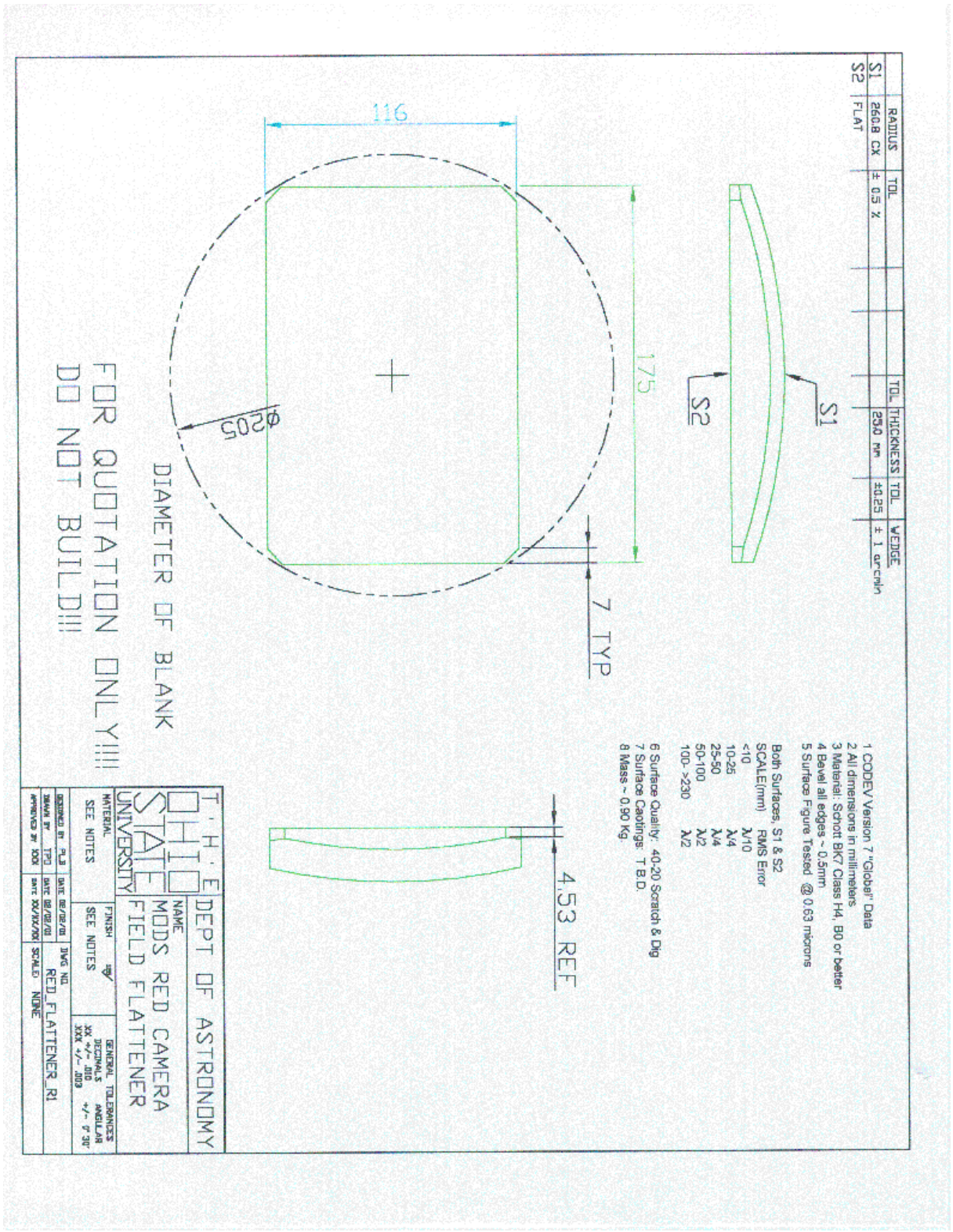
RADIUS TOL THICKNESS TOL WEDGE
S1 260.8 CX ± 0.5 % 25.0 mm ±0.25 ± 1 arc-min
S2 FLAT
S1
S2
116
175
205
7 TYP
4.53 REF
DIAMETER OF BLANK
1 CODEV Version 7 "Global" Data
2 All dimensions in millimeters
3 Material: Schott BK7 Class H4, B0 or better
4 Bevel all edges ~ 0.5mm
5 Surface Figure Tested @ 0.63 microns
Both Surfaces, S1 & S2
SCALE(mm) RMS Error
<10 λ/10
10-25 λ/4
25-50 λ/4
50-100 λ/2
100- >230 λ/2
6 Surface Quality: 40-20 Scratch & Dig
7 Surface Coatings: T.B.D.
8 Mass ~ 0.90 kg.
FOR QUOTATION ONLY!!!!
DO NOT BUILD!!!
THE OHIO STATE UNIVERSITY
DEPT OF ASTRONOMY
NAME MODS RED CAMERA FIELD FLATTENER
MATERIAL SEE NOTES
FINISH SEE NOTES
GENERAL TOLERANCES DECIMALS XX +/- .010 XXX +/- .003 ANGULAR +/- 0° 30'
DRAWN BY PLB DATE 08/02/01
CHECKED BY TPO DATE 08/02/01
APPROVED BY XXX DATE XX/XX/XX
DWG NO. RED_FLATTENER_R1
SCALE: NONE

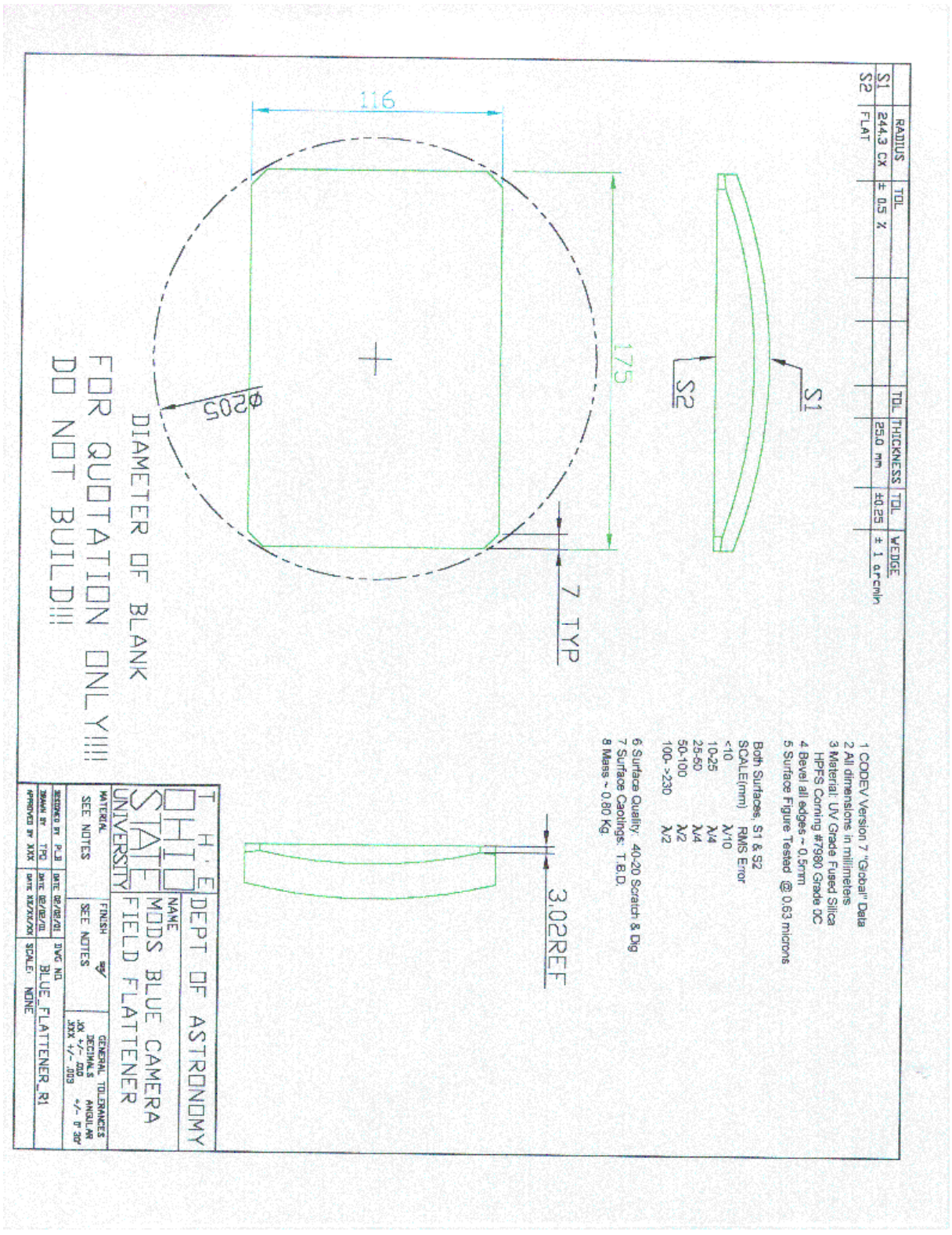
RADIUS TOL THICKNESS TOL WEDGE
S1 244.3 CX ± 0.5 % 25.0 mm ±0.25 ± 1 arcmin
S2 FLAT
1 CODEV Version 7 "Global" Data
2 All dimensions in millimeters
3 Material: UV Grade Fused Silica
HPFS Corning #7980 Grade 0C
4 Bevel all edges ~ 0.5mm
5 Surface Figure Tested @ 0.63 microns
Both Surfaces, S1 & S2
SCALE(mm) RMS Error
<10 λ/10
10-25 λ/4
25-50 λ/4
50-100 λ/2
100- >230 λ/2
6 Surface Quality: 40-20 Scratch & Dig
7 Surface Coatings: T.B.D.
8 Mass ~ 0.80 Kg.
S1
S2
116
175
Ø205
7 TYP
3.02REF
DIAMETER OF BLANK
FOR QUOTATION ONLY!!!!
DO NOT BUILD!!!
THE OHIO STATE UNIVERSITY
DEPT OF ASTRONOMY
NAME
MODS BLUE CAMERA
FIELD FLATTENER
MATERIAL
SEE NOTES
FINISH
SEE NOTES
GENERAL TOLERANCES
DECIMALS ANGULAR
.XX +/-.010 +/- 0°30'
.XXX +/-.003
DRAWN BY TPO DATE 02/08/01
CHECKED BY P.J.B DATE 02/08/01
APPROVED BY XXX DATE XX/XX/XX
DWG. NO. BLUE_FLATTENER_R1
SCALE: NONE

Appendix C: LBT Optical Spectrograph Working Group Documents

In this appendix we provide copies of two historical documents of interest to the PDR:

1. *Summary of the March 1999 Meeting of the LBTOSWG*. At this meeting the conceptual design for MODS was presented to members of the LBT consortium. Out of the meeting came a series of questions and recommendations for the MODS team.
2. *MODS Team Responses to the LBTOSWG*. This gives the detailed responses to the LBTOWSG. Out of this exercise came the current MODS design described in this PDR document.

The current MODS design evolved from this exercise. Note that some of the numbers presented for performance have been superceded in the current design.

Summary of the March 1999 Meeting of the LBTOSWG

Following its 1998 October meeting in Tucson, the LBT Scientific Advisory Committee (SAC) asked all consortium members to form a working group for concept definition of the first-light optical/UV spectrograph that is to be built by Ohio State. The SAC instructed us to adopt the proposed Ohio State Multi-Object Double Spectrograph (MODS) as a straw man design, and consider carefully what additions or refinements might be made to better accommodate consortium-wide science goals while keeping the cost of the instrument as low as possible. In addition to this general charge, the SAC had several specific questions for the MODS team to address.

In response to this charge, the LBT Optical/UV Spectrograph Working Group (LBTOSWG) was formed by open invitation to all LBT consortium members. The LBTOSWG met in Columbus on 1999 March 8-9. Present were Bruce Atwood (Ohio State, MODS project manager and director of the Ohio State Imaging Sciences Lab), Ralph Belville (Ohio State, Imaging Sciences Lab), Paul Byard (Ohio State, MODS team), Darren DePoy (Ohio State, representing the LBT SAC), John Hill (Arizona, representing the LBT Project Office), Mike Lesser (Arizona), Jerry Mason (Ohio State, Imaging Sciences Lab) Klaus Meisenheimer (Heidelberg), Tom O'Brien (Ohio State. MODS team), Pat Osmer (Ohio State, MODS PI), Roberto Pallavicini (Palermo), Dan Pappalardo (Ohio State, Imaging Sciences Lab), Brad Peterson (Ohio State, representing the LBT SAC), Rick Pogge (Ohio State, MODS Project Scientist), Jesper Storm (Potsdam), Giampaolo Vettolani (Bologna), R. Mark Wagner (Ohio State, representing the LBT Project Office), and Rogier A. Windhorst (Arizona State). Jill Bechtold (Arizona) participated in part of the meeting by telephone. The following is intended to provide a summary of the results of the meeting.

The major conclusions of the LBTOSWG meeting are the following:

UV Sensitivity

There was consensus that there are strong science drivers for retaining high UV throughput to atmospheric cutoff (about 320 nm). The LBTOSWG notes that this also

provides a unique niche for LBT, as the comparable facility instruments for the other 8–10m class telescopes will not work below 380–400 nm. The LBTOSWG also notes that the overall response of the UV side of the MODS spectrograph can be significantly better than it appears to be in the MODS proposal if a more appropriate grating and CCD coating are used. The MODS team pointed out in answer to the specific question from the SAC about the cost of UV response to atmospheric cutoff that extending the response from 400 nm to 320 nm is a small incremental cost because MODS is using reflective rather than refractive optics.

MODS Field-of-View

MODS will produce high-quality (D_{80}<0.25 arcsec, where D_{80} is the diameter that encompasses 80% of the light in a point-source image) images over a 4×4' field, and this was deemed to be acceptable given that an "extended field" option can be implemented; with reduced image quality (D_{80}<0.8 arcsec), a 5×6' field (i.e., a factor of 1.9 larger) is usable.

Given that many of the proposed science drivers for the spectrograph are essentially "survey" type observations, it is obvious that, all other things being equal, multiplexing greatly improves efficiency. For the very faint quasars and galaxies that are MODS targets, increasing the field size over the originally proposed 4×4' size thus has a dramatic effect. However, there are a number of important barriers to implementation of a wider field at the f/15 Gregorian focus. First, the Gregorian focal surface is curved, not flat. Slit masks larger than 5–6' (or thereabouts) would have to be curved. Second, implementation of a significantly wider field would require a completely different spectrograph from MODS. Collimator aberrations will cause poor images far from field center, though as noted above, images comparable to those obtainable in median uncorrected seeing can be obtained throughout a 5×6' field.

Two important points must be noted:

1. The f/4 focus is really the wide-field focus for LBT. A wide-field spectrograph ought to be designed for the f/4 focus, but not at present since the f/4 focus will not be implemented at first light.
2. The niches for MODS are high throughput, broad wavelength coverage, and excellent image quality. An affordable instrument at the f/15 focus is simply not going to be competitive in terms of field of view. Relative to the field sizes of other wide-field optical spectrographs for 8-10m class telescopes, the MODS field is competitive only with Gemini (5×5').

High-Resolution

It would be desirable for MODS to have a high-resolution mode in the R=15,000 to 20,000 range. However, very high resolution (R=30,000 to R=50,000) will require an echelle-type spectrograph optimized for single-object spectroscopy at very high resolution; attempting to meet the MODS science goals and achieve very high resolution will result in a design that does not serve any science goals well.

There are at least two ways that the current MODS design can achieve higher resolution. One possible solution is to simply use a higher-dispersion grating. However, this will

overfill the camera and thus decrease efficiency, though the design will need additional study to quantify this. A cross-dispersed mode will also be investigated. A second possible solution is to design a longer-focal length camera, either as an upgrade option, or as the baseline camera. The latter would be possible if in the R=8000 mode on-chip binning (2×2) is used; a positive aspect of such a design is that the required design change would eliminate an obstruction (the detector) in the beam, and a negative aspect would be an increased cosmic-ray problem (4 times as many cosmic rays per binned pixel) and a gap between two sections of the spectrum that would result from the necessity of using two CCDs butted together.

We also note that the higher resolution mode also provides an upgrade path to work with the adaptive optics (AO) system. The possible adaptive correction might range from rapid tip-tilt guiding, to partial (low-order) adaptive correction. In the unbinned mode, the camera pixel scale is 0.15 arcsec/pixel.

Integral Field Mode

It should be possible to implement in the future an integral field mode. The LBTOSWG envisages an integral-field module that can be inserted between the telescope and the spectrograph. This is regarded as a future upgrade path, and the MODS design will preserve the integral-field capability as a future option. We note that in any case a conventional long-slit mode (4 arcmin) will be available.

Action Items for the MODS Team

The LBTOSWG has identified the following specific action items for the MODS team. The MODS team has agreed to provide their responses to these items by no later than 31 March 1999, at which time they will be circulated to the LBTOSWG for further consideration.

1. Evaluate an unobstructed longer focal length (approximately 700 mm) camera for both sides (red and blue) and performance in both binned and unbinned modes.
2. Elaborate on the “extended field” (5'×6') concept. Include commentary on the likely availability and cost of the atmospheric dispersion corrector for this larger format.
3. Provide updated throughput and quantum efficiency curves based on a range of realistic gratings and CCD coatings.

The LBTOSWG has also requested descriptions of science programs that will require “extended field” capabilities (from Klaus Meisenheimer) and R=20,000 resolution in both the red and blue channels (from Jim Liebert).

When the MODS team response to the action items outlined above is received, the LBTOSWG will continue discussion via electronic mail. Our goal is to have written recommendations on the MODS proposal and possible modifications and/or upgrade paths ready for the next LBT SAC meeting in early May 1999.

MODS Team Responses to the LBTOSWG, 1999 April 5

At the 1999 March meeting in Columbus, the LBTOSWG identified three specific action items for the MODS team. The MODS team agreed to provide their responses to these items by the end of March.

The LBTOSWG's specific requests to the MODS team were the following:

1. Evaluate an unobstructed longer focal length (approximately 700 mm) camera for both sides (red and blue) and performance in both binned and unbinned modes.
2. Elaborate on the "extended field" (5' × 6') concept. Include commentary on the likely availability and cost of the atmospheric dispersion corrector for this larger format.
3. Provide updated throughput and quantum efficiency curves based on a range of realistic gratings and CCD coatings.

The MODS team responses to these issues appear below.

Image characteristics for a 700mm focal length camera for MODS

The camera is a modification of the one discussed at the meeting last month. The focal length was increased to 700 mm and the camera was decentered to allow an unobstructed design while imaging on to a 8K detector in the dispersion direction. The detector size in the cross-dispersion direction is 4K with 2K used for a 4 arcminute slit height. If the field is extended to 5 arc minutes in the slit direction the used area will be increased appropriately.

The results below show the diameter of the circle containing 80% of the image point spread function (D_{80}) values in arcseconds for different slit heights as a function of wavelength with the dispersed spectrum covering 4000 pixels

Table 2: D_{80} for a 700mm Camera

Slit Height (arcmin)	Wavelength (nm)				
	564	530	499	460	434
2	0.20	0.25	0.19	0.27	0.21
1.3	0.13	0.15	0.16	0.16	0.11
0.6	0.13	0.13	0.14	0.12	0.10
0	0.15	0.12	0.14	0.09	0.13
0.6	0.17	0.10	0.10	0.05	0.16
1.3	0.20	0.10	0.13	0.10	0.20
2	0.25	0.15	0.22	0.23	0.29

The D_{80} values are less than 0.3 arcseconds for all points in the spectrum. Near the center of the slit the image quality will allow narrow slits to be used if adaptive optics are used to improve the image quality through the atmosphere. The above values correspond to a

resolution of R=8000 when 4–5 pixels are binned in the dispersion direction, and double this resolution with a narrow slit with 2 pixels binned.

Overall the performance of this camera is similar to the shorter focal length camera discussed at the meeting. Furthermore, it provides a higher throughput since it is unobstructed by the detector.

Performance of the "extended field" mode

The issue is image quality over the extended field. The Table below gives the image quality in terms of D_{80} as a function of displacement from field center in the V band.

Table 3: Variation in D80 across the extended MODS Field

Y Displacement (arcmin)	X Displacement (arcmin)						
	-3	-2	-1	0	1	2	3
3	0.69	0.63	0.48	0.51	0.49	0.64	0.91
2	0.64	0.36	0.24	0.18	0.24	0.39	0.69
1	0.51	0.24	0.17	0.15	0.13	0.27	0.56
0	0.47	0.22	0.18	0.16	0.13	0.23	0.53
-1	0.54	0.28	0.19	0.17	0.15	0.31	0.60
-2	0.72	0.45	0.30	0.25	0.31	0.46	0.80

In this mode the D_{80} image diameter grows to as much as 0.46 arcseconds in the corner of a 4 arcminute field and reaches a values of 0.9 arcseconds at the corner of a 5×6 arcminute field. The field is limited on one side by the proximity of the camera corrector to the collimated beam.

The image diameters for the different wavelength values when used in a multislit mode have not been evaluated individually. However, the values in the first table closely track the sizes and are usually less because the monochromatic images in the spectrum are not broadened by lateral color. Therefore the imaging mode D_{80} values give a good indication of the spectral values for a multislit mode. This assumption will be verified in future analyses.

Revised MODS Throughput Calculation

The goal of this study is to predict the throughput of the MODS spectrograph. The atmosphere, telescope and the slit are not included. All surfaces are assumed to be clean and new. In general all values are taken from actual measurements. The model for the sol-gel coatings is the Sandia Labs base catalyzed fixed index process not the acid catalyzed graded process studied at OSU. The dichroic is assumed to be 85% efficient in both transmission and reflection which appears to be conservative. A filter is included in the red channel to block second order “blue”, in many configurations this will not be required. Available designs for the ADC require glasses that would limit the throughput at the extreme blue end. Other combinations of glasses will be investigated for better throughput. The blue response is shown both with and without the ADC.

ADC:

Both surfaces of the ADC are coated with a sol-gel coating tuned for an index equal to the square root of the index of fused silica. The internal absorption is for 25 mm of LLF 6 glass. Note that the absorption will be a function of field position and zenith distance. No allowance is made for the index mismatch between the fused silica and LLF6 glass.

Field Lens:

Both surfaces of the field lens are coated with a sol-gel coating tuned for an index equal to the square root of the index of fused silica. The pupil position may be acceptable without a Fabry lens or it may be possible to use the rear surface of the ADC to control pupil position. Thus it remains to be determined if the field lens will be required.

Dichroic:

The dichroics is assumed to have an in-band reflectivity of 85% and the first surface is assumed to have an in-band transmission of 85%. The rear surface is assumed to be coated with same sol-gel coating used for the previous surfaces.

Collimators:

The blue collimator is coated with aluminum while the red collimator is coated with silver.

Gratings:

The blue grating is coated with aluminum. The blaze efficiency published by Milton Roy for their 600 groove/mm 5.2 degree blaze grating is used. The P and S curves are averaged. No correction is made for the departure from Littrow condition. The red grating is coated with aluminum. The blaze efficiency published by Milton Roy for their 600 groove/mm 8.6 degree blaze grating is used. The P and S curves are averaged. No correction is made for the departure from Littrow condition. Improved performance could be obtained with a silver coated grating in the red channel.

Camera Correctors:

The corrector for the blue camera is coated with ZC&R's broad band coating. The corrector for the red camera is coated with the Sol-gel coating.

Camera Primary Mirrors:

The primary mirror of the blue camera is coated with aluminum. The primary mirror of the red camera is coated with silver.

Camera Field Flatteners:

The field flattener for the blue camera is coated with ZC&R's broad band coating. The field flattener for the red camera is coated with the Sol-gel coating.

CCDs:

The quantum efficiency for the blue detector is taken from the room temperature measured values for the Steward CCD lab processed Lick-Loral 3 CCD L4-W9-(1,0). The quantum efficiency for the red detector is taken from the low temperature values for the LBNL deep depletion CCD measured at Lick Observatory.

The overall throughput of MODS, based on the above is shown below [omitted, see §2.7]

Appendix D: Supplemental Optical Performance Figures

This section presents additional diagrams illustrating the performance of the MODS optics. For each camera and mode (imaging and spectroscopy), we present plots of D_{80} (80% encircled energy diameter) as a function of field/slit position and wavelength and more traditional "spot" diagrams.

Imaging Performance

Imaging performance is evaluated in standard UBVRI filter bandpasses. Optimal focus is chosen for 4×4' and 2×2' "AO" fields of view (the latter Red channel only).

Unless otherwise noted, Blue camera imaging performance is evaluated in the UBV filters, while the Red camera performance is evaluated for the VRI filters.

MODS Blue Camera

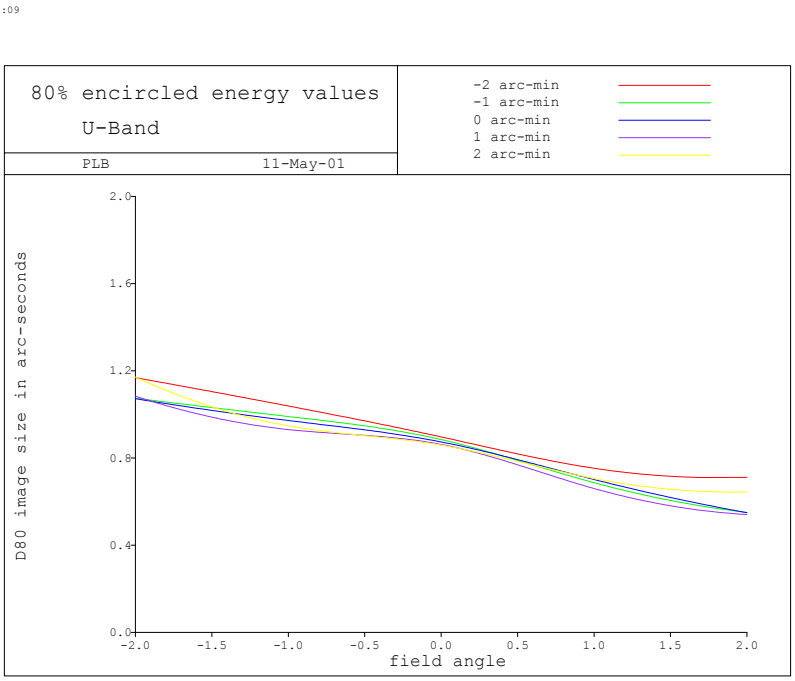

Figure D.1: D_{80} for the U-band (340nm) at optimal focus for 4x4' FOV**.**

14:27:17

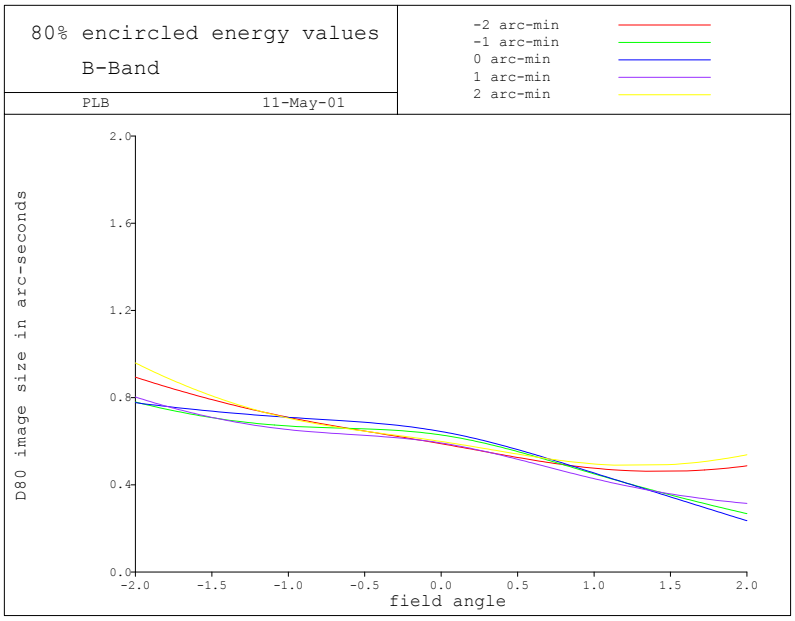

Figure D.2: D_{80} for B-band (440nm) at optimal 4x4' FOV focus.

14:29:37

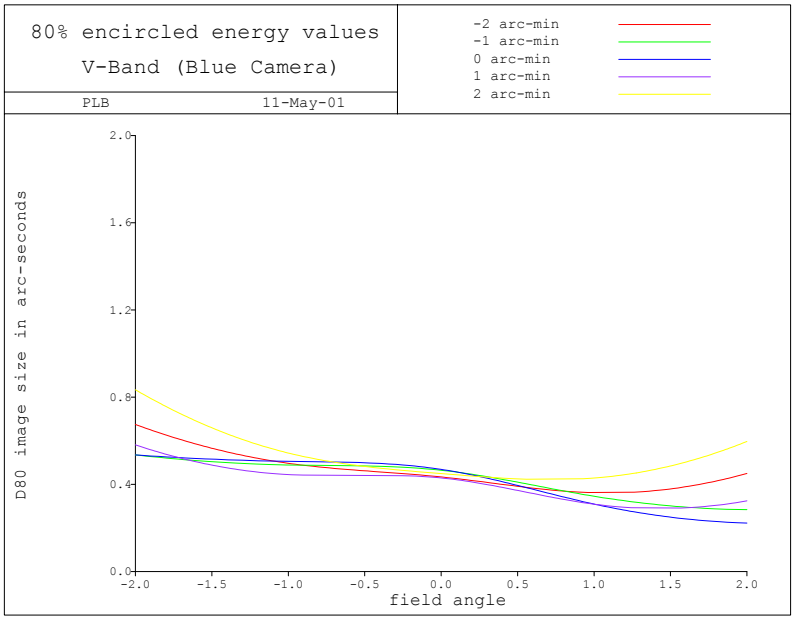

Figure D.3: D_{80} for V-band (550nm) at optimal 4x4' FOV focus.

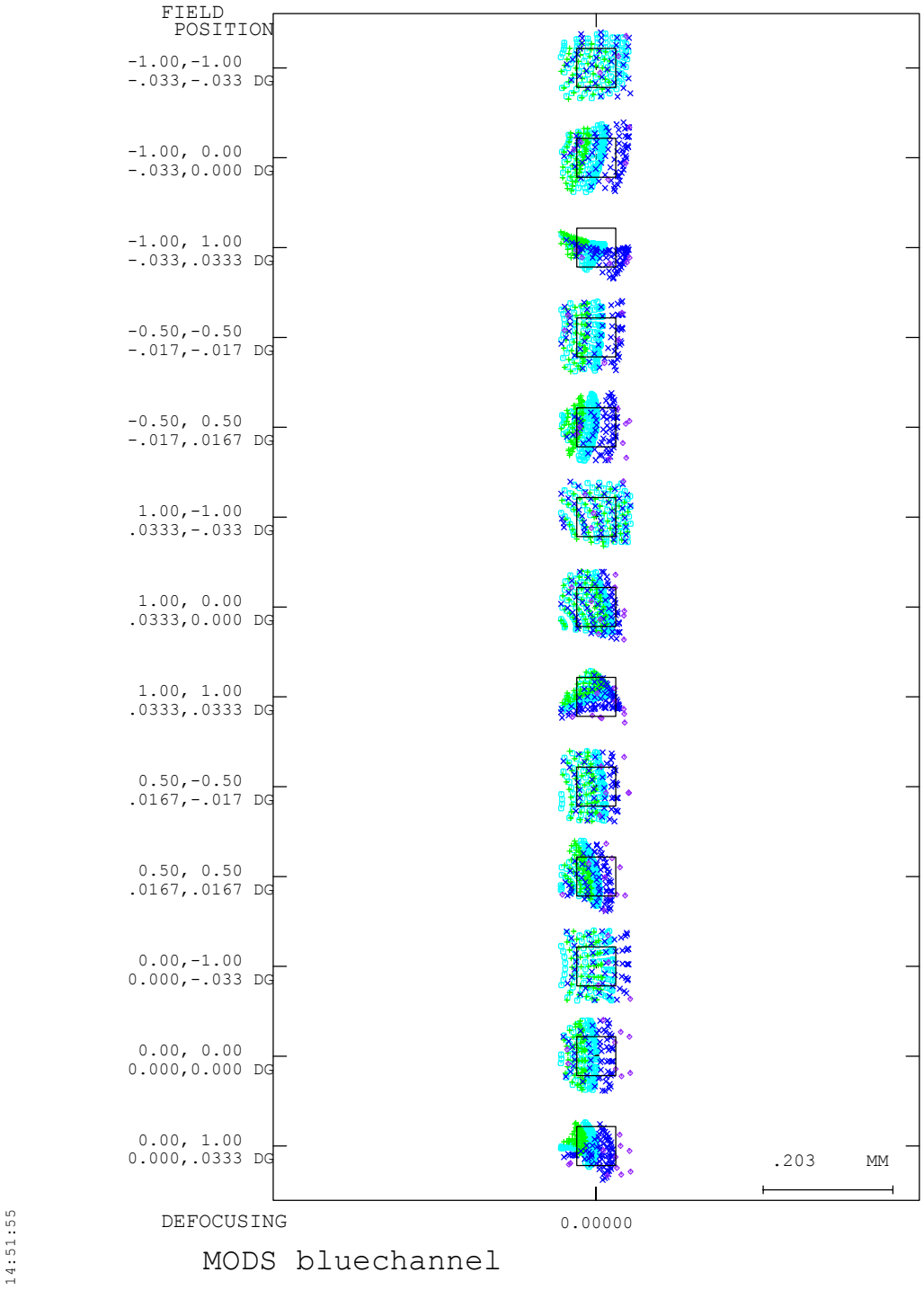

Figure D.4: Spot diagrams for the U-band imaging with the blue camera at optimal 4x4' FOV focus. Box size is 60μm.

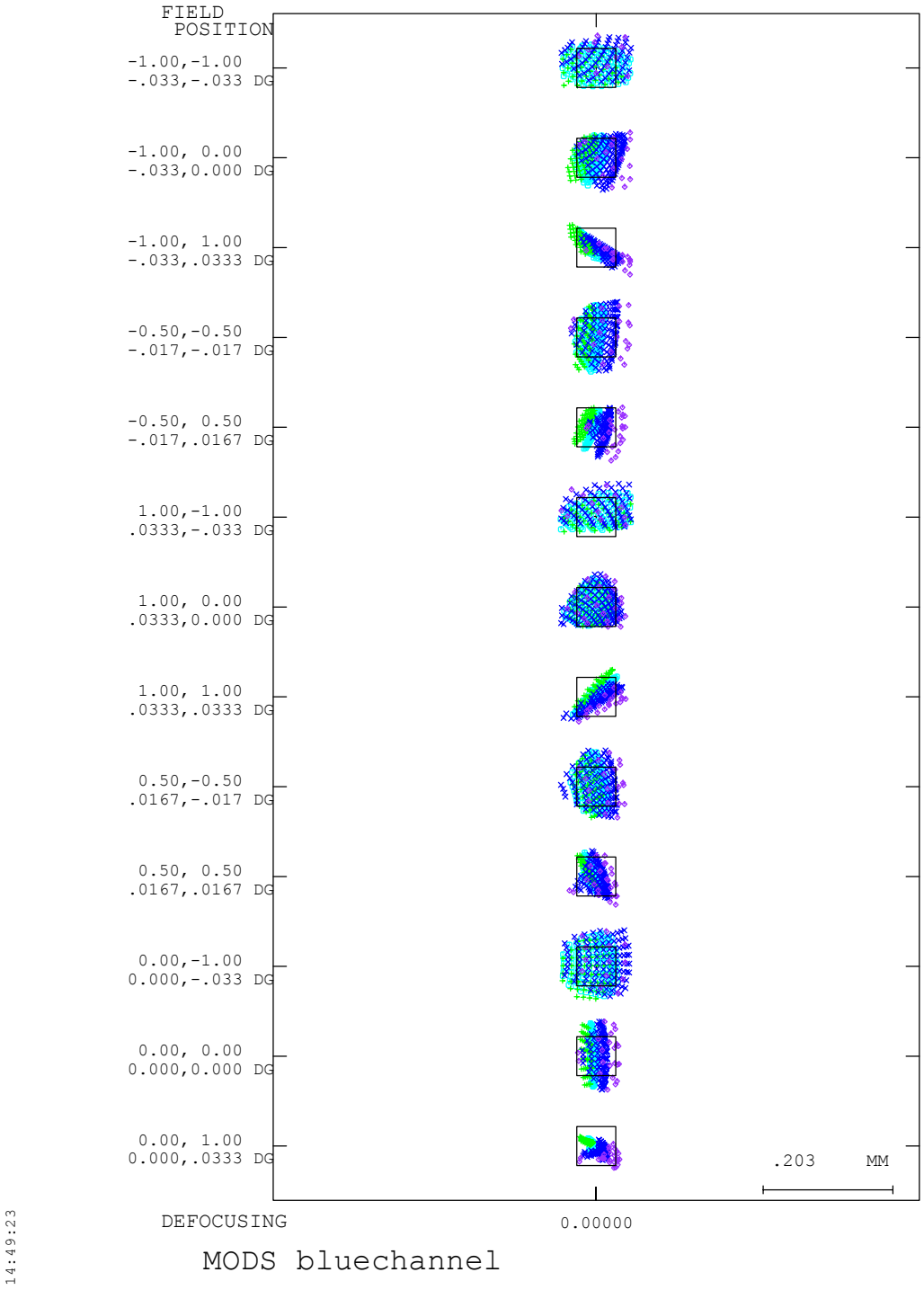

Figure D.5: Spot diagrams for B-band imaging**.** Box size is 60μm.

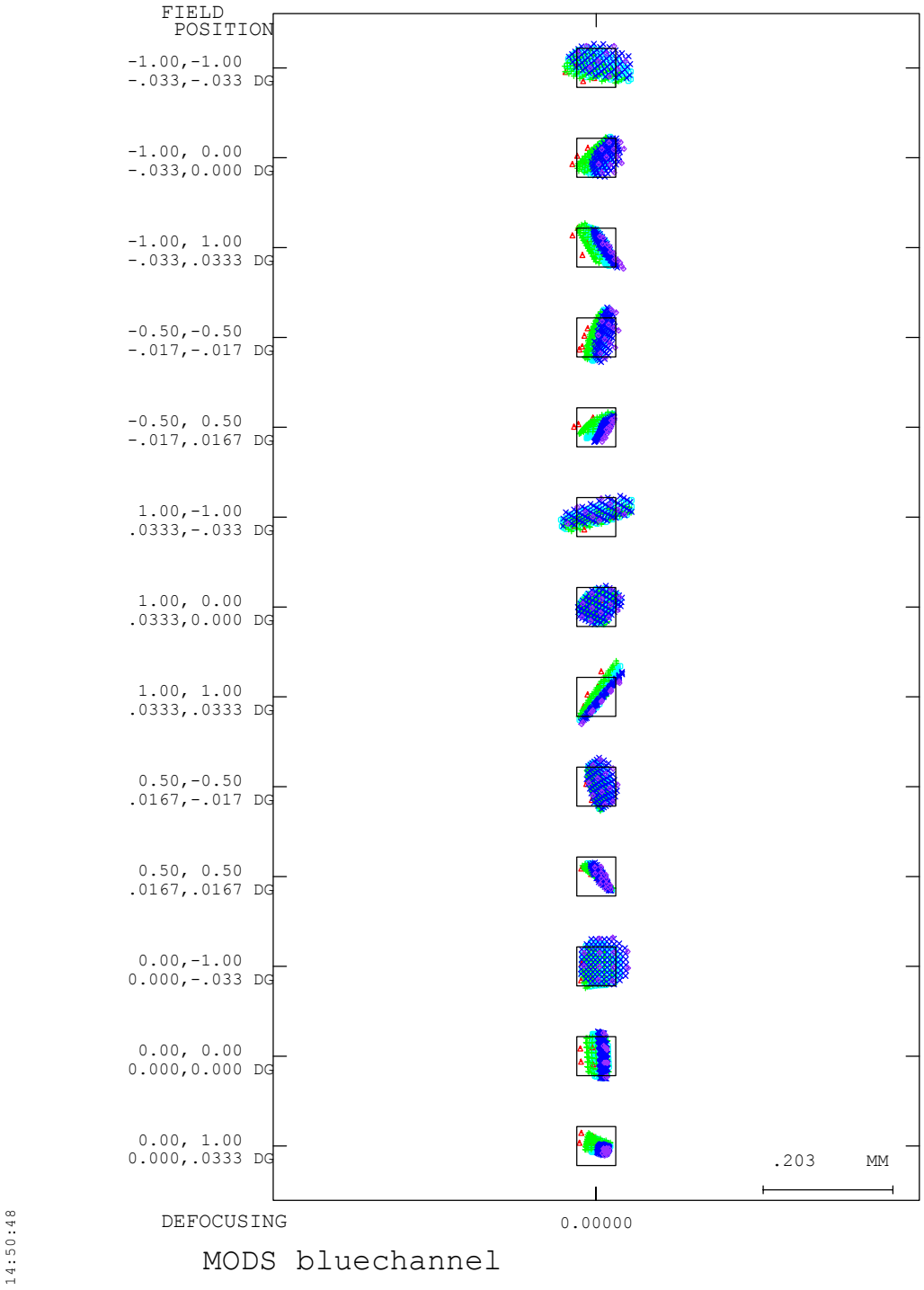

Figure D.6: Spot Diagrams for V-band imaging. Box size is 60μm.

MODS Red Camera

14:33:59

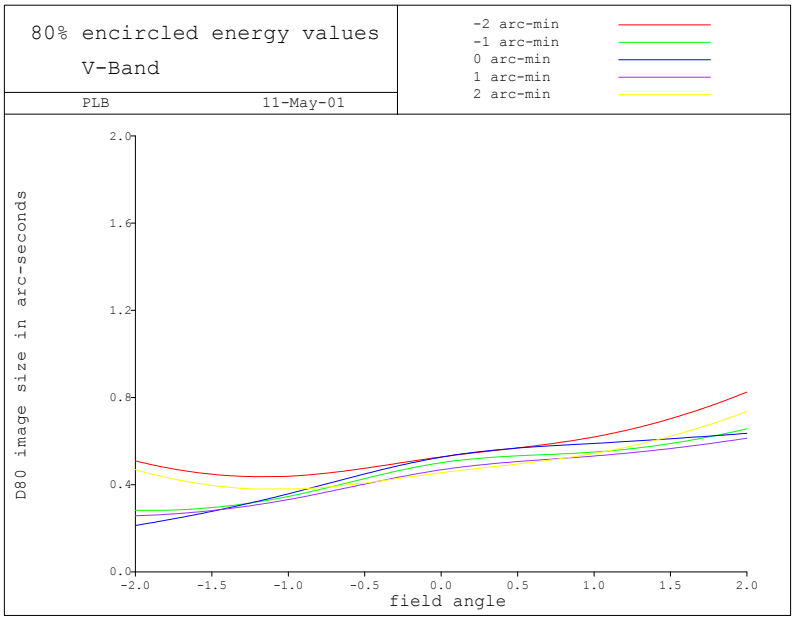

Figure D.7: D_{80} for MODS Red camera in V-band (550nm) at optimal 4x4' FOV focus.

14:36:03

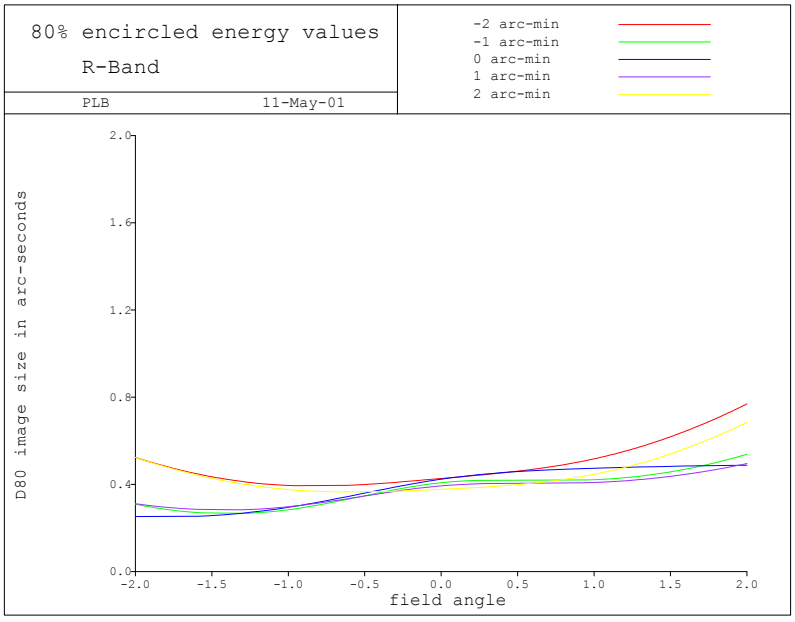

Figure D.8: D_{80} for the R-band (640nm) at optimal 4x4' FOV focus.

14:37:23

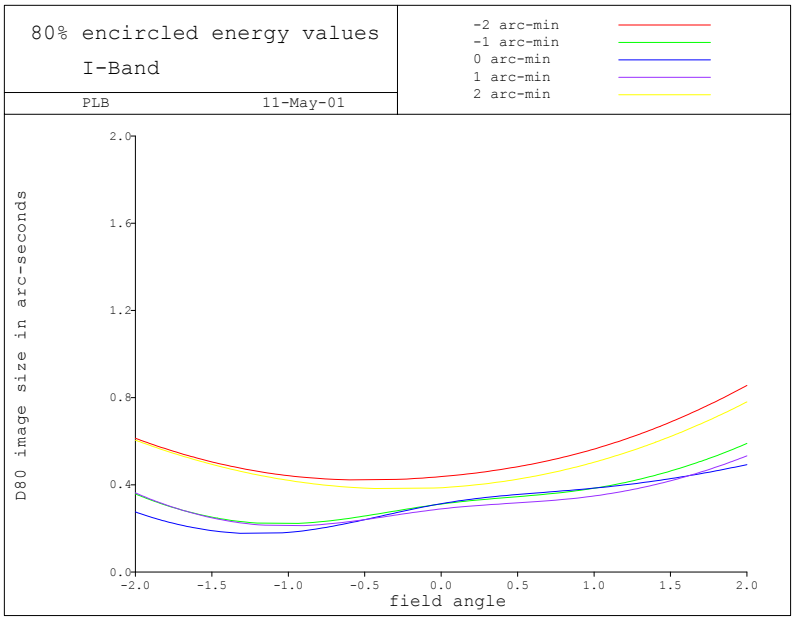

Figure D.9: D_{80} for the I-band (790nm) at optimal 4x4' FOV focus.

15:30:11

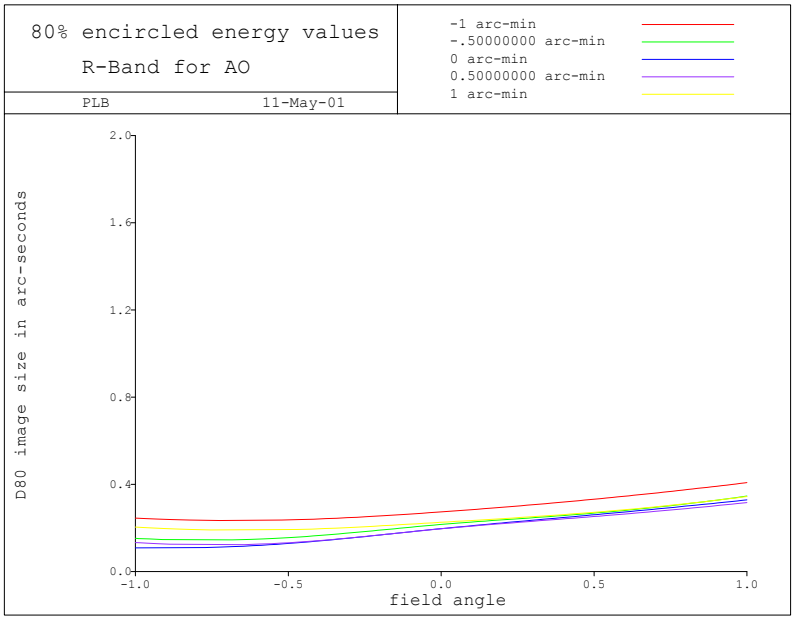

Figure D.10: D_{80} in the R-band for the red camera at optimal-focus for a 2x2' FOV "AO" imaging mode.

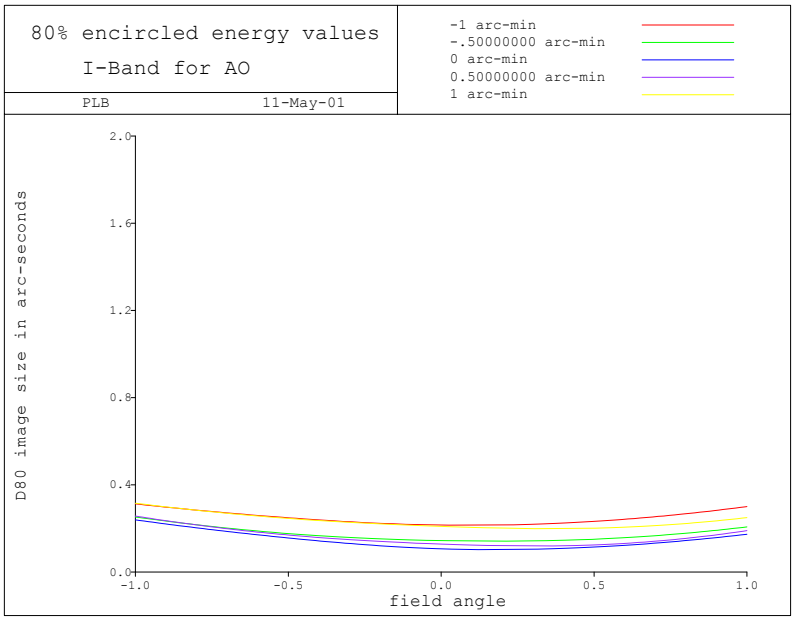

Figure D.11: D_{80} in the I-band for the red camera at optimal focus for a 2x2' "AO" FOV.

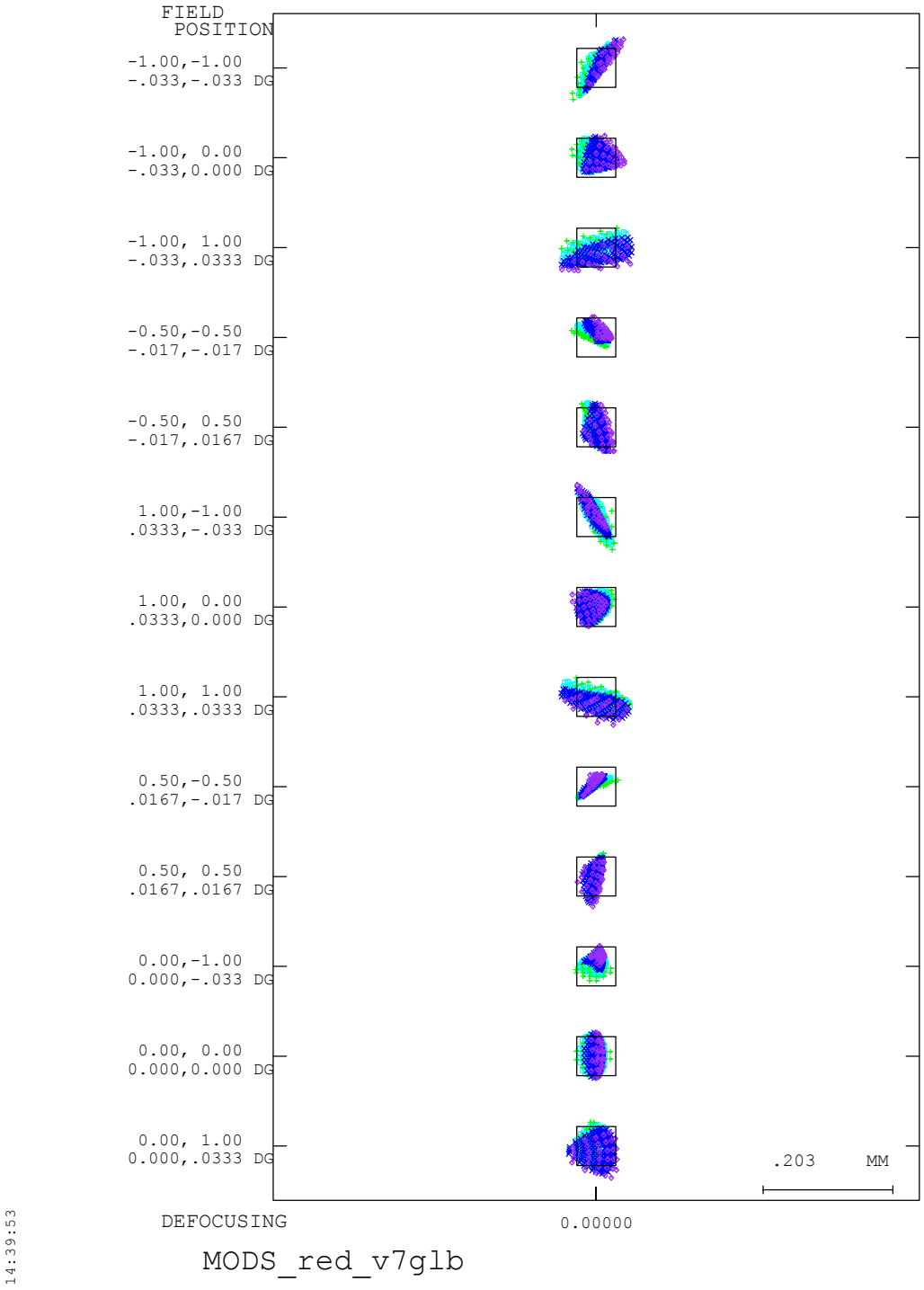

Figure D.12: Spot diagrams for the Red Camera in the V-band at optimal focus for a 4x4' FOV. Box size is 60μm.

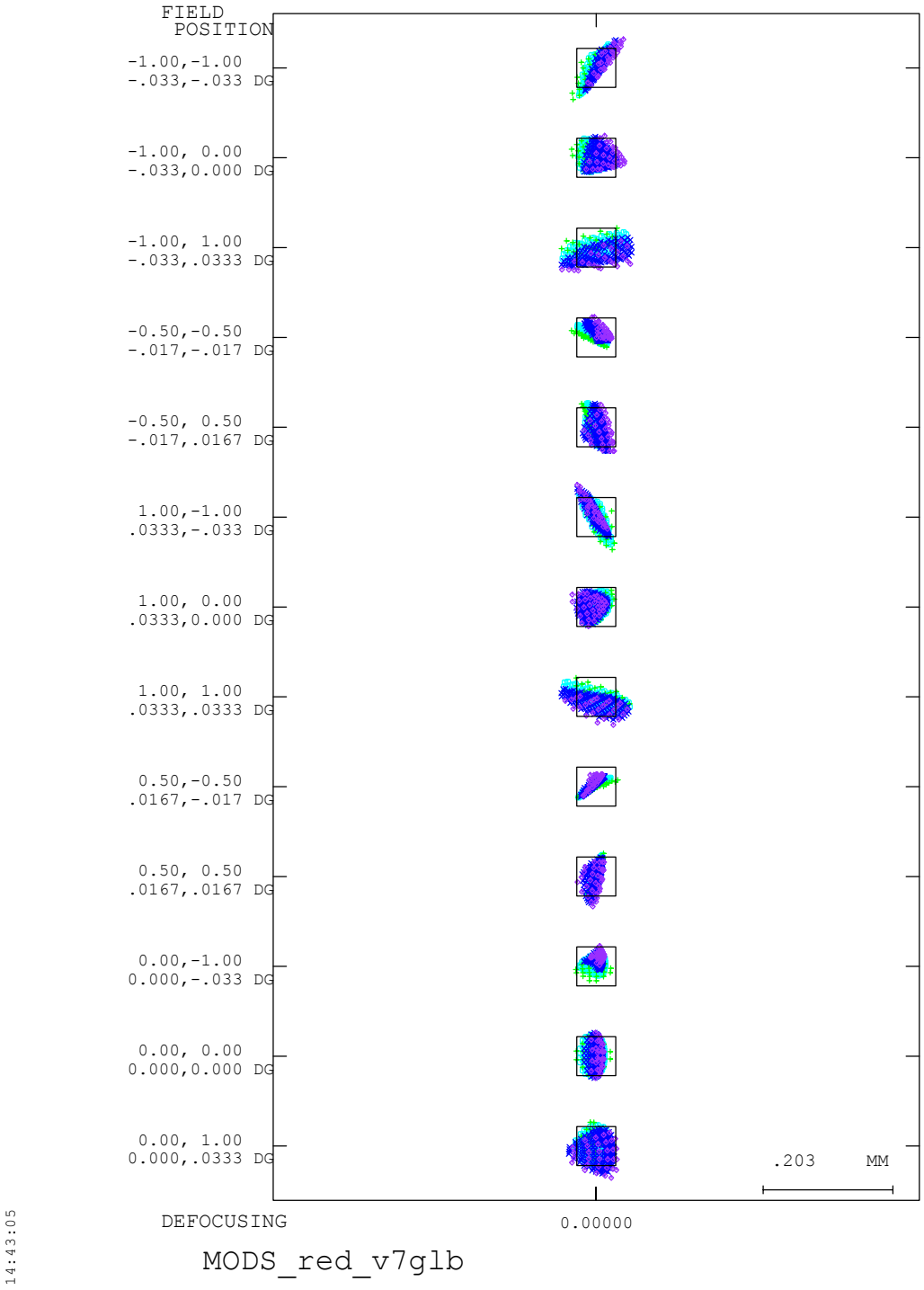

Figure D.13: Spot diagram for the R-band at optimal 4x4' FOV focus. Box size is 60μm.

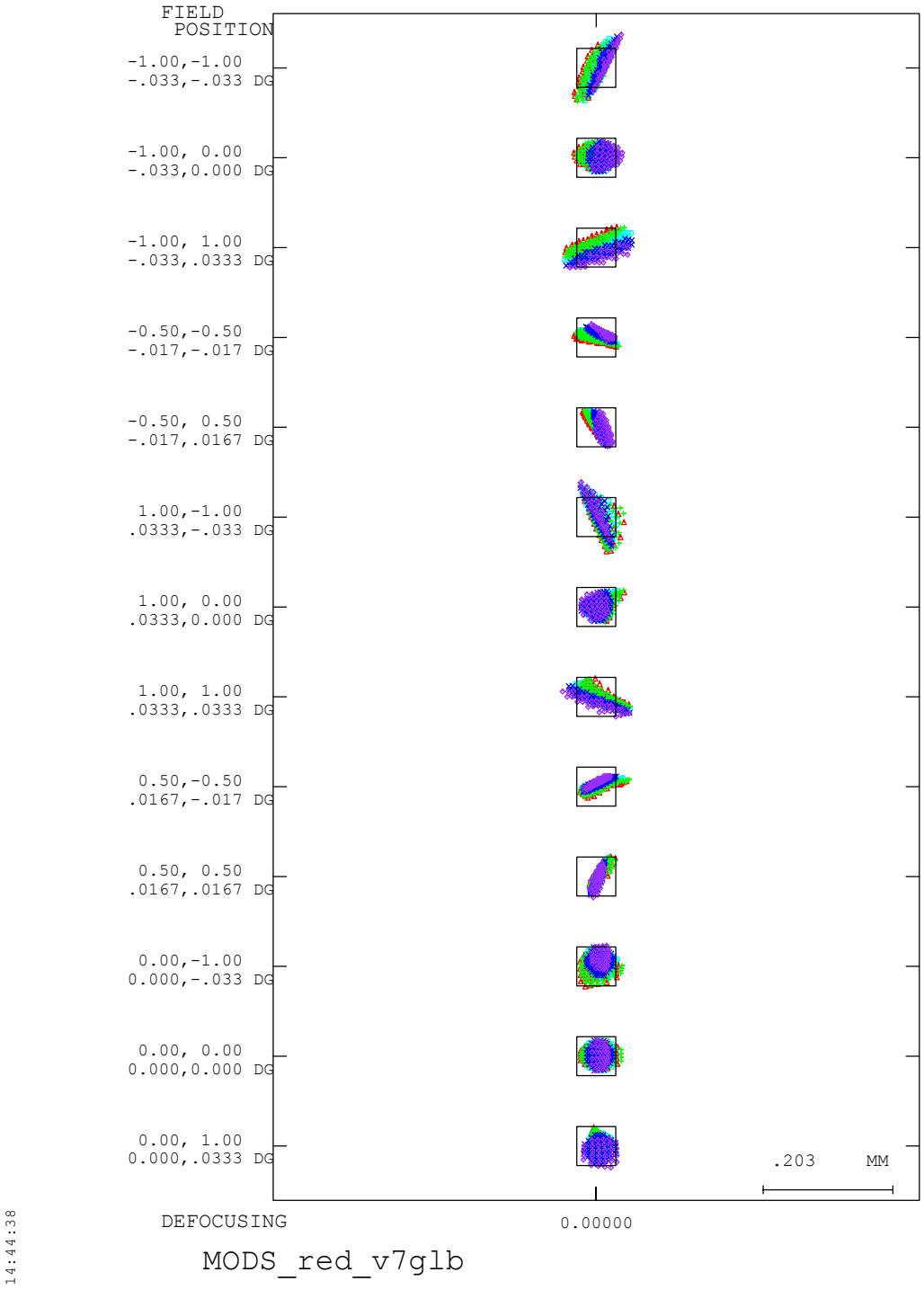

Figure D.14: Spot diagram for the I-band at optimal 4x4' FOV focus. Box size is 60μm.

Spectroscopic Performance

Spectroscopic performance is shown graphically in two ways:

1. D80 as a function of wavelength measured along the slit at optimal focus for 6', 4', and 2' long-slits.
2. Monochromatic Spot diagrams as a function of slit position.

MODS Blue Channel

10:18:08

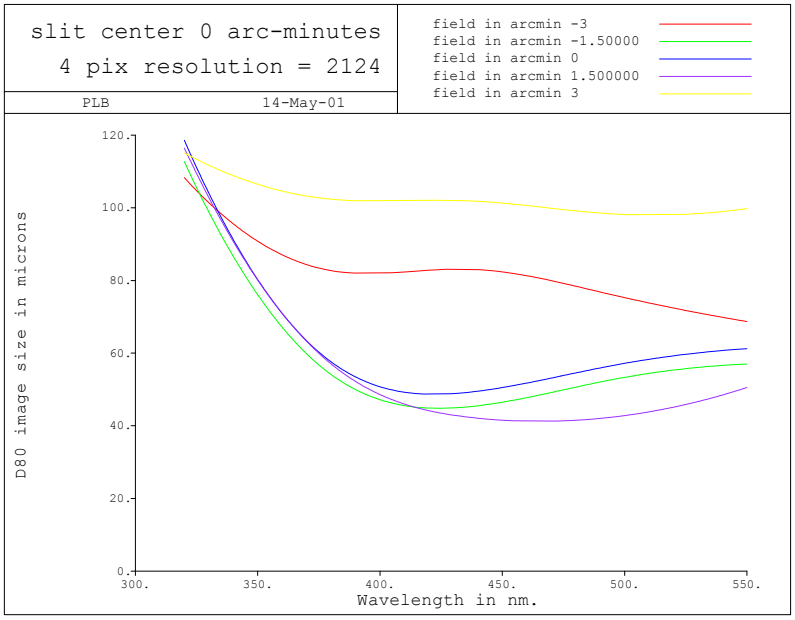

Figure D.15: D_{80} as a function of wavelength for the blue camera and an optimally focused 6' long slit.

10:16:47

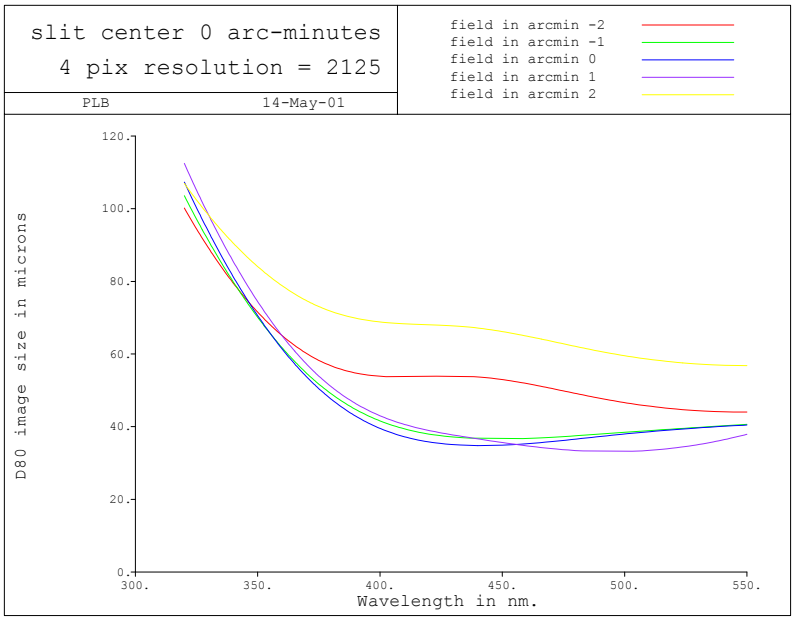

Figure D.16: D_{80} with wavelength for the blue camera and an optimally-focused 4' long slit.

10:14:36

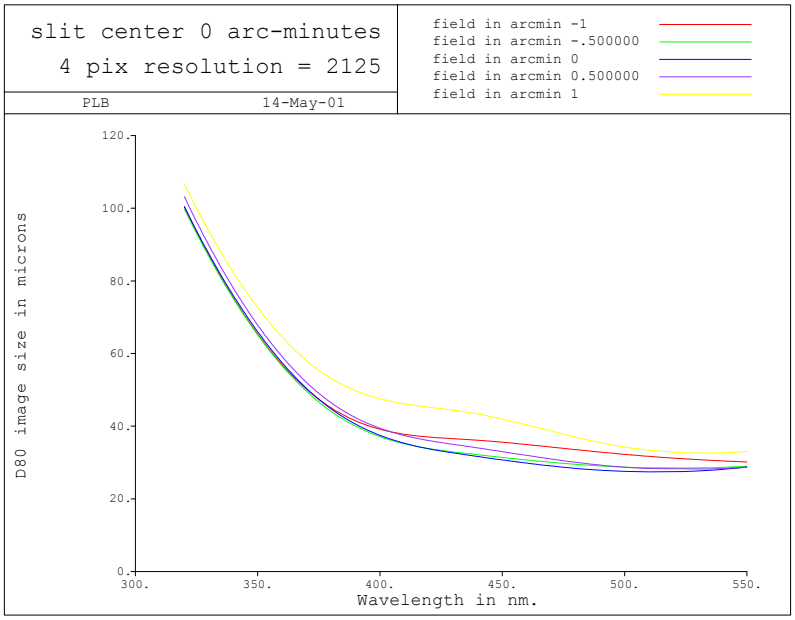

Figure D.17: D_{80} with wavelength for the blue camera and an optimally-focused 2' long slit**.**

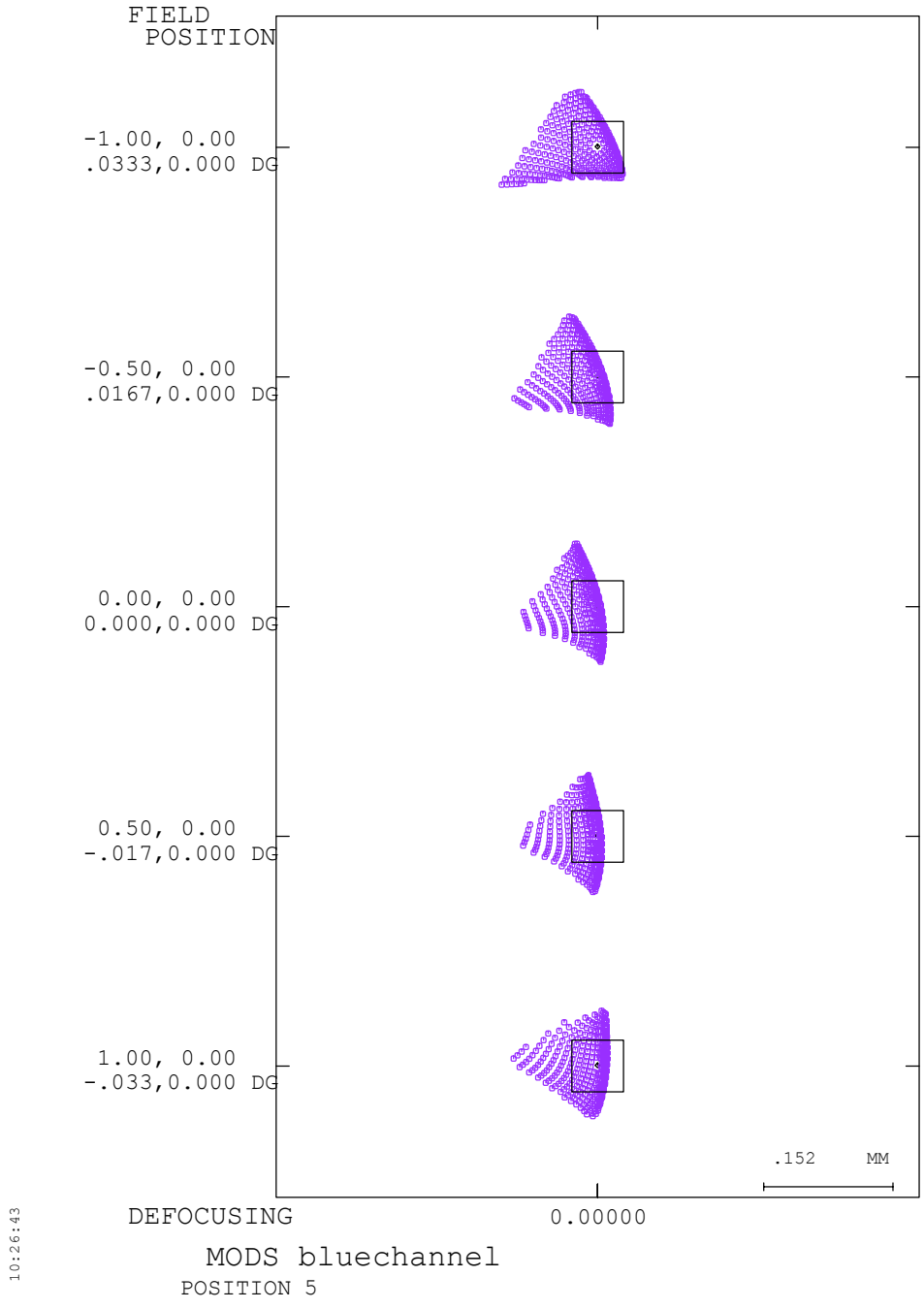

Figure D.18: Blue Camera spot diagrams for λ=320nm and an optimally-focused 4' long slit. Box size is 60μm.

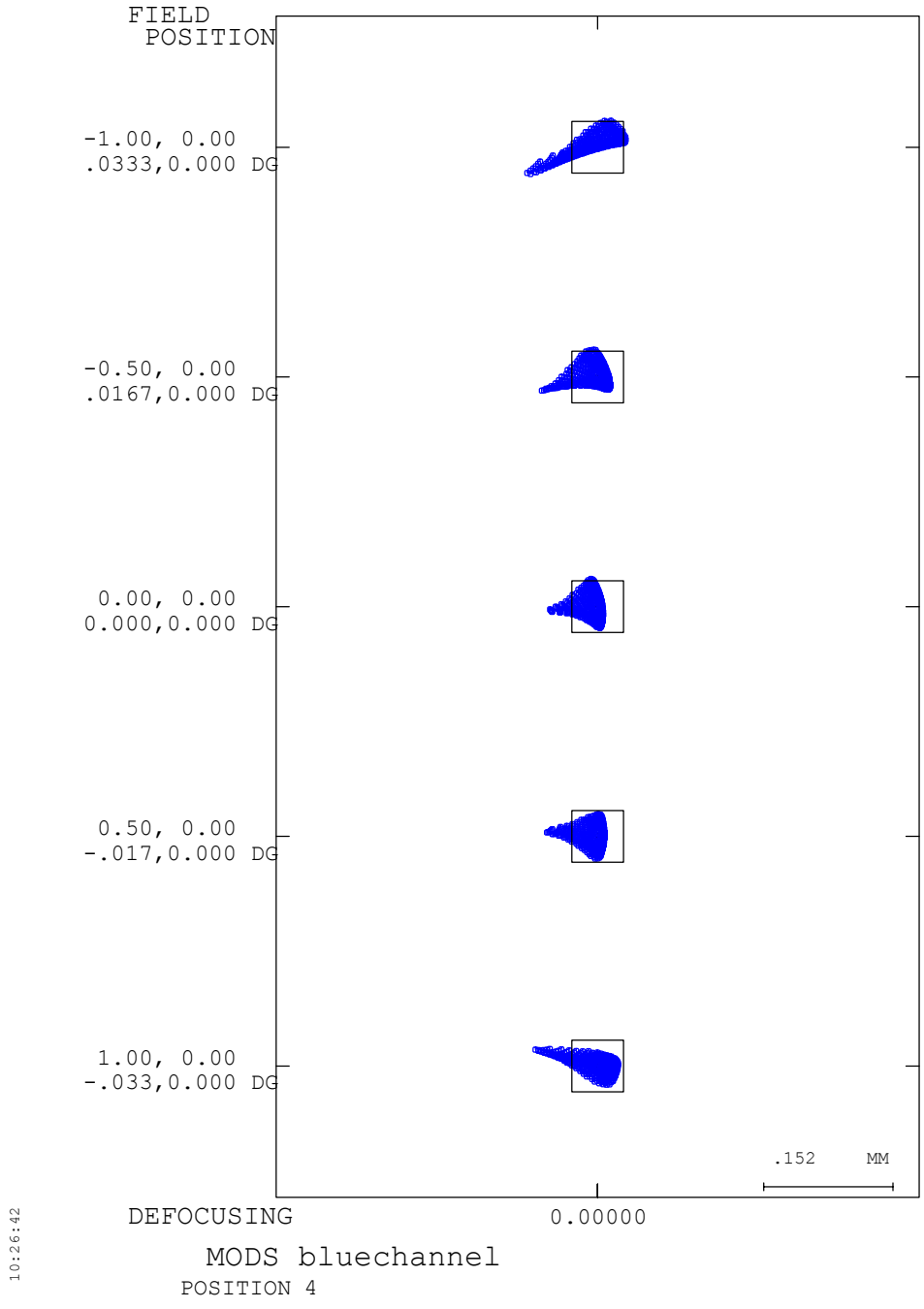

Figure D.19: Blue Camera spot diagrams for λ=377nm and an optimally-focused 4' long slit. Box size is 60μm.

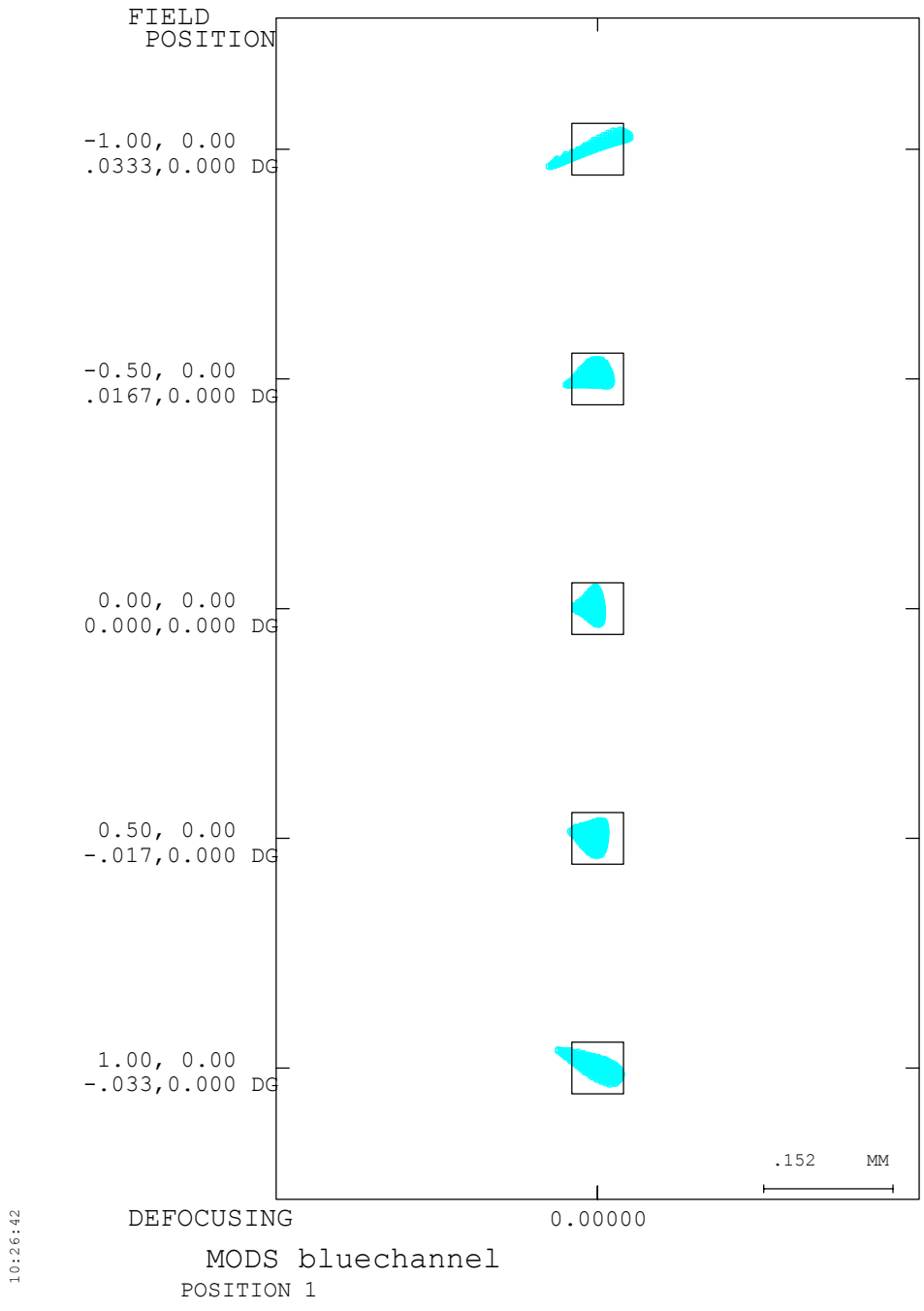

Figure D.20: Blue Camera spot diagrams for λ=435nm and an optimally-focused 4' long slit. Box size is 60μm.

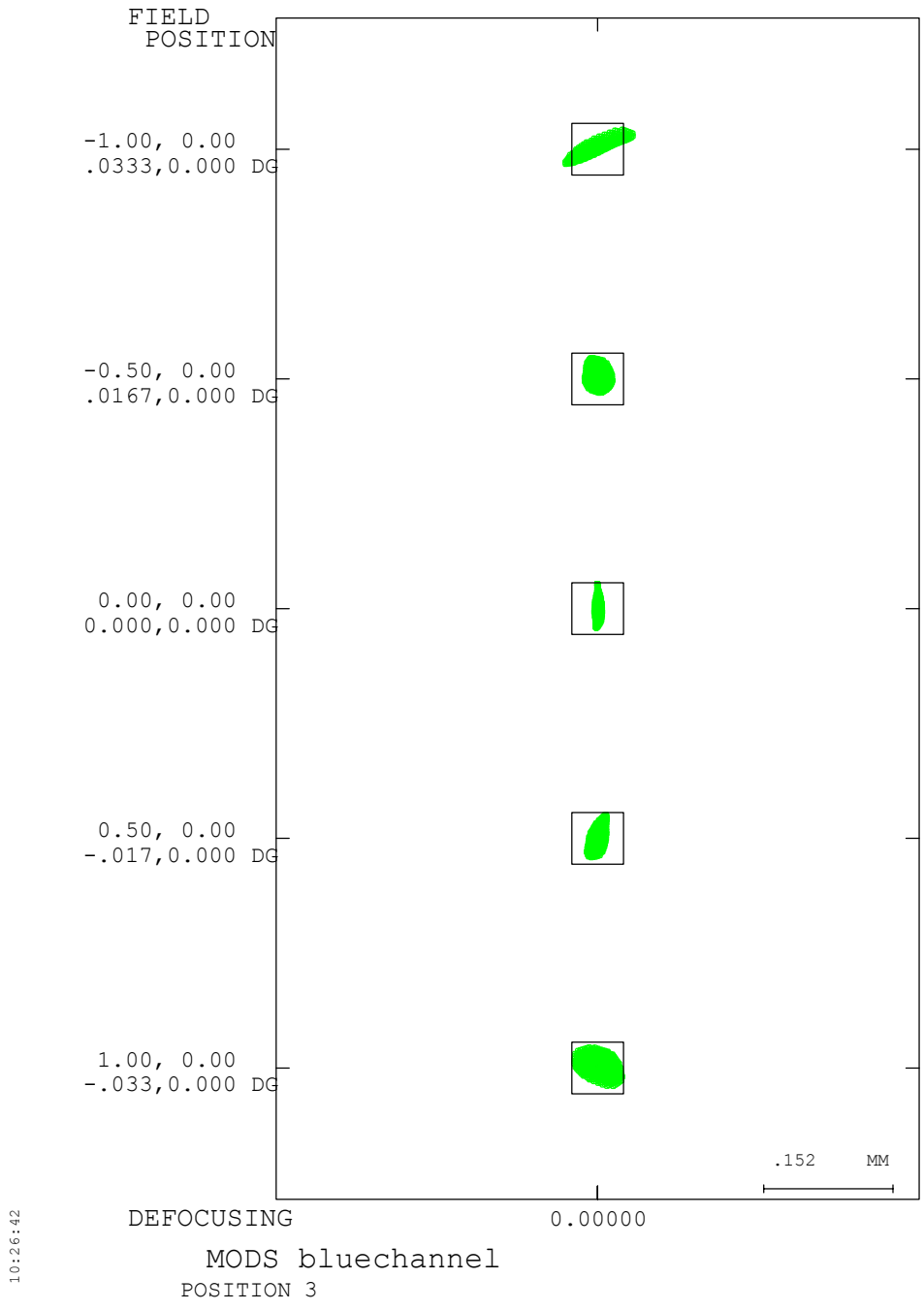

Figure D.21: Blue Camera spot diagrams for λ=492nm and an optimally-focused 4' long slit. Box size is 60μm.

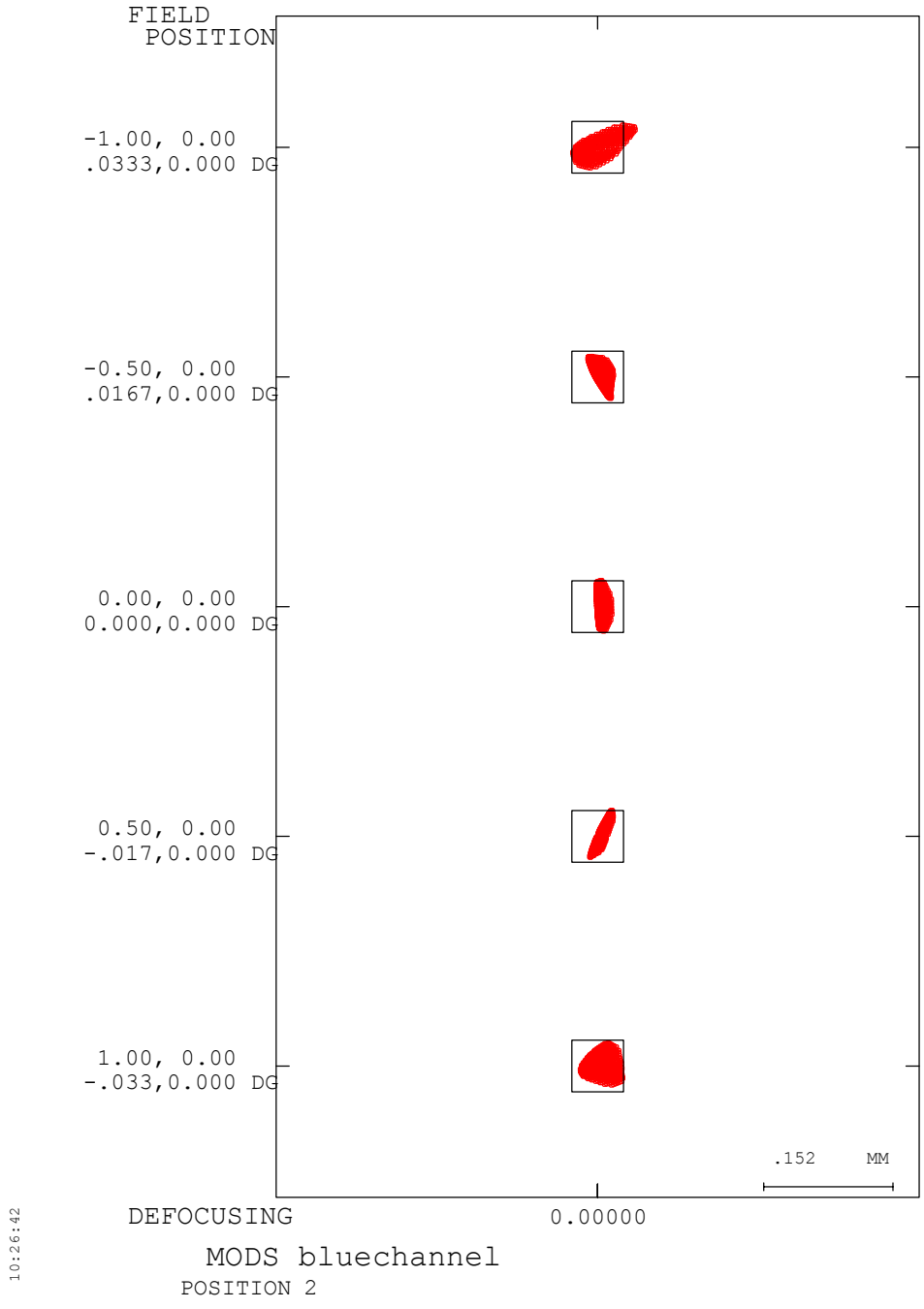

Figure D.22: Blue Camera spot diagrams for λ=550nm and an optimally-focused 4' long slit. Box size is 60μm.

MODS Red Channel

09:49:15

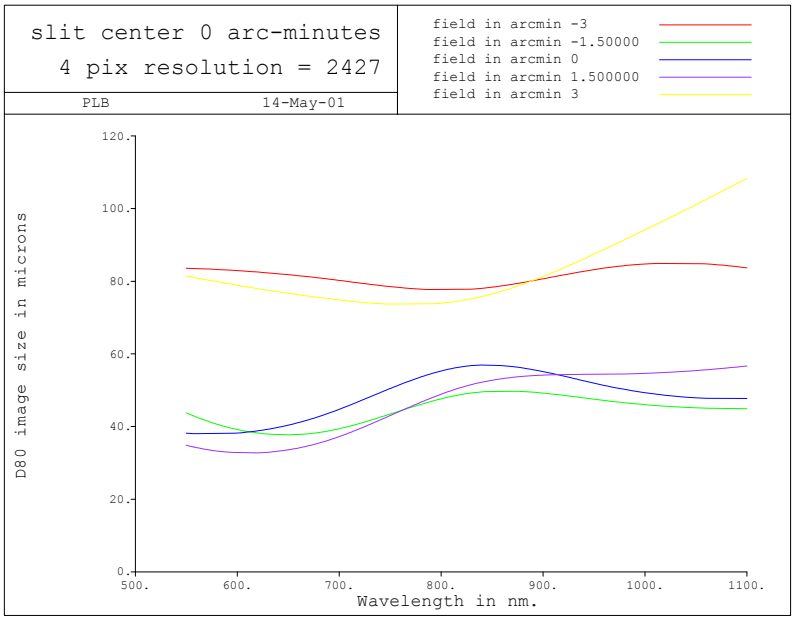

Figure D.23: D_{80} with wavelength for the red camera and an optimally-focused 6' long slit**.**

09:47:11

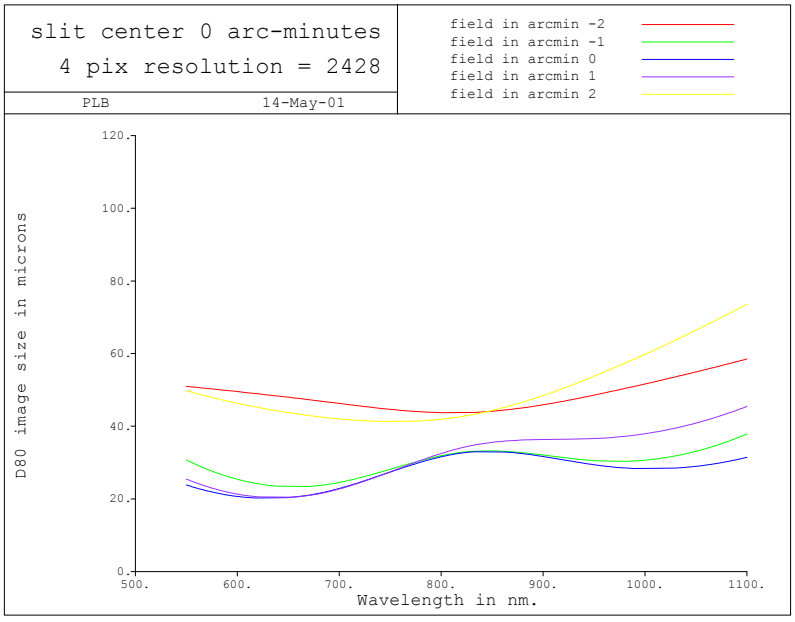

Figure D.24: D_{80} with wavelength for the red camera and an optimally-focused 4' long slit.

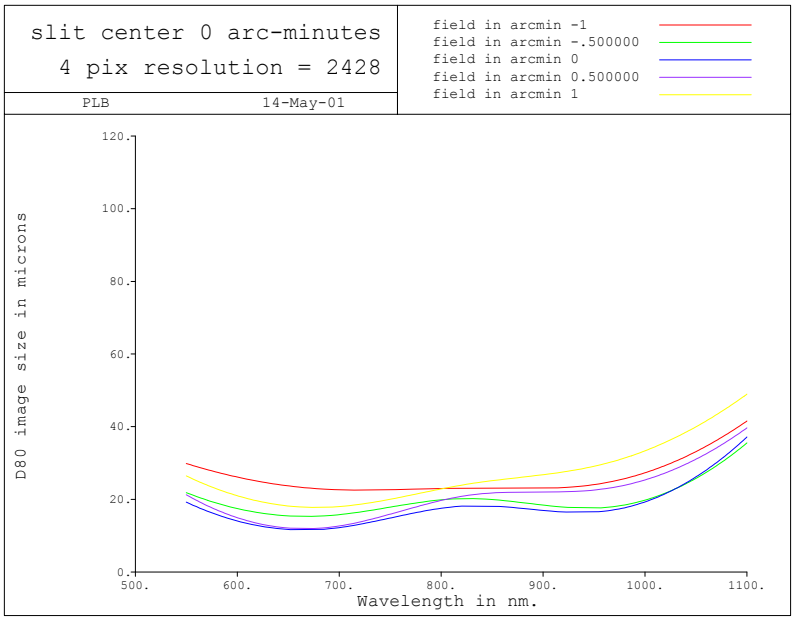

Figure D.25: D_{80} with wavelength for the red camera and an optimally-focused 2' long slit**.**

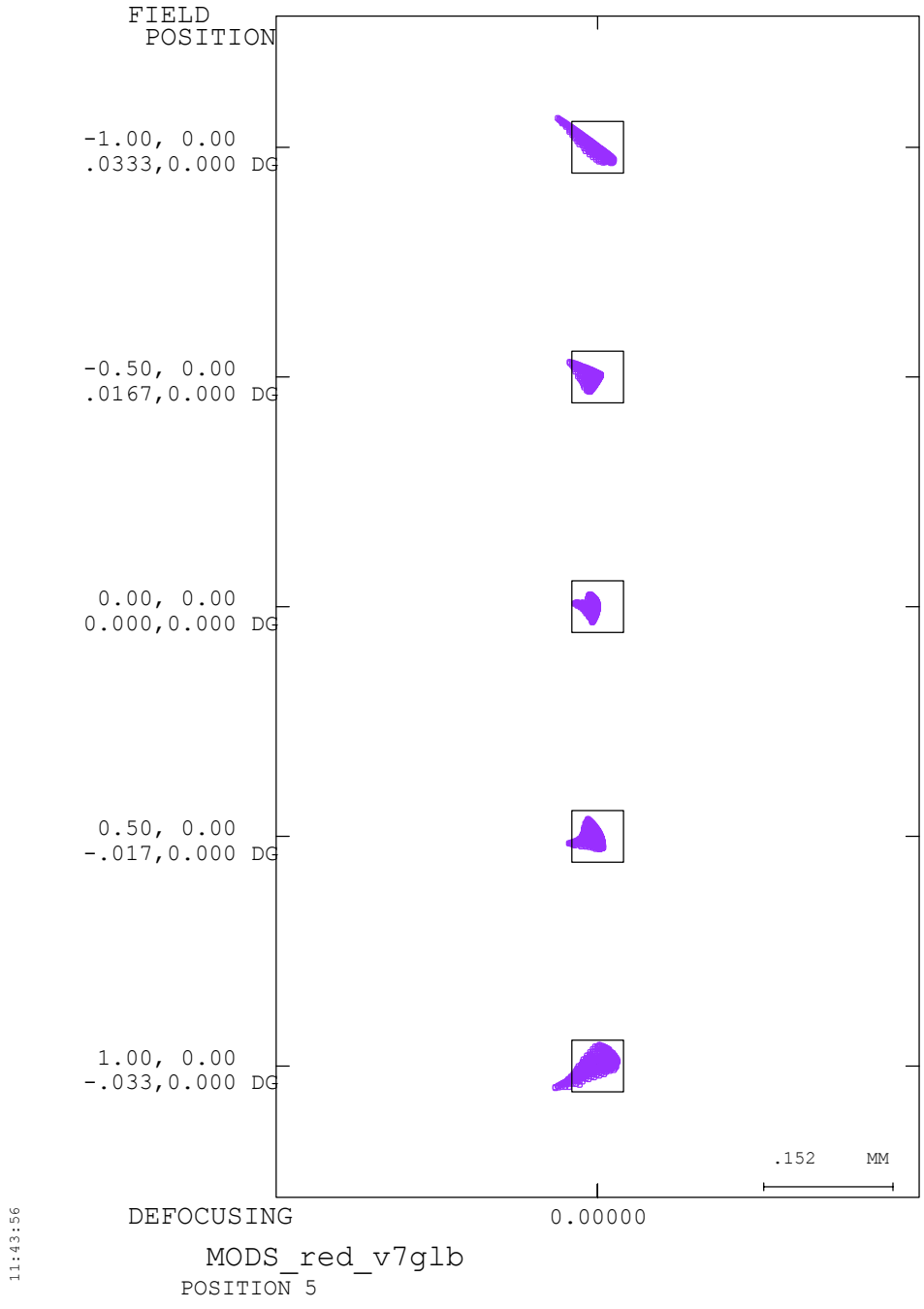

Figure D.26: Red Camera spot diagrams for λ=550nm and an optimally-focused 4' long slit. Box size is 60μm.

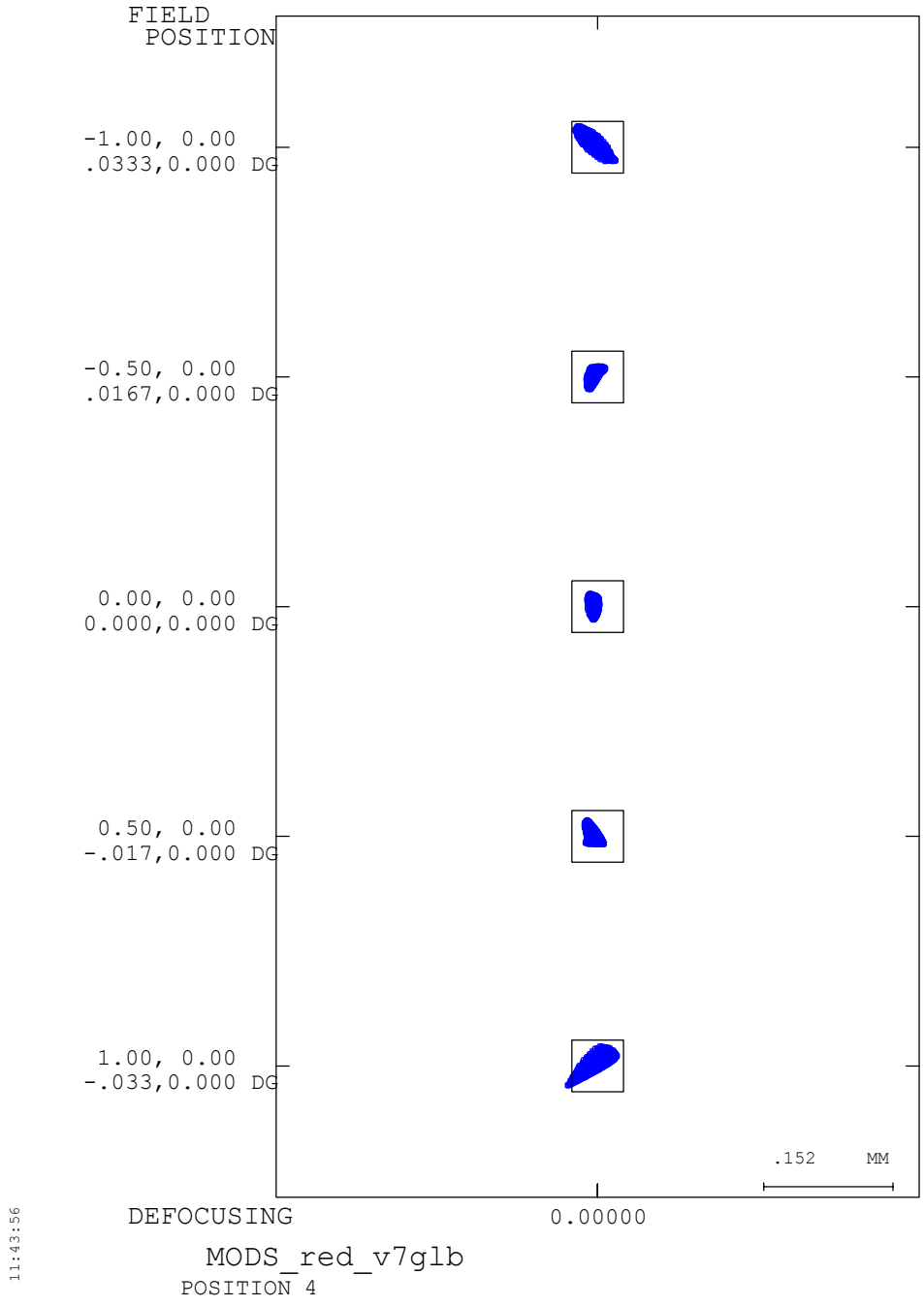

Figure D.27: Red Camera spot diagrams for λ=687nm and an optimally-focused 4' long slit. Box size is 60μm.

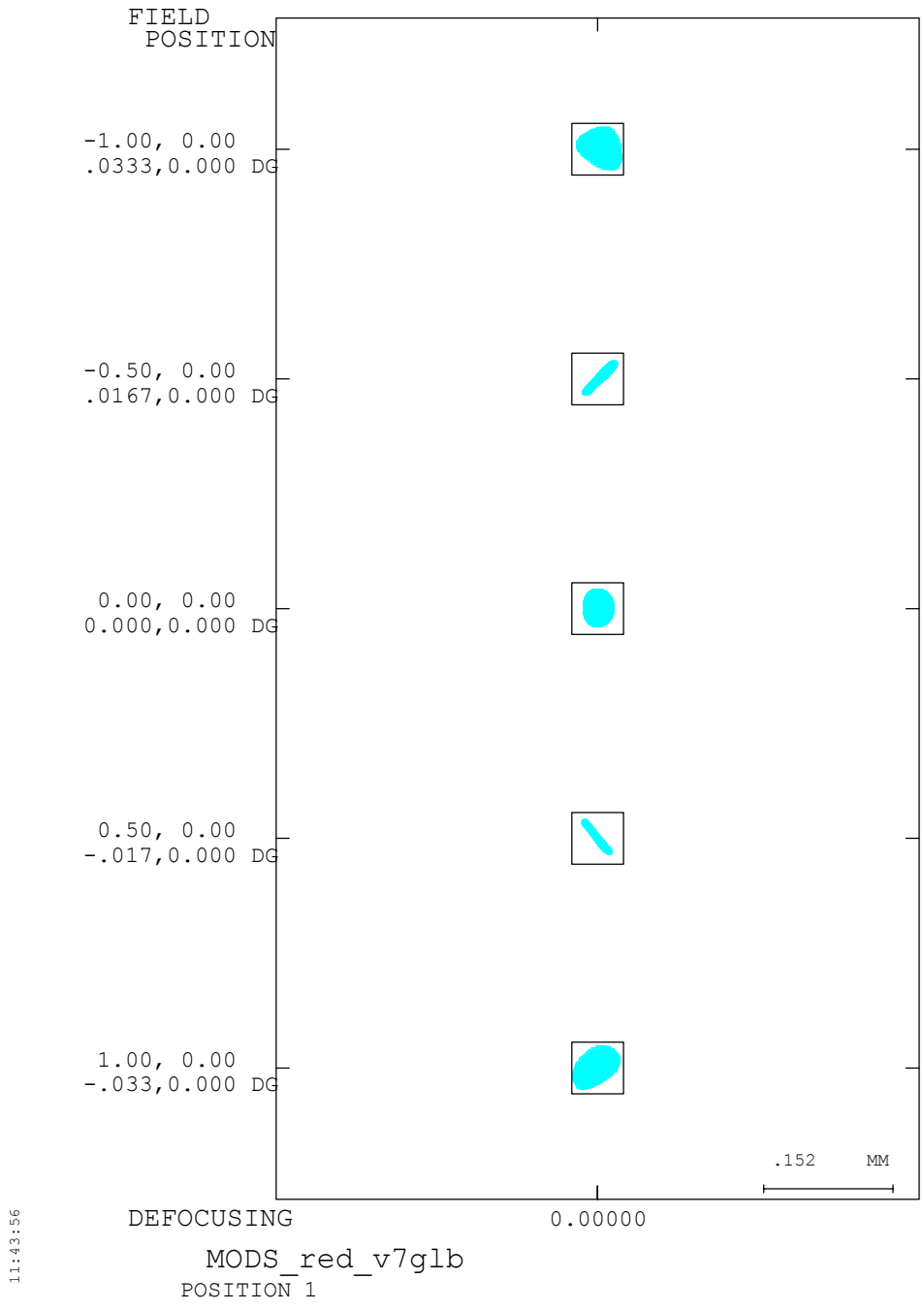

Figure D.28: Red Camera spot diagrams for λ=825nm and an optimally-focused 4' long slit. Box size is 60μm.

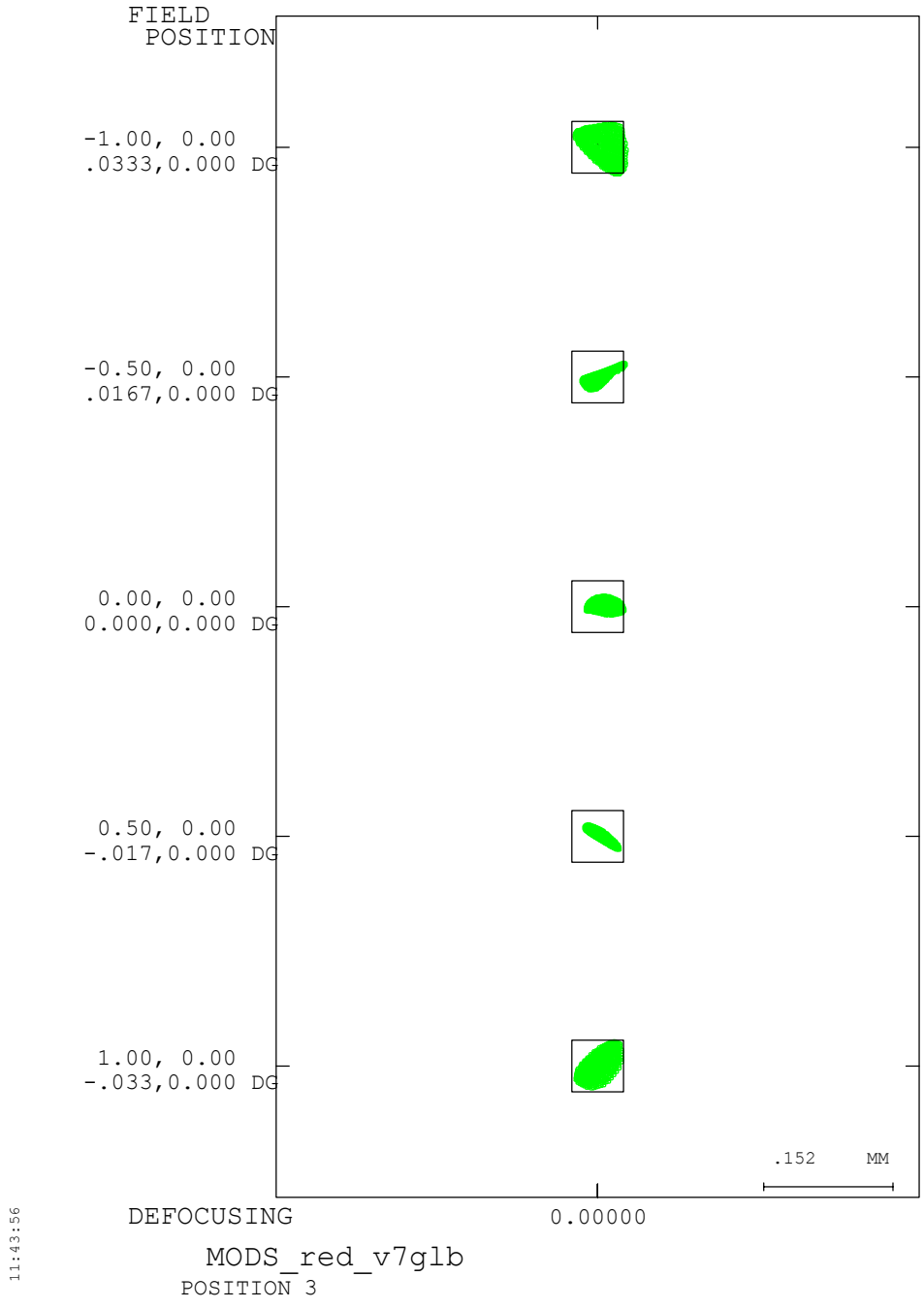

Figure D.29: Red Camera spot diagram for λ=962nm and an optimally-focused 4' long slit. Box size is 60μm.

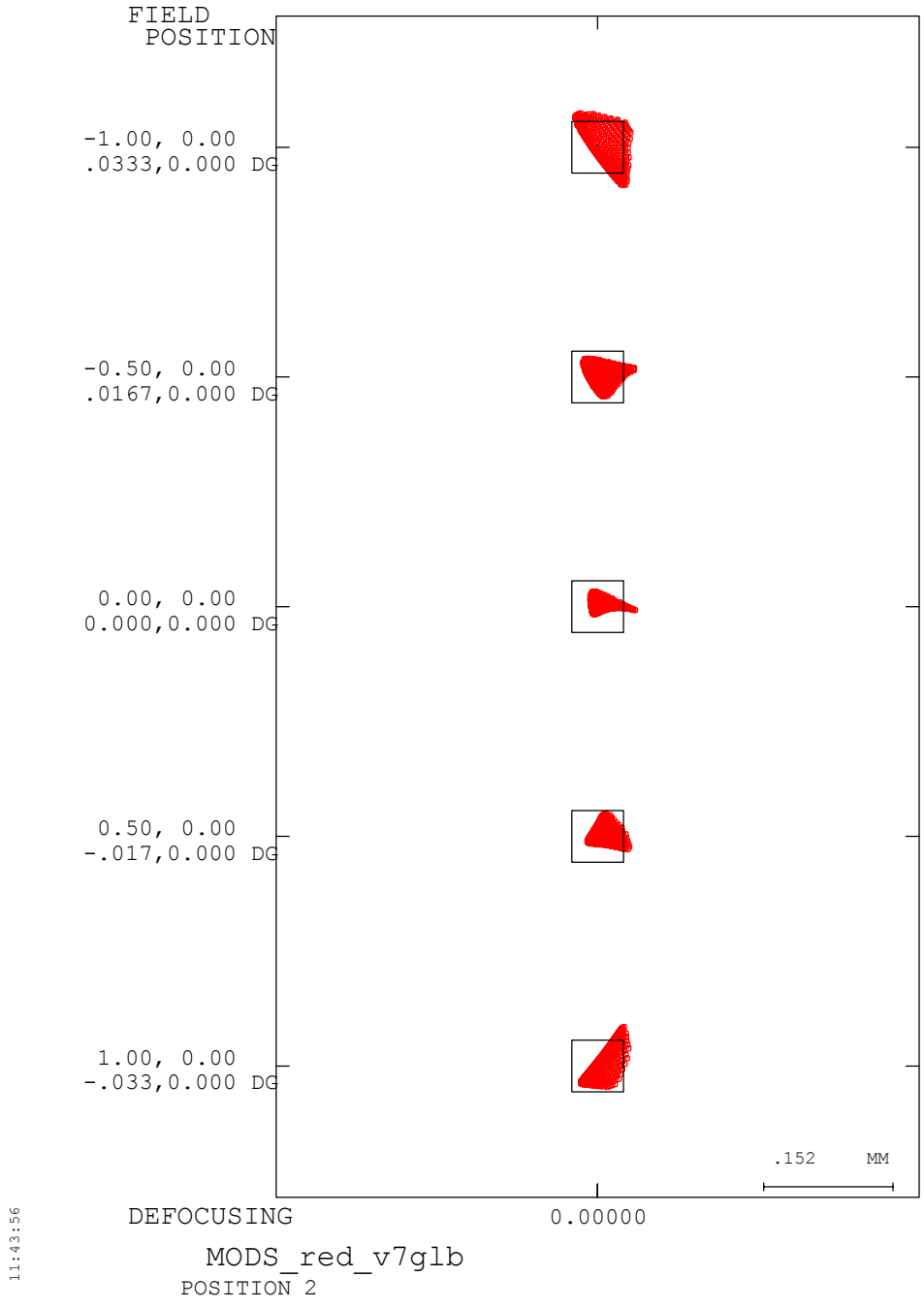

Figure D.30: Red Camera spot diagrams for λ=1100nm and an optimally-focused 4' long slit. Box size is 60μm.